Aus der

Neurologischen Universitätsklinik Tübingen

Abteilung Neurologie mit Schwerpunkt neurovaskuläre Erkrankungen

Impact of sensory inputs in TMS-EEG measurements

Inaugural-Dissertation

zur Erlangung des Doktorgrades

der Medizin

der Medizinischen Fakultät

der Eberhard Karls Universität

zu Tübingen

vorgelegt von

Caldana Gordon, Pedro

2025

Dekan:	Professor Dr. B. Pichler
1. Berichterstatter:	Professor Dr. U. Ziemann
2. Berichterstatter:	Professor Dr. C. Schwarz
3. Berichterstatter:	Professor Dr. R. Ilmoniemi

Tag der Disputation: 29.10.2025

A. Table of Contents

B. List of abbreviations

%MSO	percentage of the maximal stimulator output
EEG	electroencephalography
EMG	electromyography
ES	electric stimulation
GABA	gamma-aminobutyric acid
ICF	intracortical facilitation
LICI	long-interval cortical inhibition
MEP	motor evoked potential
PEP	peripheral evoked potentials
RMT	resting motor threshold
SAI	short-latency afferent inhibition
SICI	short intracortical inhibition
TMS	transcranial magnetic stimulation
TEP	TMS evoked potentials

1. Introduction, aims and objectives

1.1 Basis of Transcranial Magnetic Stimulation

In 1985, Barker et al demonstrated that it is possible to stimulate the cerebral cortex non-invasively by means of electromagnetic induction, dubbing the technique transcranial magnetic stimulation (TMS) (Barker et al., 1985). TMS offers significant advantages in comparison to electric stimulation as a non-invasive brain stimulation method, providing tolerable and spatially well-defined cortical stimuli.

The basic physical mechanism of TMS is the generation of a magnetic field by means of electromagnetic induction, which occurs when running an electric current through the conductive windings of a coil. For this purpose, a TMS device requires an energy storage element (a capacitor), an inductor (the TMS coil) and a switch (Figure 1A-C). By closing the circuit at the switch, the resulting flow of electric charges stored in the capacitor generates an electric current through the circuit, and the consequent displacement of electric charges induces a magnetic field orthogonal to the moving charges' direction, as described by the laws of classical electromagnetism. The wiring composition within the inductor allows for the superposition of the induced magnetic fields from each loop, thus potentiating the total magnetic field in its surroundings. The variation in time of the magnetic field's strength, which occurs when delivering a short TMS pulse, results then in the induction of an electric field orthogonal to that magnetic field (Figure 1D). It is the electric potential gradient from this induced electric field that is capable of depolarizing neuronal tissues near to the TMS coil without the need to apply direct electrical current (Davey & Epstein, 2000; Dayan et al., 2013; Ruohonen et al., 1997).

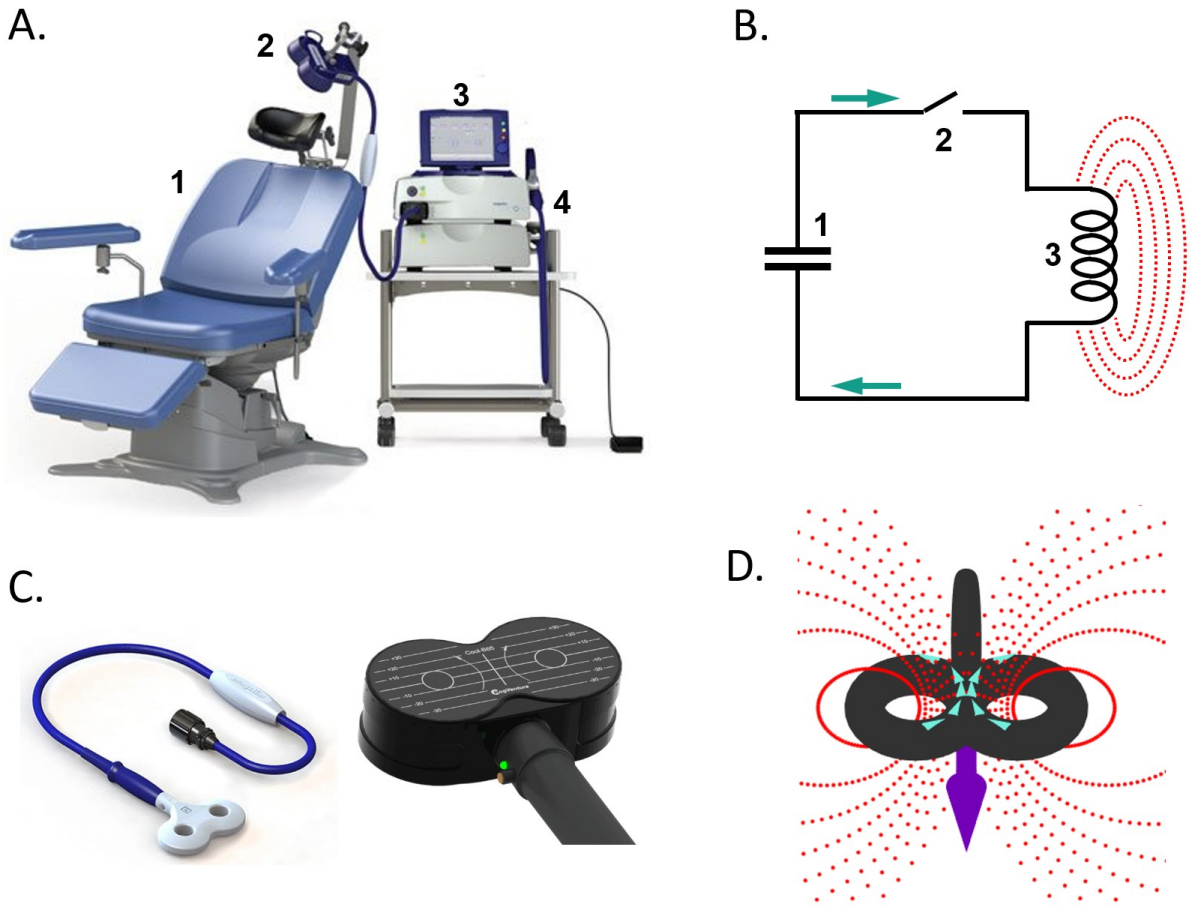

Figure 1

A. Example of a TMS set-up showing a reclining chair (1), a TMS coil (2), a digital display which allows the setting of stimulation parameters (3), and the main unit, which contains the capacitor (4). (from TMS Therapy System - Magstim Co Ltd, *www.magstim.com*)
B. Simplified representation of TMS device components. Electric charge is stored in the capacitor (1). As the trigger (2) closes the circuit, electric current (cyan arrows) flows through the inductor (3), resulting in the induction of a magnetic field (red circles) orthogonal to the current flow.
C. Example of TMS coils, “figure of 8” type, as used in the project’s experiments (left: Magstim 70-mm figure-of-8 coil; right: MagVenture Double TMS coil - Cool-B65)
D. Illustration of a figure-of-8 coil, containing two circular wirings next to each other, on which electric currents of opposite directions are delivered (cyan arrows). The induced magnetic fields from both loops become superimposed (red circles), resulting in a focal induced electric field (purple arrow) of highest intensity underneath the center of the coil.

These mechanisms have meaningful implications for a non-invasive brain stimulation method. Firstly, the induced magnetic field permeates the space around the coil undisturbed by biological tissues, due to the high magnetic permeability of water and organic tissues. This is a considerable advantage in comparison to transcranial electric stimulation, which requires high intensities to overcome the electric resistance of the scalp, skull and cerebral-spinal fluid to finally achieve cortical neurons depolarization. Moreover, when applying transcranial electrical stimulation, the current dissipates

through biological tissues and activates large brain regions, whereas the TMS induced electromagnetic field in the cortex is highly focal and of predictable intensity (Dayan et al., 2013; Peterchev et al., 2012).

The consequences of directly activating the cortex with TMS can be immediately detected in a subject, with different effects observed depending on the cortical region targeted. For instance, delivering TMS to the occipital cortex can elicit the visual perception of flickering lights, and TMS to the primary motor cortex can elicit a motor twitch from the contralateral limb. By applying TMS to the motor cortex and observing the motor evoked response one can obtain information on the functioning of the motor system. It was observed that by increasing the current run through the TMS coil (stated as the percentage of the maximal stimulator output – %MSO) while targeting the precentral gyrus, it's possible to obtain increasingly stronger motor responses (motor evoked potential - MEP), measured with surface electromyography (van der Kamp et al., 1996). Moreover, by slowly increasing the %MSO it's possible to determine the minimal energy necessary to elicit an MEP, referred to as the "resting motor threshold" (RMT). The RMT assessment is commonly used as a calibration procedure to determine optimal %MSO to use in a particular subject to promote effective cortical activation (Groppa et al., 2012).

The possibility of non-invasively probing the brain in a safe, tolerable way has clear applications in medicine. The observation of MEPs with TMS can be used to accurately identify the cortical location of motor areas when coupled with neuronavigation (Lefaucheur & Picht, 2016; Pitkanen et al., 2018), which can be used in planning neurosurgery in patients with lesions next to motor areas, allowing lesion removal while sparing motor function (Schramm et al., 2021). Similarly, TMS can also be applied for mapping language areas by delivering pulses to different cortical regions, while the subject performs an object-naming task. In this context, a language eloquent region is identified once the stimulation causes the subject to mispronounce a word or halt speech production (Lefaucheur & Picht, 2016; Picht et al., 2013).

1.2 Transcranial Magnetic Stimulation – Electromyography (TMS-EMG)

The use of RMT values and MEP amplitude to single TMS pulses were thought to provide quantitative information on the state of the stimulated motor cortex. However, these measures were found to be highly variable across and within individuals, as

several factors have been shown to influence them, including skull thickness, muscle strength, individual cortical motor representation, type of TMS coil used, among others (Burke et al., 1995; Rosler et al., 2002). The development of further stimulation protocols provided more reliable measures of motor cortex excitability, such as paired-pulse TMS. These protocols involve the application of a TMS pulse of subthreshold intensity to the motor cortex (conditioning stimulus), followed by a pulse of suprathreshold intensity (test stimulus) (Valls-Sole et al., 1992). It was observed that the MEP amplitude of the suprathreshold pulse is modulated as a function of the temporal distance between the conditioning and test stimuli. For interstimulus intervals below 5ms the MEP amplitude is reduced, a phenomenon called short intracortical inhibition (SICI), whereas interstimulus intervals above 5ms lead to MEP amplitude increase, called intracortical facilitation (ICF) (Kujirai et al., 1993; Ziemann et al., 1996). These phenomena are thought to test intracortical neuronal circuits, with the SICI representing inhibitory systems and the ICF excitatory systems (Ziemann et al., 2015).

Evidence of the physiological mechanisms of these measures was offered by pharmaco-TMS experiments. The administration of benzodiazepines, which are known positive allosteric modulators of GABA-A receptors, led to a significant increase in the SICI (i.e., further decrease in the MEP amplitude in the paired-pulse condition) (Di Lazzaro, Oliviero, et al., 2005; Di Lazzaro, Pilato, et al., 2005), although little effect was observed in the administration of GABA-B agonists (McDonnell et al., 2006) or glutamate antagonists (Liepert et al., 1997). This supports the notion that SICI reflects the activity of parvalbumine-positive GABA-A interneurons in inhibiting the pyramidal neuron. Likewise, the administration of glutamate receptor antagonists led to the suppression of the ICF, which is expected from a phenomenon resulting from the activation of excitatory interneurons (Liepert et al., 1997). Finally, long-interval cortical inhibition (LICI), which is the MEP amplitude reduction observed with interstimulus intervals above 100ms, was potentiated with the administration of GABA-B receptor agonists, but not GABA-A receptor agonists (McDonnell et al., 2006; Mohammadi et al., 2006), in agreement with the hypothesis that LICI reflects cortical inputs from subcortical structures, modulated by the metabotropic GABA-B receptor.

These discoveries hinted on the use of TMS paradigms for probing the cortical function in neuropsychiatric disorders as possible as biomarkers, and even diagnostic tools. Studies investigating subjects with obsessive compulsive disorder and schizophrenia

found lower SICI compared to healthy controls, in line with models of intracortical dysfunction and inhibitory deficits as hallmarks of these neuropsychiatric disorders (Radhu et al., 2013). Although these measures have only been used experimentally for these mental disorders, a clinical application has been established in the differential diagnosis of dementia. This involves the short-latency afferent inhibition (SAI) protocol, in which the MEP amplitude elicited by TMS decreases when it is preceded by 20ms by an electrical stimulus to the median or ulnar nerve at the wrist of the contralateral arm (Tokimura et al., 2000). Importantly, pharmacological studies demonstrated that the acetylcholine receptor antagonist scopolamine reduces SAI, suggesting that the protocol probes the state of central cholinergic neurotransmission (Di Lazzaro et al., 2000). The impairment of cholinergic transmission in Alzheimer's disease can then be detected by reduced SAI, whereas the intracortical dysfunction in frontotemporal dementia can be detected by abnormal SICI-ICF values. It has been found that the ratio SICI-ICF/SAI can accurately differentiate both clinical conditions even in the initial stages of the disease, helping to clarify the diagnosis and consequent prognosis of patients with dementia (Benussi et al., 2017; Benussi et al., 2020).

A clear limitation of these methods is that they require a motor response as an output. Firstly, it limits the scope to motor system investigations. Secondly, it provides only an indirect measure of cortical responsivity, as the state of spinal circuitry, peripheral nerves and muscles can influence the output, i.e., MEP amplitude. To obtain a direct response from cortical activation by TMS from any non-motor region would require a method other than TMS-EMG. This would be particularly valuable in investigating specific dysfunctions to (non-motor) cortical regions, as well as the neuromodulatory effects of focal cortical interventions (Tremblay et al., 2019).

1.3 Transcranial Magnetic Stimulation – Electroencephalography (TMS-EEG)

A considerable advance in cortical excitability probing with TMS came with the combination of electroencephalography (EEG). It was observed that the activation of cortical targets by TMS leads to neuronal responses measurable by scalp EEG, an output named "TMS evoked potentials" (TEP) (Ilmoniemi & Kicic, 2010; Ilmoniemi et al., 1997). As was the case with TMS-EMG, TMS-EEG has since been used in the investigation of cortical imbalances associated with neuropsychiatric disorders, as well as in the investigation of pharmacological effects of drugs acting on the central nervous system and neuromodulatory therapeutic interventions (Tremblay et al., 2019).

Analogous to pharmacological TMS-EMG experiments, TMS-EEG signatures have also been associated with specific changes in cortical functioning (Belardinelli et al., 2021; Cash et al., 2017; Premoli, Biondi, et al., 2017; Premoli et al., 2014). Measures of whole cortex responsivity also provide information of the global state of the central nervous system, with potential clinical applications for diagnosis and prognosis of disorders of consciousness (Casarotto et al., 2016).

Despite these advances, there is still considerable controversy regarding the interpretation of TMS-EEG response signals. Of particular importance, there is evidence that the observed EEG responses are not only caused by direct cortical activation by TMS, but also contain cortical responses to sensory input (Nikouline et al., 1999; Paus et al., 2001). This occurs because triggering the TMS device also generates sensory stimuli: the TMS coil activation causes a high pitch “click” sound, while the induced electric field aimed at stimulating the cortex also traverses superficial tissues, activating cranial nerves and muscles close to the TMS target. These auditory and somatosensory stimuli have been consistently found to elicit peripheral evoked potentials (PEP) in the TMS-EEG response signal (Ilmoniemi & Kicic, 2010). The superposition of these 2 responses, TEP and PEP, pose a considerable challenge for TMS-EEG experiments, as failure to take sensory inputs into account can lead to misinterpretation of the results. Likewise, given the possibility that different cortical states and modulatory interventions can also change the responses to sensory input, some of the results observed in TMS-EEG measurements might simply reflect a change in PEP, which can severely compromise the relevance of the method (Siebner et al., 2019).

The ideal solution for this issue would be to block all possible sensory inputs from the TMS activation. To tackle the auditory input, the use of masking noise through headphones or earbuds can be used to blur the perception of the TMS click sound, thus not resulting in an event potential (Massimini et al., 2005; Russo et al., 2022). There is some evidence that this method is effective in suppressing the auditory PEP (Gosseries et al., 2015; Russo et al., 2022; ter Braack et al., 2015), although others report that the method could not completely block the sound perception for a considerable proportion of subjects (Conde et al., 2019). Moreover, tackling the somatosensory input is a considerably more challenging endeavor, and until the

present date no successful attempt to block the somatosensory input has been described, frustrating the solution of blocking all TMS generated sensory inputs.

An alternative solution is to apply a control condition, a sham TMS which would recreate the same sensory inputs as the real TMS, but without the direct cortical activation caused by TMS. In this design, the matching response signals caused by sham and real TMS are attributed to PEPs, whereas components only observed in the real TMS are then the “true” TEPs, as has been attempted in several experiments (Conde et al., 2019; Du et al., 2017; Gordon et al., 2018; Herring et al., 2015; Rocchi et al., 2021). Unfortunately, this endeavor has proven to be considerably more challenging than first thought, with repeated failures in the sham design. Some studies have only used auditory control while neglecting the somatosensory input (Du et al., 2017; Harquel et al., 2016), others have used somatosensory stimuli outside the head and thus not properly matching the sensory input from sham and real TMS (Biabani et al., 2019; Herring et al., 2015), and even those that used somatosensory stimuli on the same region of TMS application still failed to elicit PEPs that properly matched those from real TMS conditions (Conde et al., 2019; Gordon et al., 2018; Rocchi et al., 2021). Until this matter is resolved it is not possible to attribute results from TMS-EEG measurements to the cortical response to direct activation by TMS or PEPs, or both (Conde et al., 2019; Siebner et al., 2019).

1.4 Aims/Objectives

The objective of this project is to design and test an optimized sham procedure for TMS-EEG experiments that would overcome the limitations of previously proposed sham procedures. This optimized sham procedure for TMS-EEG needs to satisfy 2 conditions: 1) It should reliably recreate the same sensory inputs as the real TMS pulse, and 2) it should evoke the same electrophysiological responses to sensory inputs from the real TMS. By having precisely matched PEPs, the response signal from the sham could then be subtracted from the EEG response to real TMS, thus revealing the specific electrophysiological signature to direct cortical activation by TMS, the true TEPs.

The objective of the project is also to apply this method to disentangle modulatory effects of an intervention on TEPs from effects on PEPs. For this purpose, the aim is to reproduce the findings of a previous TMS-EEG study, specifically a report that

investigated the neuromodulatory effects of Diazepam on TMS-EEG responses (Premoli et al., 2014), and ascertain to what extent these neuromodulatory effects are attributed to changes in TEPs or PEPs.

Specific Aims:

1) To design an optimized sham method for TMS-EEG that recreates the same sensory inputs and evokes the same electrophysiological responses as real TMS.

2) To apply the optimized sham in a TMS-EEG experiment to identify and remove all responses attributed to PEPs, allowing the description of the true TEPs.

3) To apply the optimized sham in a pharmacological TMS-EEG experiment, aiming at isolating the modulatory effects of the drug on PEPs from the effects on the responses to direct cortical activation by TMS (TEPs).

2. Results

To attain the objectives of this project, three experiments were conducted and described in the following publications.

2.1 ***Recording brain responses to TMS of primary motor cortex by EEG –utility of an optimized sham procedure*** (by Pedro C. Gordon, D. Blair Jovellar, YuFei Song, Christoph Zrenner, Paolo Belardinelli, Hartwig Roman Siebner and Ulf Ziemann; published in Neuroimage. 2021 Dec 15:245:118708. doi: 10.1016/j.neuroimage.2021.118708.)

NeuroImage 245 (2021) 118708

Contents lists available at ScienceDirect

NeuroImage

journal homepage: www.elsevier.com/locate/neuroimage

Recording brain responses to TMS of primary motor cortex by EEG – utility of an optimized sham procedure

Pedro C. Gordon[a,b], D. Blair Jovellar[a,b], YuFei Song[a,b], Christoph Zrenner[a,b], Paolo Belardinelli[a,b,c], Hartwig Roman Siebner[d,e,f], Ulf Ziemann[a,b,*]

[a] Department of Neurology & Stroke, University of Tübingen, Hoppe-Seyler-Straße 3, Tübingen 72076, Germany
[b] Hertie Institute for Clinical Brain Research, University of Tübingen, Germany
[c] CIMeC, Center for Mind/Brain Sciences, University of Trento, Italy
[d] Danish Research Centre for Magnetic Resonance, Centre for Functional and Diagnostic Imaging and Research, Copenhagen University Hospital – Amager and Hvidovre, Copenhagen, Denmark
[e] Department of Clinical Medicine, Faculty of Health and Medical Sciences, University of Copenhagen, Denmark
[f] Department of Neurology, Copenhagen University Hospital – Bispebjerg and Fredriksberg, Copenhagen, Denmark

ARTICLE INFO

Keywords:
Transcranial magnetic stimulation
Electroencephalography
TMS-EEG
Sham stimulation
Peripherally evoked potentials

ABSTRACT

Introduction: Electroencephalography (EEG) is increasingly used to investigate brain responses to transcranial magnetic stimulation (TMS). A relevant issue is that TMS is associated with considerable auditory and somatosensory stimulation, causing peripherally evoked potentials (PEPs) in the EEG, which contaminate the direct cortical responses to TMS (TEPs). All previous attempts to control for PEPs suffer from significant limitations.

Objective/Hypothesis: To design an optimized sham procedure to control all sensory input generated by subthreshold real TMS targeting the hand area of the primary motor cortex (M1), enabling reliable separation of TEPs from PEPs.

Methods: In 23 healthy (16 female) subjects, we recorded EEG activity evoked by an optimized sham TMS condition which masks and matches auditory and somatosensory co-stimulation during the real TMS condition: auditory control was achieved by noise masking and by using a second TMS coil that was placed on top of the real TMS coil and produced a calibrated sound pressure level. Somatosensory control was obtained by electric stimulation (ES) of the scalp with intensities sufficient to saturate somatosensory input. ES was applied in both the sham and real TMS conditions. Perception of auditory and somatosensory inputs in the sham and real TMS conditions were compared by psychophysical testing. Transcranially evoked EEG signal changes were identified by subtraction of EEG activity in the sham condition from EEG activity in the real TMS condition.

Results: Perception of auditory and somatosensory inputs in the sham vs. real TMS conditions was comparable. Both sham and real TMS evoked a series of similar EEG signal deflections and induced broadband power increase in oscillatory activity. Notably, the present procedure revealed EEG potentials and a transient increase in beta band power at the site of stimulation that were only present in the real TMS condition.

Discussion: The results validate the effectiveness of our optimized sham approach. Despite the presence of typical responses attributable to sensory input, the procedure provided evidence for direct cortical activation by subthreshold TMS of M1. The findings are relevant for future TMS-EEG experiments that aim at measuring regional brain target engagement controlled by an optimized sham procedure.

1. Introduction

The combined use of electroencephalography (EEG) and transcranial magnetic stimulation (TMS) allows the probing of immediate cortical responses to brain stimulation in a safe and non-invasive approach, expanding the available tools for understanding human neurophysiology. TMS-EEG can potentially be employed in the investigation of local neuronal excitability of any cortical region targeted by TMS, and alterations in cortical responses associated with drugs acting on the central nervous system, neuromodulatory interventions or neuropsychiatric disorders (Ilmoniemi et al., 1997; Esser et al., 2006; Rogasch and Fitzgerald, 2013; Tremblay et al., 2019). Despite its potentials, the technique

* Corresponding author at: Department of Neurology & Stroke, University of Tübingen, Hoppe-Seyler-Straße 3, Tübingen 72076, Germany.
E-mail address: ulf.ziemann@uni-tuebingen.de (U. Ziemann).

https://doi.org/10.1016/j.neuroimage.2021.118708.
Received 23 June 2021; Received in revised form 31 October 2021; Accepted 2 November 2021
Available online 4 November 2021.

is not free of caveats. One significant issue is that the EEG responses to TMS are not limited to transcranial cortical activation (the so called TMS evoked potentials – TEPs), but in addition reflect activation by multisensory inputs also caused by TMS. These peripherally evoked potentials (PEPs) are cortical responses that follow the sensory (auditory and somatosensory) input, and present as EEG deflections of considerable amplitude starting at around 100 ms (Ilmoniemi and Kicic, 2010). Consequently, PEPs are superimposed to TEPs, significantly hindering TMS-EEG data interpretation (Ilmoniemi and Kicic, 2010). Several attempts have been proposed to overcome this limitation. However, most have failed to consistently control for sensory inputs from real TMS. Also, attempts to reproduce the PEPs by sham procedures were limited by failure to generate sensory inputs comparable to those produced by real TMS (Belardinelli et al., 2019; Conde et al., 2019; Siebner et al., 2019).

The contamination of TMS-EEG data with PEPs has been identified since the implementation of the technique, with auditory input found responsible for significant evoked potentials in TMS-EEG experiments (Nikouline et al., 1999; Paus et al., 2001). TMS-related auditory input involves a high-pitched "click" sound generated during coil discharge—a result of the brief coil vibration as the electric current runs through its windings—which is clearly audible by subjects (Nikouline et al., 1999), and sound pressure level can significantly exceed 100 dB (Counter and Borg, 1992; Koponen et al., 2020). It has been suggested that the auditory PEP accounts for most of the undesired indirect cortical activation in TMS-EEG experiments, stressing the importance of a proper control method to allow experiments to retrieve the true TEPs in the EEG signal (Paus et al., 2001; Ilmoniemi and Kicic, 2010; Rocchi et al., 2021). The use of earplugs to muffle significantly attenuates the sound pressure level in the ear canal (Counter and Borg, 1992), but was found to be largely insufficient in suppressing the auditory PEP (Nikouline et al., 1999; ter Braack et al., 2015). Alternatively, the use of masking noise has been suggested, specifically one that contains the same frequency spectrum distribution as the TMS click (Massimini et al., 2005), a procedure which was found very effective in suppressing the auditory PEP (Gosseries et al., 2015; ter Braack et al., 2015). Another proposed approach is the use of a sham condition in which an equivalent click sound is generated by a sham procedure, usually a sham coil, or a real coil placed away from the cortex. Studies that used this procedure aimed to compare the signals from the sham and real TMS conditions, as concurrent responses in both signals would indicate the PEP, and the remaining response in the real TMS condition can then be attributed to the true direct cortical activation by TMS (Casali et al., 2010; Herring et al., 2015; Du et al., 2017; Gordon et al., 2018; Conde et al., 2019).

In addition to the auditory input, somatosensory inputs from TMS were also found to contribute to the PEP in TMS-EEG experiments. The electric field induced by the time-varying magnetic field of TMS extends inevitably through extracranial tissue and activates trigeminal axons and scalp muscles. The trigeminal somatosensory input and reafferents from the muscle twitches result in somatosensory responses in the EEG signal (Herring et al., 2015; Conde et al., 2019). Proposed solutions involve the use of a sham condition that would reproduce the somatosensory input generated by TMS, analogous to the principle behind the auditory sham control. Previous studies proposed electric stimulation with electrodes placed on the same scalp region as the TMS target (Rossi et al., 2007; Mennemeier et al., 2009), which would deliver a similar scalp sensation, theoretically generating PEPs equivalent to those in the real TMS condition.

Despite these proposed solutions, only few studies attempted to employ these control methods. It is unclear to what extent the results obtained by these uncontrolled TMS-EEG studies represent EEG responses from direct cortical activation, or rather non-specific PEPs. Moreover, critical reports have identified that even those studies that attempted to employ these methods have failed to design a realistic sham control condition that properly matched the multisensory inputs of real TMS (Belardinelli et al., 2019; Siebner et al., 2019). So far, no consensus has been reached on how to create an ideal sham procedure in TMS-EEG studies, resulting in a critical view on the validity and interpretability of current TMS-EEG studies.

Here, we aim to design and test an optimized sham procedure for TMS-EEG experiments that will overcome the limitations presented by the previously proposed sham procedures. Specifically, the optimized sham would deliver the same multisensory stimuli as real TMS, meaning that their perception is identical in psychophysical testing, and PEPs are equivalent between sham and real TMS. By meeting these conditions, a comparison between the signals from the sham and the real TMS conditions should imply that any differences are largely to be attributed to direct cortical activation by TMS, thus revealing TEPs in a specific manner. The objectives of the present study were: (1) To design such optimized sham TMS condition; (2) to test the perception of the sensory inputs from the optimized sham TMS and compare them with the real TMS condition; and (3) to compare the EEG responses in the optimized sham vs. real TMS conditions.

2. Methods

2.1. Subjects and design

The experiment involved right-handed healthy volunteers that participated in a single session. Inclusion criteria were age between 18 and 50 years and competency to provide informed consent to participate in the study. Exclusion criteria were presence or history of psychiatric or neurological diseases, intake of drugs acting on central nervous system, presence or history of alcohol or illicit drugs abuse, and current pregnancy. Subjects with resting motor threshold (RMT) > 60% of the maximum stimulator output (MSO) were also excluded, as higher intensities would involve higher auditory input and compromise the sham procedure (see section *Optimized sham TMS design*).

A total of 23 (16 female) subjects was included in this study, with a mean age of 25 years (SD ± 4.4). All subjects provided written informed consent prior to participation. The study was approved by the ethics committee of the medical faculty of the University of Tübingen (456/2019BO2) and conformed to the latest version of the Declaration of Helsinki.

2.2. Experimental set-up

The experiment was conducted in a quiet room with the subjects sitting comfortably on a reclined chair, instructed to keep their eyes opened during the measurements. Prior to the TMS-EEG session, all subjects underwent magnetic resonance imaging (MRI) using a 3T Siemens PRISMA scanner with T1-weighted anatomical sequences. MRI was required for proper positioning of the TMS coil with respect to the individual's brain anatomy, using a neuronavigation system (Localite GmbH, Sankt Augustin, Germany), and also for the EEG forward model and source reconstruction, explained below.

Scalp EEG was recorded from a TMS compatible 64-channel Ag/AgCl sintered ring electrode cap (EasyCap GmbH, Germany). Additionally, surface EMG was recorded through bipolar EMG adhesive hydrogel electrodes (Kendall, Covidien) over the abductor pollicis brevis (APB) and first dorsal interosseus (FDI) muscles of the right hand in a bipolar belly-tendon montage (5 kHz sampling rate, 0.16 Hz–1.25 kHz bandpass filter). EMG was used for determination of RMT with standard methods (Groppa et al., 2012), using the individual MRI and neuronavigation to guide the coil position and maintain its orientation perpendicular to the precentral sulcus, and then selecting the cortical target that elicited highest motor evoked potentials (MEP) amplitudes as the *hot-spot*. EMG was also recorded for detection of possible MEPs during the TMS-EEG measurements. TMS was delivered using a figure-of-eight coil (external diameter of each wing 90 mm) connected to a Magstim 200^2 magnetic stimulator (Magstim Company Ltd., UK) with a monophasic current waveform. Two identical stimulators and coils were used in this

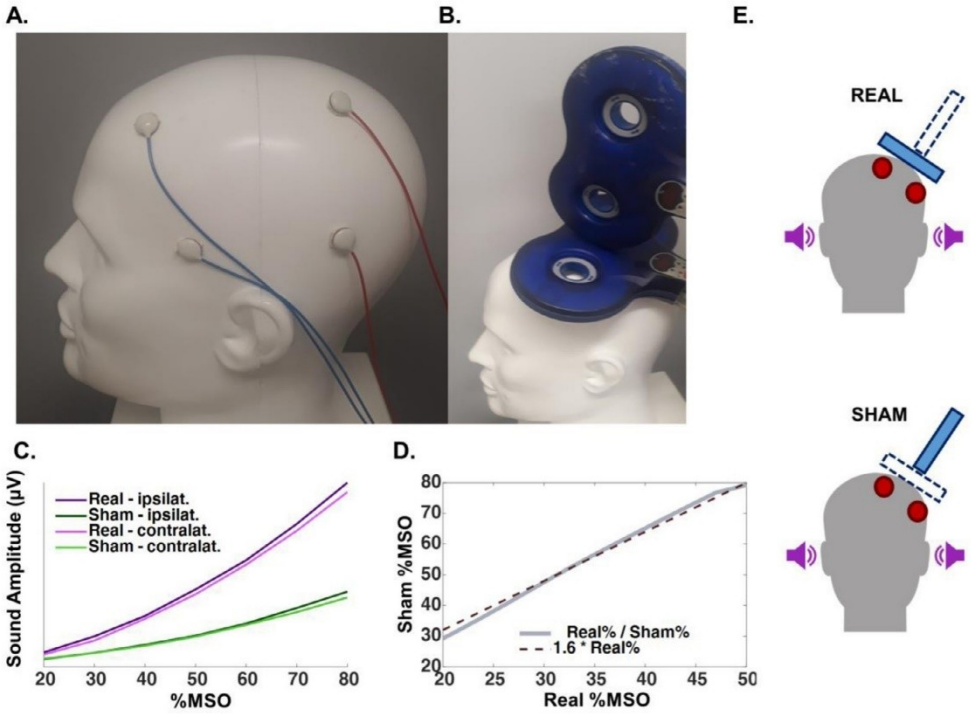

Fig. 1. **A.** Head model illustrating the positioning of the electrodes for electric stimulation, 2 electrodes of the same polarity at FFT9h and AFF5h (blue cables), and 2 electrodes of the opposite polarity at CPP3h and TPP7h (red cables). Polarities switched after each pulse. **B.** Illustration of the positioning of the real TMS coil (in contact with the head) and sham TMS coil (above the real coil and tilted by 90 °). **C.** Sound amplitude of the coil click summed over 50 ms, measured by microphones in the ear canals ipsilateral and contralateral to real and sham TMS. **D.** Sound amplitude relation between the real and the sham TMS conditions according to TMS intensity (%MSO), which follows approximately a linear function, with real%MSO = 1.6 x sham%MSO. **E.** Depiction of the real and sham TMS set-up, both showing delivery of masking noise (purple sound-icons) and electric stimulation (red electrodes), but differ with respect of the TMS coil activated, as real TMS involved discharging the coil tangentially on the scalp, but sham TMS the coil on top of the real TMS coil and tilted 90 ° with respect to the scalp (blue rectangles) (For interpretation of the references to color in this figure legend, the reader is referred to the web version of this article).

experiment, one for the real TMS condition and the other for the sham TMS condition. Finally, electric stimulation (ES) of the scalp was delivered by a Digitimer DS7A (Digitimer Ltd. UK).

TMS targeted the hand area of left primary motor cortex (M1), with coil orientation perpendicular to the central sulcus, as informed by the neuronavigation system. The intensity used for the real TMS condition was 90% RMT. This subthreshold intensity was chosen to avoid somatosensory input via re-afferent feedback from MEP-related muscle twitches (Paus et al., 2001; Fecchio et al., 2017), while this intensity is sufficient to produce TEPs (Komssi and Kahkonen, 2006; Fecchio et al., 2017)

2.3. Optimized sham TMS design

As described in the Introduction, the two major sources of sensory input elicited by TMS are auditory and somatosensory. To control for the auditory input, we applied masking noise of the same spectral distribution as the coil click during the measurements (Massimini et al., 2005). Despite the reported success of this procedure in suppressing auditory PEPs, there is evidence that the procedure is not sufficient to completely cancel the auditory input (Conde et al., 2019). We share this experience in our laboratory, as some subjects can still hear the TMS click despite application of masking noise at maximum tolerable intensity. To account for this potential limitation, we added another control method in the form of a sham TMS procedure, involving an identical TMS stimulator and coil as for the real TMS condition, but having the coil tilted at a 90-degree angle with respect to the scalp and positioned on top of the real TMS coil, so that the sham coil would not induce current in the cortex (Fig. 1B). However, the difference in the distance from the source of the auditory stimulus to the ear will lead to differences in sound pressure level at the ear, if both coils are discharged with identical stimulus intensity. To account for this, we performed measurements using a head model and 3 mm microphones (Zero-Height SiSonic Microphone, Knowles Electronics) attached to the regions corresponding to the ear canals on both sides, ipsilateral and contralateral to TMS. Seven TMS intensities for both sham and real TMS conditions were tested, applying 25 pulses each at intensities from 20 to 80% of the MSO in 10% steps. By analyzing the absolute amplitude of the signal in the first 50 ms after the pulse (Fig. 1C), we observed an approximately linear relation between the sound amplitude generated by sham TMS and real TMS at different intensity (within the range of intensities between 20 and 50% MSO), i.e., the average sound pressure level from the sensors ipsilateral and contralateral to stimulation caused by real TMS could be matched by sham TMS when increasing sham TMS intensity by a factor of 1.6 (Fig. 1D).

To control for the somatosensory input, we aimed to reproduce the somatic input caused by real TMS by delivering ES using an electric stimulator and electrodes placed over the scalp. During a pilot experiment we explored several different stimulation intensities and electrode montages. This was necessary as the scalp sensations produced by TMS and ES were easily distinguishable: subjects reported real TMS as causing a blunt sensation in a broad area of the scalp and leading to a slight contraction of the temporal muscle, whereas the ES sensation was described as sharp and focal. We observed that shorter ES pulse widths were re-

ported as less sharp and more similar to TMS, leading us to set it to 50 μs, the lowest pulse width allowed by the stimulator. To generate a broad region covered by stimulation, and a cranial muscle twitch, we positioned 2 pairs of electrodes of 1 cm in diameter between the EEG electrodes over a broad area of the left fronto-temporal region: 2 electrodes of the same polarity at the positions corresponding to FFT9h and AFF5h, according to the international 10–5 system for EEG (Seeck et al., 2017), and 2 electrodes of opposite polarity at CPP3h and TPP7h (Fig. 1A).

Despite these efforts, we realized that individuals could still distinguish between the sham and real TMS sensory input. This could represent a significant limitation, as this discernibility might indicate different levels of sensory input between conditions, potentially eliciting PEPs with different characteristics. However, even an indistinguishable sham condition does not guarantee that the resulting PEPs from the two conditions are identical, which would have to be carefully tested to confirm the validity of the optimized sham condition.

Our strategy to overcome these problems was to use high-intensity ES applied to *both* sham and real TMS conditions. The rationale is that high enough ES intensities will saturate the somatosensory input. If successful, any further somatosensory input would not result in a detectable increase in the PEP amplitude, including the somatosensory input from real TMS.

By testing different ES intensities, set as multiples of the individual's sensory perception threshold (SPT), we anticipated PEP saturation to occur with intensities around 300% of the SPT, as suggested by previous reports (Torquati et al., 2002; Lin et al., 2003), and also by our own pilot measurements. The mean SPT of the final sample was 8.7 mA (SD $\pm$ 2.5 mA).

In summary, the sham TMS condition involved (Fig. 1E, lower part): (1) masking noise, (2) sham coil click (sham TMS coil on top of the real TMS coil, tilted by 90 °, intensity 1.6 × 90%RMT) and (3) concomitant application of ES (intensity as a function of the individual's SPT). The real TMS condition involved (Fig. 1E, upper part): (1) masking noise, (2) real coil stimulation (real TMS coil placed tangentially on the scalp, with peak induced electrical field targeting M1, intensity 90%RMT) and (3) concomitant application of ES (intensity as a function of the individual's SPT, identical to ES in the sham condition). Standard ES intensity was 300%SPT, but for a few subjects (n = 5) who could clearly distinguish between real and sham TMS conditions, the intensity was increased to 400%SPT.

2.4. Testing the optimized sham TMS condition

The first measurement was aimed to confirm the PEP saturation with increasing ES intensities. This involved the application of 5 stimulation blocks of 100 pulses each, applied with an interstimulus interval of 2 s ($\pm$1 s jitter; 1–3 s range), each containing the masking noise, auditory sham, and ES; but the ES intensity was different in each block: 0, 100, 200, 300 and 400%SPT. These blocks were delivered in pseudorandomized order balanced across subjects.

We also evaluated the perception of the real vs. sham TMS conditions with 2 different procedures. In the first procedure subjects received 4 blocks of 4 stimuli each, 2 blocks containing only the sham TMS condition and 2 blocks containing only the real TMS condition. The blocks were delivered in random order. Subjects were instructed to fill out a set of visual analog scales (VAS, values 0 to 10) after each block, referring to the perceived sensation during each block with regard to the following perception items: (1) intensity of auditory sensation; (2) intensity of scalp sensation; (3) area size of scalp sensation; (4) intensity of pain or discomfort. The second procedure consisted of a two-alternative forced choice (2AFC) test: Subjects were instructed as to the sensations caused by each condition, using stimuli probes as examples. Following that, subjects were given a panel with 2 buttons, one labeled "SHAM" and the other "REAL", and then 50 pulses were applied (25 of each condition in random order), and after each pulse subjects were forced to indicate whether they thought this was a sham or real condition by pressing the corresponding button.

The concluding TMS-EEG measurements consisted of the application of 320 pulses, 160 real TMS and 160 sham TMS, randomly interleaved and applied with an interstimulus interval of 3 s ($\pm$1 s jitter; 2–4 s range).

2.5. EEG data processing

Offline data analysis was performed using the Fieldtrip open source toolbox (Oostenveld et al., 2011). EEG data from TMS responses were segmented into epochs aligned to the TMS pulse (−1000 to 1500 ms) and baseline corrected (−1000 to −50 ms). Data containing artifacts from the TMS and ES pulses, and the associated muscle response were removed and cubic interpolated (−5 to +20 ms window around the TMS pulse). Trials were inspected visually, and epochs and channels with excessive noise were excluded, as were trials containing MEPs in the EMG of the right FDI or APB. The average percentage of trials excluded per subject was 17% (SD $\pm$ 12%; range: 4–26%), being on average 10.2% due to excessive noise (SD $\pm$ 6.5%; range: 4.6–23.8%) and 6.8% due to the presence of MEPs (SD $\pm$ 3.5%; range: 1.1–12.0%). The number of channels excluded due to excessive noise was on average 6 (SD $\pm$ 2.6; range: 1–12). Further artifacts were removed with a 2-step ICA procedure. The first step aimed at removing remnant high amplitude TMS and ES artifacts, and the second step removing artifacts related to muscle activity and eye blink (Rogasch et al., 2014). Excluded channels were spline-interpolated and the signal was then re-referenced to the average of all electrodes after the ICA procedure. The TEP signal was finally filtered with a 45 Hz low-pass filter. Furthermore, individual results were inspected for outliers, averaging the amplitude of the signal in 5 different time windows of interest (TOI: 25–40 ms, 40–60 ms, 60–90 ms, 90–130 ms and 130–250 ms), and indicating individual data deviating >3 standard deviations from the mean as outliers.

For the processing of TMS-induced oscillations, time–frequency representations (TFRs) of TMS-related changes in oscillatory power were calculated. First, the evoked TMS response (average signal time-locked to TMS stimulus) was subtracted from the signal, and the result was then decomposed into its TFRs (Premoli et al., 2017). TFR was then calculated using a Morlet wavelet decomposition on single trials, with frequency-dependent width (wavelet width of 2.6 cycles at 4 Hz, adding 0.2 cycle for each 1 Hz), followed by z-transforming the TFR of each trial with respect to the mean and standard deviation of the full trial, and baseline correction (−500 to −100 ms) (Premoli et al., 2017). By excluding the time-locked evoked response, we remove information regarding amplitude shifts of the evoked potential, which is an information already contained in the TEP analysis, thus focusing specifically in the changes in cortical oscillatory activity due to the stimuli.

Finally, the EEG signals from statistically significant results were projected into the source space. Individual cortical surfaces and dipole arrays were obtained from the individual's MRI, segmented and meshed using the Fieldtrip toolbox (Oostenveld et al., 2011), with a forward model for EEG using a customized pipeline, taking into account the positions of the EEG electrodes related to individual head anatomy (Stenroos and Sarvas, 2012; Stenroos and Nummenmaa, 2016). Source reconstruction was then obtained on the whole cortical surface using the L2-minimum-norm estimate (Hamalainen and Ilmoniemi, 1994). For the TEPs, the final result was obtained by z-transforming the signal of each trial with respect to the mean and standard deviation of the baseline (−500 to −100 ms). For induced oscillations, the EEG signal was first projected to the source space, followed by the TFR calculation, as described above. Finally, for the purpose of plotting the final result, data attributed to each individual dipole was pooled and warped into a common MNI space for a group average across all subjects.

2.6. Statistical analysis

All statistical analyses were performed on the MATLAB platform (R2018b, The Mathworks, USA). Data from the visual analog scales in

the sham and real TMS conditions were analyzed using paired comparisons, with significance threshold of $p < 0.0125$ to adjust for multiple comparisons. Given the marked skewness of some distributions, we used two-sided Wilcoxon rank sum tests for these analyses. Responses from the 2AFC test were pooled individually in order to yield each subjects accuracy (total correct answers divided by total number of trials). The individual accuracy was subtracted by the expected accuracy for random answers (0.5). The absolute value of this transformation corresponds to the distance of the observed accuracy and the expected accuracy for random answers. In order to identify the likelihood that the observed distance deviated significantly from random answers (i.e., in this case the subject was able to distinguish between sham and real TMS conditions), the distance was compared with the distribution of the medians derived from 100,000 simulations of 23 subjects responding to the test randomly.

For the PEPs elicited by different ES intensities, the signal was first analyzed by its global mean field power (GMFP) within time windows of interest (TOI) 60–90 ms, 90–130 ms and 130–250 ms after the ES pulse, based on previous reports on TMS-EEG and PEP signals (Lioumis et al., 2009; Rocchi et al., 2021). GMFP in the 5 stimulation conditions (ES intensities, 0–400%SPT, in 100% steps) were compared using one-way ANOVA. The EEG signals from the 300%SPT and 400%SPT conditions were compared by cluster-based dependent-samples t-tests from the Fieldtrip open source toolbox, using as input the averaged signal across trials for each subject, and setting the statistical threshold to $p < 0.05$ (Oostenveld et al., 2011).

Analysis of the TEPs from the real vs. sham TMS conditions was performed with identical cluster-based t-statistics. Analysis of the induced oscillations followed the same procedure, but was divided into different frequency bands of interest: theta (4–7 Hz), alpha (8–12 Hz), low beta (13–20 Hz), high beta (21–29 Hz), and gamma (30–40 Hz). Due to the increased number of tests, the threshold of statistical significance was adjusted to $p < 0.01$.

3. Results

3.1. Testing the optimized sham TMS condition – peripherally evoked potentials

We first tested the optimized sham TMS by delivering ES of increasing intensities, while concomitantly applying masking noise and auditory sham stimulation (Fig. 1E). We observed that despite the masking noise, auditory sham stimulation alone (ES set to 0%SPT, Audit.only) evoked an EEG response in central midline electrodes, starting at around 130 ms and peaking at 200 ms, albeit of small amplitude (Fig. 2A–C).

The GMFP amplitude increased with increasing ES intensity and reached a plateau with intensities ≥ 300%SPT (Fig. 2A). We tested this by comparing the GMFP across conditions in 3 different TOIs (Fig. 2D). 300%SPT and 400%SPT conditions were not different for the TOIs 90–130 ms and 130–250 ms (ANOVA $p < 0.001$; *post hoc* Audit.only = 100%SPT < 300%SPT = 400%SPT). For the TOI 60–90 ms, although there was no statistically significant difference between 300%SPT and 400%SPT, the results were not equivalent (ANOVA $p = 0.002$; *post hoc* Audit.only = 100%SPT = 200%SPT < 400%SPT). We further tested possible differences between the PEPs from the 300%SPT and 400%SPT conditions by comparing the respective EEG responses using a cluster-based *t*-test. The test revealed 2 significant clusters between 70 and 100 ms, with a higher signal amplitude in the 400%SPT condition (Fig. 2E–F). By subtracting the results from the source reconstruction of both signals in that time window, we observed that the difference was most pronounced over bilateral sensorimotor cortices (Fig. 2G). No significant differences were found beyond 100 ms.

3.2. Testing the optimized sham TMS condition – sensory perception

We compared the sensory perception from the sham and real TMS conditions using the results from the VAS. The reported sensory perceptions were not significantly different between conditions for any of the tested sensorial qualities (Fig. 3A, two-sided Wilcoxon rank sum tests: auditory intensity, $p = 0.596$; scalp intensity, $p = 0.938$; scalp area, $p = 0.484$; pain/discomfort, $p = 0.999$).

The results from the 2AFC test are shown in Fig. 3B, displayed as the distance of the individuals' accuracy to 50% (i.e., distance to expected accuracy of random responses). In our sample, the subjects' median "distance from 50% accuracy" was 0.1. By running simulations of 23 subjects answering randomly to this test, we obtained that the mean of the simulated median "distance from 50% accuracy" is 0.03 (SD ± 0.005). This places the observed median distance outside 5 SD of the simulated distribution, indicating a probability $p < 0.0001$ that our subjects as a whole sample responded randomly to the 2AFC test. This can be exemplified by the presence of 3 clear outliers (Fig. 3B-C), who were most definitely capable of making the distinction between conditions ($p<0.00001$ that any individual would attain "distance from 50% accuracy" > 0.4 by answering randomly). Note that one outlier actually had an accuracy close to zero (Fig. 3C). It is most likely that this individual could indeed make the distinction, but mistook sham TMS for real TMS, and vice versa. Since the issue is discernibility between conditions, this reinforces using the "distance from 50% accuracy" in this study, rather than accuracy *per se*.

Even after exclusion of the 3 outliers, the median "distance from 50% accuracy" was still > 5 SD away from the expected median (now simulated with $n = 20$ subjects), suggesting that at least some individuals were still somewhat capable of making a distinction between the sham and real TMS conditions. Based on the 2AFC test results we divided the sample into two groups: subjects with a small distance from 50% accuracy were considered as being "unaware" of the condition, and those with larger distance as being "aware". This procedure was performed by selecting a threshold, estimated by progressively excluding subjects with the largest distance from 50% accuracy from the statistical analysis, and correspondingly readjusting the simulation's sample size, until we obtained a median < 2 SD away from the expected median for random answers. This was reached with a threshold distance from 50% accuracy of 0.12. A total of 13 subjects (56%) were classified as "unaware" and 10 subjects (44%) as "aware".

We investigated what could have caused individuals to be able to distinguish between the sham and real TMS conditions. We first considered that the use of high TMS intensities (subjects with high RMT) or lower ES intensities (subjects with low SPT) could have been prone to distinguishable sensory inputs. However, there was no evidence for differences in TMS or ES intensities between the "aware" and "unaware" subjects (Fig. 3D, two-sided Wilcoxon rank sum test: TMS $p = 0.900$; ES $p = 0.729$). Moreover, subjects who were particularly accurate in identifying the conditions ("highly aware", corresponding to the 3 outliers. Fig. 3B, C.) did not appear to have skewed the distributions in any direction. We also investigated whether the perception of the different items of sensory input as quantified on the VAS could have explained the distinction. Likewise, there was no significant difference in the reported sensory perception regarding auditory intensity ($p = 0.642$), somatic scalp intensity ($p = 0.696$) or pain/discomfort ($p = 0.394$). Only a non-significant trend was observed towards reporting larger scalp area perception in the real TMS compared to sham condition in subjects who were "aware" ($p = 0.040$, significance threshold $p < 0.0125$; Fig. 3E). Again, the subjects who were "highly aware" of the difference did not appear to have affected these distributions.

3.3. Comparing sham and real – TMS evoked potentials

On inspection of the results of all individual subjects, we identified one subject as an outlier (amplitude of the signal in TOI 25–40 ms > 3 SD, TOI 130–250 ms > 3 SD, and TOI 90–130 ms > 4 SD, see Supplementary Results). This subject was therefore excluded from the ensuing analyses. No other subject presented deviations > 3 SD in any TOI. We then compared the evoked EEG responses in the sham and real

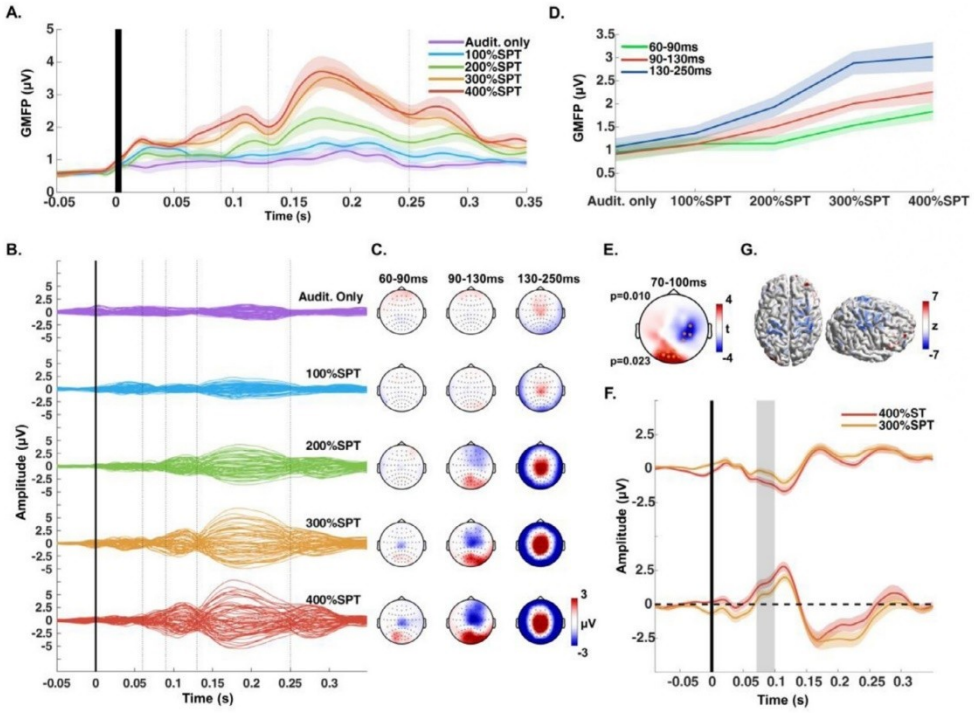

Fig. 2. **A.** Global mean field power (GMFP), averaged across all subjects, from the EEG responses to the sham condition with different electric stimulation intensities, set as multiples of the individual's sensory perception threshold (SPT). Dotted lines indicate the boundaries of the time windows of interest (TOIs). Audit.only indicates that no electric stimulation was applied. Please note that the filtering shifted the onset of EEG responses leftward. **B.** Butterfly plots of the averaged EEG response across all subjects, divided by increasing intensity of the electric stimulation (average reference, each line corresponding to one EEG channel) **C.** Scalp distribution of the signal observed in B, divided in 3 TOIs. **D.** Increase of the averaged GMFP within each TOI with increasing intensity of the electric stimulation. **E.** Results of the cluster-based *t*-test comparing the conditions applying electric stimulation intensity at 300% SPT vs. 400%SPT, showing two significant clusters (electrodes within the clusters marked by orange dots, respective *p*-values on the left) between 70 and 100 ms after the stimulus. **F.** EEG signal over time, averaged across the electrodes from the negative cluster (top plot) and positive cluster (bottom plot), from the 300%SPT and 400%SPT conditions. The shaded gray areas correspond to the time windows where the significant clusters were found **G.** Display of the difference of the EEG signal (400%SPT minus 300%SPT) within 70–100 ms, projected to the source and normalized with respect to the baseline signal (*z*-value) (For interpretation of the references to color in this figure legend, the reader is referred to the web version of this article).

TMS conditions (Fig. 4A, B). This comparison revealed significant differences, shown as a series of clusters of channels in TOIs 25–50 ms, 40–50 ms, 70–90 ms, 100–150 ms and 480–520 ms (Fig. 4C-D). More specifically, the real TMS condition caused an early positive deflection around 30 ms (P30) after stimulation in central electrodes close to the site of real TMS over left M1. This was followed by a dipole, consisting of a negative deflection around 45 ms in frontal electrodes in the midline and non-stimulated hemisphere (N45) and a positive deflection in parietal electrodes of the stimulated hemisphere (P45). This turned into a dipole of reverse polarity at around 70 ms (P70 over frontal electrodes in the non-stimulated hemisphere, N70 over parieto-occipital electrodes in the stimulated hemisphere). Moreover, while both real and sham conditions presented the deflection typically attributed to PEP, involving a frontocentral negative deflection at 100 ms (N100), the difference (real – sham TMS) suggests that real TMS caused a positive deflection peaking at around 125 ms, centered at the stimulated region of left M1 (P120). Finally, the real TMS condition evoked a long-latency positivity that peaked at central electrodes around 500 ms after the pulse (P500). Similar results were also found when only investigating subjects that were "unaware" of the difference between sham and real TMS conditions (Supplementary Results), providing evidence that the capability of distinguishing between the sham vs. real TMS conditions played no role in the TEP findings. The projection of the EEG signals to the source, followed by the subtraction of the sham from the real TMS condition suggested that P30 involves a broad response centered on the sensorimotor cortex ipsilateral to the stimulation, the N45 / P45 responses in bilateral prefrontal cortex / centered on the ipsilateral somatosensory cortex, the P70 / N70 responses in the bilateral prefrontal cortex / ipsilateral parietal cortex, and the P120 and P500 responses in the stimulated sensorimotor cortex (Fig. 4E).

3.4. Comparing sham and real – transient TMS-induced increase in beta band power

Both the sham and real TMS conditions led to considerable changes in the ongoing oscillations, with increased power in all of the investigated frequency bands after stimulation (Fig. 5A). Statistical comparison of the TFRs revealed significant differences (real TMS > sham TMS) in the low (13–20 Hz) and high beta bands (21–29 Hz) in time windows between 50 and 140–160 ms (Fig. 5B, C). These differences were expressed in the stimulated sensorimotor cortex and frontal cortex mainly ipsilateral to stimulation (Fig. 5B–D).

Spectral power changes were not different between the TFRs of sham and real TMS conditions in any other of the tested frequency bands (Fig. 5A and C).

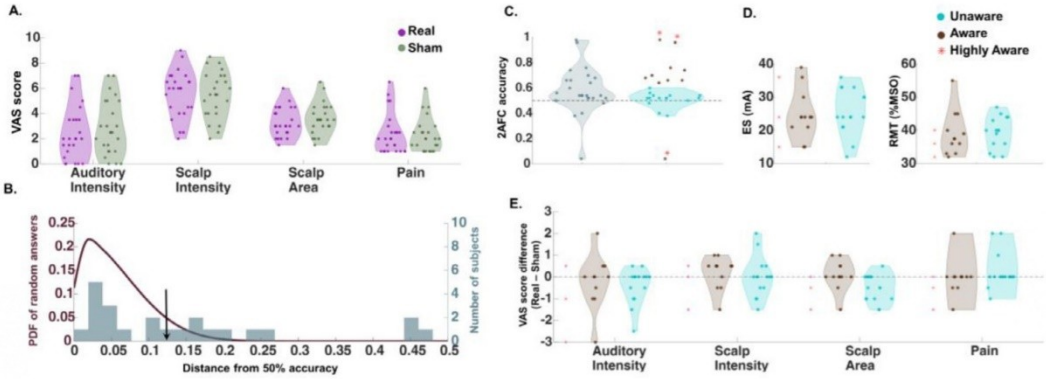

Fig. 3. **A**. Results from the visual analog scale for perceived stimuli sensation from the sham and real TMS conditions, each dot corresponds to an individual subject. **B**. Histogram of the 2AFC test's response, shown by the individuals' "distance from 50% accuracy" (grey), plotted with the expected value of the "distance from 50% accuracy" in case of random answers, shown as a probability density function (PDF) (brown). The arrow points to the threshold that divides subjects classified as being "unaware" of the distinction between the sham and real TMS condition (to the left from the arrow) and those who were "aware" (to the right). **C.** Left plot showing the overall accuracy of the subjects to the 2AFC test, and the right plot showing the same data, but separating subjects who were "unaware" (cyan) and subjects who were "aware" (brown) as to the distinction between the sham and real TMS conditions. The dots correspond to individual subjects and red asterisks indicate those subjects who were "highly aware" of the distinction. **D.** Comparison of "aware" and "unaware" subjects with respect of the ES and the TMS intensities used in the experiment, red asterisks indicating the values from the subjects who were "highly aware" of the distinction. **E.** Comparison of the "aware" and "unaware" subjects with respect of the difference of reported sensory perceptions on the visual analog scale (VAS) from each condition (real minus sham) (For interpretation of the references to color in this figure legend, the reader is referred to the web version of this article).

4. Discussion

4.1. Design and test of the optimized sham

Designing an ideal sham condition for TMS-EEG experiments is particularly challenging as, despite best efforts, sham conditions often fail to match the multisensory input from the real TMS condition (Conde et al., 2019). Given that this constitutes a major caveat of the method, it is unfortunate that most previous studies have not properly reported the subjects' perceived sensory input from real and sham conditions. In some cases only the auditory input was assessed (Rocchi et al., 2021), or only accuracy of distinction between conditions was tested (Mennemeier et al., 2009; Gordon et al., 2018), or the perceived stimulus intensity scale was solely used to set the sham intensity (Opitz et al., 2014).

The notion that most of the PEPs in TMS-EEG are attributed to auditory inputs (Paus et al., 2001; Ilmoniemi and Kicic, 2010) has probably drawn exceeding attention to this issue, leading subsequent studies to neglect the impact of somatosensory inputs. For instance, Du et al. investigated the effects of TMS to several cortical areas, but did not include a somatosensory control (Du et al., 2017). The EEG signal in the sham condition was of markedly low amplitude, and the authors attributed the frontal N100, observed at all stimulation sites, to a generic marker of direct brain activation by TMS (Du et al., 2017). This view can no longer be maintained, given the results observed here and by others (Conde et al., 2019; Ahn and Frohlich, 2021) demonstrating that the N100 is predominantly a peripherally evoked potential. Harquel et al. (2016), although correctly identifying the P200 present in all the experimental conditions as an auditory evoked potential, did not consider a possible contribution by somatosensory input .

Other studies, although including somatosensory sham control, have likely failed to employ a condition that properly matched the sensory input from real TMS. A recent report used a combined auditory and somatosensory sham approach aiming to disentangle the PEPs from the TMS-EEG signal (Rocchi et al., 2021). The study applied proper noise masking that suppressed the auditory evoked potential; however, it employed a somatosensory sham condition with electric stimulation of low intensity (on average, 6 mA), which most likely did not match the TMS somatic input. This can also be inferred from the low amplitude of the EEG response evoked by this condition, which led to a N100 potential in frontocentral regions following real TMS, most likely representing a residual PEP that was not adequately controlled for by the sham condition (Rocchi et al., 2021). One example of a more adequate control for somatosensory inputs is reported by Raffin et al. (2020), who analyzed the EEG responses to increasing TMS intensities, while also attempting to match the sensory input by increasing ES intensities (Raffin et al., 2020).

In order to overcome the limitations from these previous studies, we designed our optimized sham condition by considering these sources of sensory input from the TMS activation, auditory and somatosensory, and tested our design with a psychophysical comparison of the sham and real TMS perception. We observed that the GMFP from the auditory sham condition (Fig. 2A) was of lower amplitude than reported from sham stimuli without masking noise (Gosseries et al., 2015; Rocchi et al., 2021), corroborating a considerable suppression of the auditory evoked potential by masking. Still, a small-amplitude potential remained in a period of 130–250 ms after stimulation (Fig. 2A–C). This justifies the use of an auditory sham stimulation with equivalent sound pressure level at the ear canal compared to the real TMS condition (Fig. 1C, D), thus helping to create indistinguishable conditions. To control for the somatosensory evoked potential we applied electric stimuli to the scalp area of the TMS target, aiming to generate a highly similar somatic input to the real TMS and keeping the subject unaware as to the nature of each stimulus (Rossi et al., 2007; Mennemeier et al., 2009), a feature that cannot be claimed by other sham modalities such as shoulder stimulation (Herring et al., 2015; Biabani et al., 2019). However, only when adding the ES to both real and sham conditions subjects reported a thoroughly comparable sensory perception from these conditions.

The use of this optimized sham procedure might also be of particular advantage as a placebo condition for clinical trials using TMS. Clinical trials using non-invasive brain stimulation also face significant validity issues due to the challenge of applying a sham that consistently simulates the real TMS, which is especially problematic given the substantial placebo effect attributed to TMS (Razza et al., 2018; Burke et al., 2019). Although originally only auditory stimulation was included as sham, to properly simulate the real TMS, further sham procedures also integrated

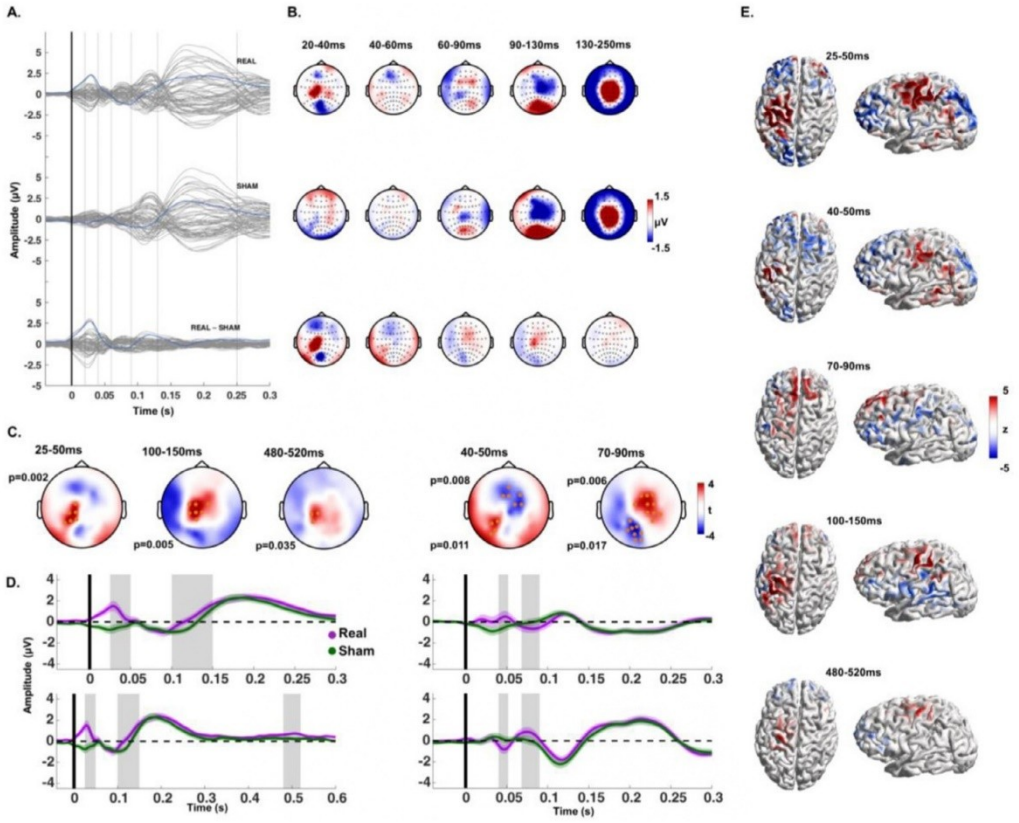

Fig. 4. A. Butterfly plots of the averaged EEG response across all subjects, divided by real TMS condition, sham TMS condition and the subtraction of the sham from the real condition (average reference, each line corresponding to an EEG channel, blue line corresponding to the C3 channel, i.e., close to the site of real TMS) **B**. Scalp distribution of the signal observed in A, divided in 5 time windows of interest. **C.** Results of the cluster-based *t*-test comparing the sham and real TMS conditions showing two significant clusters, displayed as resulting t-values of each electrode (electrodes in the clusters marked by orange dots, respective p-values on the left). **D.** Signal over time of EEG responses from the real TMS (purple) and sham TMS (green), triggered at time=0 (black line). Plots in the left column show the signal from the electrodes that composed the clusters indicated in C: 25–50 ms, 100–150 ms and 480–520 ms (note that only the bottom plot shows the 480–520 ms cluster). Plots in the right column show the signal from the electrodes that composed the clusters indicated in C: 40–50 ms and 70–90 ms (top plot corresponds to the fronto-central cluster and bottom plot to the left-hemispheric sensorimotor cluster). Shaded grey areas correspond to the time windows of the clusters (indicated in C). **E.** Difference of the source projection, displayed as *z*-scores, of the real minus sham condition EEG signals, in the time windows where the significant clusters were found (For interpretation of the references to color in this figure legend, the reader is referred to the web version of this article).

somatosensory stimulation by the means of scalp electrical stimulation (Rossi et al., 2007; Mennemeier et al., 2009). Our optimized sham goes one step further by applying electrical stimulation to both real and sham, assuring equivalent subjective perception in multiple sensory modalities and an overall indistinguishability between conditions. The method may prove capable of fully homogenizing the placebo effects of real and sham TMS in a clinical trial, thus revealing the true therapeutic effect of non-invasive brain stimulation. This, however, will require further testing.

4.2. Separating TEPs from PEPs

In TMS-EEG experiments, the sham condition must also reliably control for the peripherally evoked responses in the EEG caused by real TMS. Several procedures have been proposed to clear TMS-EEG data from PEPs, including ICA, and linear regression or cosine similarity-based analysis (Biabani et al., 2019; Freedberg et al., 2020; Raffin et al., 2020). However, these methods do not exempt the need of a sham condition, as it is necessary to inform the models what constitutes a PEP, so it can then be removed from the real TMS response. Moreover, some of these methods rely on further assumptions; for instance, ICA assumes temporal independence of the underlying sources, an assumption that is very likely violated given that both TEPs and PEPs are time-locked to the stimulus (Biabani et al., 2019).

An even more far-reaching assumption is that the TEPs and PEPs are independent phenomena and do not exert any influence on each other, meaning that their corresponding EEG signals are simply linearly superimposed. This assumption is the basis of most proposed methods so far to remove PEPs from TMS-EEG responses (Biabani et al., 2019), and also necessary for statistical comparisons between real and sham TMS conditions, as they have been widely performed in previous studies (Herring et al., 2015; ter Braack et al., 2015; Du et al., 2017; Gordon et al., 2018; Raffin et al., 2020; Rocchi et al., 2021). However, the assumption that TEPs and PEPs do not interact is unlikely, given the converging evidence for modulatory effects of sensory input on motor cortex excitability (Novembre et al., 2019) (for review (Kenemans, 2015; Wessel and Aron, 2017)). As a consequence, changes in cortical excitability induced by the multisensory TMS-induced inputs, which include vibration, tactile sensation, direct activation of trigeminal afferents and contraction of cranial muscles, likely cause changes to the

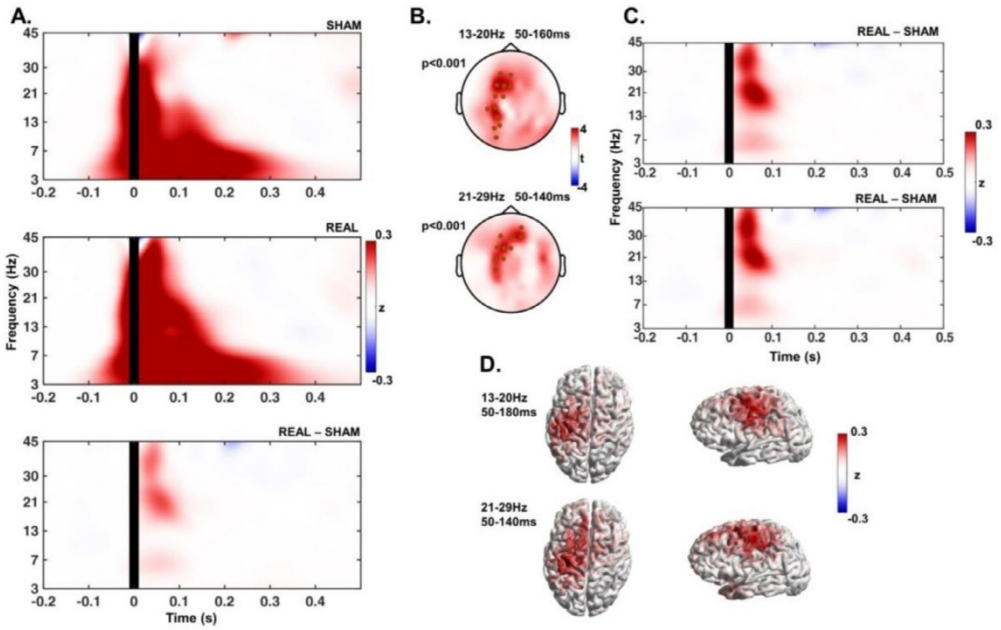

Fig. 5. **A.** Time-frequency response (TFR) plots show the change in spectral power with respect to baseline, averaged across all subjects and electrodes, from the sham and real TMS condition, and the subtraction of the sham TFR from the real. **B.** Results of the cluster-based t-tests comparing the real and sham conditions showing two significant clusters (marked as black dots, respective *p*-values on the left) in the low beta band (13–20 Hz) around 50–160 ms after the stimuli, and a single cluster in the high beta band (21–29 Hz) around 50–140 ms after the stimuli, displayed as *t*-values of each electrode. **C.** TFR plots show the response to the real TMS condition after subtraction of the sham condition, with the TFR shown in each plot corresponding to the average signal of the electrodes that composed the clusters indicated in B (top-plot corresponds to the 13–20 Hz cluster and bottom-plot to the 21–29 Hz cluster). **D.** Difference of the source reconstruction of the oscillatory response to real TMS minus sham condition, displayed as *z*-scores, in the frequency bands and time windows where the significant clusters were found.

"true" TEP that would be obtained by direct cortical activation in isolation. Even though the issue has not been explored in TMS-EEG studies, this interaction imposes a significant limitation to the aforementioned methods to remove PEPs from TMS-EEG responses.

Despite these limitations, we chose to follow previous studies in the assumption of linear superposition, which is a prerequisite for the subtraction of the sham response from the real TMS response. It follows that the resulting signals should not be understood as corresponding to "true" TEPs, due to the potential modulatory effect of the sensory input. Nevertheless, by designing a method that generates closely comparable sensory inputs and evoked potentials in sham and real TMS conditions, we could consistently match PEP contributions in the real and sham condition. We accomplished this by applying supramaximal ES in sham and real TMS conditions, thereby saturating the EEG responses to somatosensory input. Logarithmic input-output curves have been demonstrated for PEPs, i.e., linear increases of stimulus intensity result in progressively smaller increases in PEP amplitude, approaching asymptotically a plateau (Torquati et al., 2002; Lin et al., 2003). We demonstrated saturation of PEP amplitude at ES intensities ≥ 300%SPT (Fig. 2). An early-latency PEP component at around 80 ms, however, did not reach a plateau (Fig. 2D–G). Nevertheless, the comparison of the EEG signals in the real minus sham TMS conditions revealed a potential of opposite polarity in this time window of interest (Fig. 4C), indicating that an incomplete saturation of this early somatosensory potential, if anything, had resulted in underestimation of the amplitude of the underlying TEP.

The results from using the present method to remove PEPs from early (i.e., within the first 90 ms) EEG responses to TMS of motor cortex are mostly in agreement with previous reports (for review, (Komssi and Kahkonen, 2006; Hill et al., 2016; Hallett et al., 2017)). However, a close inspection shows that only the P30 and the N45/P45 have been clearly described, while a dipolar P70/N70 with the P70 expressed in bilateral prefrontal cortex and the N70 in parietal cortex ipsilateral to TMS was not described in uncontrolled or incompletely sham-controlled studies (Komssi et al., 2004; Bonato et al., 2006; Premoli et al., 2014; Cash et al., 2017; Gordon et al., 2018; Darmani and Ziemann, 2019; Ahn and Frohlich, 2021; Belardinelli et al., 2021), with the exception of one study that however failed to demonstrate the preceding dipolar N45/P45 response (Premoli et al., 2014). A recent study has described a negative deflection at around 45 ms and a positive deflection at 60 ms, respectively N45 and P60, which were located in the ipsilateral somatosensory cortex, whereas the P30 was localized in the stimulated motor cortex, in line with our present findings (Ahn and Frohlich, 2021).

The confirmation of early TEPs (below 100 ms after the TMS pulse) was expected, as this time windows is mostly free of PEPs (Conde et al., 2019; Ahn and Frohlich, 2021). Beyond 100 ms the superposition of the PEPs hinders the analysis of TEPs, and sham control procedures that do not fully reproduce the sensory input from the real TMS may lead to components of PEPs erroneously interpreted as TEPs. Using the present optimized sham procedure, we observed a close match of the EEG signals from the sham and real TMS conditions beyond 100 ms, despite the real TMS condition contained objectively more sensory input (TMS + ES). This supports that we attained PEP saturation and that the resulting PEPs from both conditions was equivalent, representing a thorough control of multisensory input in the real TMS condition by the sham condition.

Nevertheless, we were able to identify significant differences in this time window that can most likely be attributed to direct cortical activation by TMS, namely positive deflections around 120–130 ms and 480–520 ms after the TMS pulse (Fig. 4). These differ from PEPs as their peaks are shifted from the expected PEPs, and they are located

specifically in the stimulated cortical region, the left M1, further suggesting that they correspond to direct cortical activation responses. The existence of a response specific to TMS activation around 120 ms has also been suggested by previous studies, despite these being partially or mostly attributed to sensory inputs in the form of PEPs (Nikulin et al., 2003; Komssi et al., 2004; Lioumis et al., 2009; Herring et al., 2015). In line with this, several interventions that aimed at modulating cortical excitability identified changes in the response signal within this time window (Premoli et al., 2014; Cash et al., 2017; Chung et al., 2019), but retrospective interpretation needs to acknowledge the possibility that these changes are combined effects of intervention on TEPs and PEPs. Finally, we found a significant positivity in the stimulated area around 500 ms after the stimulus, specific to the real TMS condition, which might have gone undetected in previous reports by being in a time window beyond of what usually is investigated in TMS-EEG studies, and might deserve further investigation of its relevance and physiological implication.

4.3. Extracting sensory induced oscillations from TMS induced oscillations

The results presented here corroborate the notion that also cortical oscillatory activity can be modulated by indirect sensory input. Both real and sham TMS induced considerable changes in the oscillatory activity, observed by a power increase in all of the analyzed frequency bands immediately after stimulation (Fig. 5). After subtracting the EEG signals of the sham from the real TMS condition we observed that the only remaining oscillatory change is an increased beta power within the first 200 ms, mostly located in the stimulated sensorimotor cortex. The induced increase in beta oscillations (13–29 Hz) most likely reflects direct TMS responses typical of motor cortex, whereas lower frequency responses that have been eliminated by subtraction of the sham from the real TMS condition likely correspond to activity induced by sensory input (Rosanova et al., 2009; Fecchio et al., 2017; Biabani et al., 2021).

Our previous report on TMS-induced oscillations found differences between sham and real TMS conditions that are replicated in the present report, concerning the early increase in beta power while, retrospectively, later decreases in alpha and beta power likely have to be attributed to induced oscillations resulting from non-controlled sensory inputs (Gordon et al., 2018). The same problem occurred in other studies that did not apply a realistic sham control (Fuggetta et al., 2005; Fecchio et al., 2017). These examples underscore the importance of masking and matching sensory inputs, as it has been largely achieved in this study.

4.4. Limitations

Despite achieving a method that could remove PEP components in a TMS-EEG experiment, caution should be applied with respect to generalization of the reported findings. It is well recognized that TMS applied to different cortical regions and at different stimulus intensities leads to different cortical responses, mostly due to different neuronal populations being activated (Komssi et al., 2004; Rosanova et al., 2009). It follows that the present methodological procedures and findings cannot be simply transposed to TMS of other cortical areas or intensities, given that the present measurements were limited to subthreshold stimulation of motor cortex. Changing the cortical target may require adapting the sham condition. For example, use of high-intensity TMS, such as required for stimulating the cerebellum (Fernandez et al., 2021) may generate a sensory input of greater order of magnitude compared to the sham procedure described here, and thus a higher-intensity sham sensory control would be necessary for saturation of PEPs. Also, the sound pressure level equivalence function (Fig. 1D) will require recalibration if the real and sham TMS coils are moved to a different target. Finally, as mentioned before, the results cannot be generalized to TMS-EEG responses elicited by suprathreshold intensities, which have different characteristics, including higher amplitudes. Nevertheless, suprathreshold TMS pulses to M1 lead by definition to MEPs, which are responsible for an additional re-afferent somatosensory evoked response (Komssi et al., 2004; Fecchio et al., 2017; Premoli et al., 2017; Biabani et al., 2021). This response would further add to confounding signals to TEPs and induced oscillations.

Further technical aspects of the sham procedure deserve critical review. Firstly, whereas the real TMS coil was placed in contact with the scalp, the sham coil was placed atop the real coil (Fig. 1B, E). This led to different degrees of auditory input via bone conduction between sham and real TMS. The use of a spacer underneath the real TMS coil (Ruddy et al., 2018) would have allowed avoidance of vibratory input from both conditions. However, this would have required higher TMS intensities for effective cortical stimulation, and higher air conduction auditory input in the auditory sham control, with a possible compromising effect on the linear relation of real/sham sound pressure level (Fig. 1C, D). The close match of the EEG signals in the sham and real TMS conditions between 100 and 200 ms indicates that these slight differences in the sensory input did not result in a detectable PEP difference. Another issue concerns the electrical stimulation to control for somatosensory input. ES caused a sizable decaying artifact after the stimulus, due to the proximity of ES and EEG electrodes, requiring discarding the EEG signal in the first 25 ms after the stimulus. This may have resulted in omission of short-latency TEPs (Ilmoniemi et al., 1997; Ferreri et al., 2011).

Finally, the delivery of considerable multisensory input in both real and sham conditions might have altered the genuine TEP signature. Although TMS-EEG measurements in general might be subject to this effect due to the ubiquity of sensory stimuli from TMS, by applying peripheral stimulation at supramaximal intensity likely has increased the risk of changing the spatiotemporal patterns of the transcranially evoked EEG signature, as increased sensory inputs lead to more pronounced motor cortex modulation (Novembre et al., 2019). As a result, although the differences we observed successfully removed PEP components from the EEG response, there is no guarantee that the remaining TEP responses have not been warped by sensory inputs, and thus may not represent “true” TEPs.

These observations suggest that, despite its success in the objectives proposed in this study, the method of optimized sham need to be further developed. Matching the PEP corresponding to the motor re-afferent feedback will allow investigation of suprathreshold TMS intensities in studies of motor cortex. Future studies may also calibrate the optimized sham procedure, possibly lowering the amount of sensory stimulus needed for a consistent TEP and PEP pairing, thus minimizing the potential confounding effects of sensory input on the TEP response.

5. Conclusions

We present here an optimized sham for TMS-EEG experiments of the primary motor cortex hand area that matched the multisensory input from the real TMS condition, by delivering masking noise in addition to an auditory sham, combined with supramaximal somatosensory stimuli in both sham and real TMS conditions to saturate the PEPs. This method enables the identification of EEG responses caused by the direct cortical activation with TMS, while removing responses attributed to the procedure’s multisensory input.

Declaration of Competing Interest

P.C.G. and C.Z. report funding through the EXIST translational research program from the German Federal Ministry for Economic Affairs and Energy. H.S. received honoraria as speaker from Sanofi Genzyme, Denmark and Novartis, Denmark, as consultant from Sanofi Genzyme, Denmark, Lophora, Denmark, and Lundbeck AS, Denmark, and as editor-in-chief (Neuroimage Clinical) and senior editor (NeuroImage) from Elsevier Publishers, Amsterdam, The Netherlands. He has received royalties as book editor from Springer Publishers, Stuttgart, Germany and from Gyldendal Publishers, Copenhagen, Denmark. U.Z. received

grants from the German Ministry of Education and Research (BMBF), European Research Council (ERC), German Research Foundation (DFG), Janssen Pharmaceuticals NV and Takeda Pharmaceutical Company Ltd., and consulting fees from Bayer Vital GmbH, Pfizer GmbH and CorTec GmbH, all not related to this work. The other authors declare no further competing financial interests.

Credit authorship contribution statement

Pedro C. Gordon: Conceptualization, Visualization, Investigation, Formal analysis, Data curation, Writing – review & editing. **D. Blair Jovellar:** Investigation, Writing – review & editing. **YuFei Song:** Investigation, Writing – review & editing. **Christoph Zrenner:** Investigation, Writing – review & editing. **Paolo Belardinelli:** Formal analysis, Visualization, Conceptualization, Writing – review & editing. **Hartwig Roman Siebner:** Conceptualization, Visualization, Writing – review & editing. **Ulf Ziemann:** Conceptualization, Visualization, Writing – review & editing.

Data and code availability statement

MATLAB scripts—including the EEG pre-processing pipeline and statistics—are available at https://github.com/pcgordon/optimized_supraliminal_sham. These codes were designed for using the open source toolbox Fieldtrip, version 20210212 (https://www.fieldtriptoolbox.org/).

Data can be made available upon request.

Ethics statement

This study was conducted in accordance with the Declaration of Helsinki and following approval from the local ethics committee of the medical faculty of the University of Tübingen (registration number 456/2019BO2). The inclusion of subjects and data gathering started only after their signing the written informed consent approved by the local ethics committee.

Acknowledgments

C.Z. acknowledges support from the Clinician Scientist Program at the Faculty of Medicine at the University of Tübingen [grant number 391–0-0]. The project has received funding from the European Research Council (ERC Synergy) under the European Union's Horizon 2020 research and innovation program (ConnectToBrain) [grant number 810377], and from an EXIST Transfer of Research grant by the German Federal Ministry for Economic Affairs and Energy [grant number 03EFJBW169]. H.S. holds a 5-year professorship in precision medicine at the Faculty of Health Sciences and Medicine, University of Copenhagen which is sponsored by the [grant number R186–2015–2138].

Supplementary materials

Supplementary material associated with this article can be found, in the online version, at doi:10.1016/j.neuroimage.2021.118708.

References

Ahn, S., Frohlich, F., 2021. Pinging the brain with transcranial magnetic stimulation reveals cortical reactivity in time and space. Brain Stimul. 14 (2), 304–315. doi:10.1016/j.brs.2021.01.018.

Belardinelli, P., Biabani, M., Blumberger, D.M., Bortoletto, M., Casarotto, S., David, O., et al., 2019. Reproducibility in TMS-EEG studies: a call for data sharing, standard procedures and effective experimental control. Brain Stimul. 12 (3), 787–790. doi:10.1016/j.brs.2019.01.010.

Belardinelli, P., Konig, F., Liang, C., Premoli, I., Desideri, D., Muller-Dahlhaus, F., et al., 2021. TMS-EEG signatures of glutamatergic neurotransmission in human cortex. Sci. Rep. 11 (1), 8159. doi:10.1038/s41598-021-87533-z.

Biabani, M., Fornito, A., Coxon, J.P., Fulcher, B.D., Rogasch, N.C., 2021. The correspondence between EMG and EEG measures of changes in cortical excitability following transcranial magnetic stimulation. J. Physiol. 599 (11), 2907–2932. doi:10.1113/JP280966.

Biabani, M., Fornito, A., Mutanen, T.P., Morrow, J., Rogasch, N.C., 2019. Characterizing and minimizing the contribution of sensory inputs to TMS-evoked potentials. Brain Stimul. 12 (6), 1537–1552. doi:10.1016/j.brs.2019.07.009.

Bonato, C., Miniussi, C., Rossini, P.M., 2006. Transcranial magnetic stimulation and cortical evoked potentials: a TMS/EEG co-registration study. Clin. Neurophysiol. 117 (8), 1699–1707. doi:10.1016/j.clinph.2006.05.006.

Burke, M.J., Kaptchuk, T.J., Pascual-Leone, A, 2019. Challenges of differential placebo effects in contemporary medicine: the example of brain stimulation. Ann. Neurol. 85 (1), 12–20. doi:10.1002/ana.25387.

Casali, A.G., Casarotto, S., Rosanova, M., Mariotti, M., Massimini, M., 2010. General indices to characterize the electrical response of the cerebral cortex to TMS. Neuroimage 49 (2), 1459–1468. doi:10.1016/j.neuroimage.2009.09.026.

Cash, R.F., Noda, Y., Zomorrodi, R., Radhu, N., Farzan, F., Rajji, T.K., et al., 2017. Characterization of Glutamatergic and GABAA-mediated neurotransmission in motor and dorsolateral prefrontal cortex using paired-pulse TMS-EEG. Neuropsychopharmacology 42 (2), 502–511. doi:10.1038/npp.2016.133.

Chung, S.W., Sullivan, C.M., Rogasch, N.C., Hoy, K.E., Bailey, N.W., Cash, R.F.H., et al., 2019. The effects of individualised intermittent theta burst stimulation in the prefrontal cortex: a TMS-EEG study. Hum. Brain Mapp. 40 (2), 608–627. doi:10.1002/hbm.24398.

Conde, V., Tomasevic, L., Akopian, I., Stanek, K., Saturnino, G.B., Thielscher, A., et al., 2019. The non-transcranial TMS-evoked potential is an inherent source of ambiguity in TMS-EEG studies. Neuroimage 185, 300–312. doi:10.1016/j.neuroimage.2018.10.052.

Counter, S.A., Borg, E., 1992. Analysis of the coil generated impulse noise in extracranial magnetic stimulation. Electroencephalogr. Clin. Neurophysiol. 85 (4), 280–288. doi:10.1016/0168-5597(92)90117-t.

Darmani, G., Ziemann, U., 2019. Pharmacophysiology of TMS-evoked EEG potentials: a mini-review. Brain Stimul. 12 (3), 829–831. doi:10.1016/j.brs.2019.02.021.

Du, X., Choa, F.S., Summerfelt, A., Rowland, L.M., Chiappelli, J., Kochunov, P., et al., 2017. N100 as a generic cortical electrophysiological marker based on decomposition of TMS-evoked potentials across five anatomic locations. Exp. Brain Res. 235 (1), 69–81. doi:10.1007/s00221-016-4773-7.

Esser, S.K., Huber, R., Massimini, M., Peterson, M.J., Ferrarelli, F., Tononi, G., 2006. A direct demonstration of cortical LTP in humans: a combined TMS/EEG study. Brain Res. Bull. 69 (1), 86–94. doi:10.1016/j.brainresbull.2005.11.003.

Fecchio, M., Pigorini, A., Comanducci, A., Sarasso, S., Casarotto, S., Premoli, I., et al., 2017. The spectral features of EEG responses to transcranial magnetic stimulation of the primary motor cortex depend on the amplitude of the motor evoked potentials. PLoS One 12 (9), e0184910. doi:10.1371/journal.pone.0184910.

Fernandez, L., Biabani, M., Do, M., Opie, G.M., Hill, A.T., Barham, M.P., et al., 2021. Assessing cerebellar-cortical connectivity using concurrent TMS-EEG: a feasibility study. J. Neurophysiol. doi:10.1152/jn.00617.2020.

Ferreri, F., Pasqualetti, P., Maatta, S., Ponzo, D., Ferrarelli, F., Tononi, G., et al., 2011. Human brain connectivity during single and paired pulse transcranial magnetic stimulation. Neuroimage 54 (1), 90–102. doi:10.1016/j.neuroimage.2010.07.056.

Freedberg, M., Reeves, J.A., Hussain, S.J., Zaghloul, K.A., Wassermann, E.M., 2020. Identifying site- and stimulation-specific TMS-evoked EEG potentials using a quantitative cosine similarity metric. PLoS One 15 (1), e0216185. doi:10.1371/journal.pone.0216185.

Fuggetta, G., Fiaschi, A., Manganotti, P., 2005. Modulation of cortical oscillatory activities induced by varying single-pulse transcranial magnetic stimulation intensity over the left primary motor area: a combined EEG and TMS study. Neuroimage 27 (4), 896–908. doi:10.1016/j.neuroimage.2005.05.013.

Gordon, P.C., Desideri, D., Belardinelli, P., Zrenner, C., Ziemann, U., 2018. Comparison of cortical EEG responses to realistic sham versus real TMS of human motor cortex. Brain Stimul. 11 (6), 1322–1330. doi:10.1016/j.brs.2018.08.003.

Gosseries, O., Sarasso, S., Casarotto, S., Boly, M., Schnakers, C., Napolitani, M., et al., 2015. On the cerebral origin of EEG responses to TMS: insights from severe cortical lesions. Brain Stimul. 8 (1), 142–149. doi:10.1016/j.brs.2014.10.008.

Groppa, S., Oliviero, A., Eisen, A., Quartarone, A., Cohen, L.G., Mall, V., et al., 2012. A practical guide to diagnostic transcranial magnetic stimulation: report of an IFCN committee. Clin. Neurophysiol. 123 (5), 858–882. doi:10.1016/j.clinph.2012.01.010.

Hallett, M., Di Iorio, R., Rossini, P.M., Park, J.E., Chen, R., Celnik, P., et al., 2017. Contribution of transcranial magnetic stimulation to assessment of brain connectivity and networks. Clin. Neurophysiol. 128 (11), 2125–2139. doi:10.1016/j.clinph.2017.08.007.

Hamalainen, M.S., Ilmoniemi, R.J., 1994. Interpreting magnetic fields of the brain: minimum norm estimates. Med. Biol. Eng. Comput. 32 (1), 35–42.

Harquel, S., Bacle, T., Beynel, L., Marendaz, C., Chauvin, A., David, O., 2016. Mapping dynamical properties of cortical microcircuits using robotized TMS and EEG: towards functional cytoarchitectonics. Neuroimage 135, 115–124. doi:10.1016/j.neuroimage.2016.05.009.

Herring, J.D., Thut, G., Jensen, O., Bergmann, T.O., 2015. Attention modulates TMS-locked alpha oscillations in the visual cortex. J. Neurosci. 35 (43), 14435–14447. doi:10.1523/JNEUROSCI.1833-15.2015.

Hill, A.T., Rogasch, N.C., Fitzgerald, P.B., Hoy, K.E., 2016. TMS-EEG: a window into the neurophysiological effects of transcranial electrical stimulation in non-motor brain regions. Neurosci. Biobehav. Rev. 64, 175–184. doi:10.1016/j.neubiorev.2016.03.006.

Ilmoniemi, R.J., Kicic, D., 2010. Methodology for combined TMS and EEG. Brain Topogr. 22 (4), 233–248. doi:10.1007/s10548-009-0123-4.

Ilmoniemi, R.J., Virtanen, J., Ruohonen, J., Karhu, J., Aronen, H.J., Naatanen, R., et al.,

1997. Neuronal responses to magnetic stimulation reveal cortical reactivity and connectivity. Neuroreport 8 (16), 3537–3540.
Kenemans, J.L., 2015. Specific proactive and generic reactive inhibition. Neurosci. Biobehav. Rev. 56, 115–126. doi:10.1016/j.neubiorev.2015.06.011.
Komssi, S., Kahkonen, S., 2006. The novelty value of the combined use of electroencephalography and transcranial magnetic stimulation for neuroscience research. Brain Res. Rev. 52 (1), 183–192. doi:10.1016/j.brainresrev.2006.01.008.
Komssi, S., Kahkonen, S., Ilmoniemi, R.J., 2004. The effect of stimulus intensity on brain responses evoked by transcranial magnetic stimulation. Hum. Brain Mapp. 21 (3), 154–164. doi:10.1002/hbm.10159.
Koponen, L.M., Goetz, S.M., Tucci, D.L., Peterchev, A.V., 2020. Sound comparison of seven TMS coils at matched stimulation strength. Brain Stimul. 13 (3), 873–880. doi:10.1016/j.brs.2020.03.004.
Lin, Y.Y., Shih, Y.H., Chen, J.T., Hsieh, J.C., Yeh, T.C., Liao, K.K., et al., 2003. Differential effects of stimulus intensity on peripheral and neuromagnetic cortical responses to median nerve stimulation. Neuroimage 20 (2), 909–917. doi:10.1016/S1053-8119(03)00387-2.
Lioumis, P., Kicic, D., Savolainen, P., Makela, J.P., Kahkonen, S., 2009. Reproducibility of TMS-Evoked EEG responses. Hum. Brain Mapp. 30 (4), 1387–1396. doi:10.1002/hbm.20608.
Massimini, M., Ferrarelli, F., Huber, R., Esser, S.K., Singh, H., Tononi, G., 2005. Breakdown of cortical effective connectivity during sleep. Science 309 (5744), 2228–2232. doi:10.1126/science.1117256.
Mennemeier, M., Triggs, W., Chelette, K., Woods, A., Kimbrell, T., Dornhoffer, J., 2009. Sham transcranial magnetic stimulation using electrical stimulation of the scalp. Brain Stimul. 2 (3), 168–173. doi:10.1016/j.brs.2009.02.002.
Nikouline, V., Ruohonen, J., Ilmoniemi, R.J., 1999. The role of the coil click in TMS assessed with simultaneous EEG. Clin. Neurophysiol. 110 (8), 1325–1328.
Nikulin, V.V., Kicic, D., Kahkonen, S., Ilmoniemi, R.J., 2003. Modulation of electroencephalographic responses to transcranial magnetic stimulation: evidence for changes in cortical excitability related to movement. Eur. J. Neurosci. 18 (5), 1206–1212. doi:10.1046/j.1460-9568.2003.02858.x.
Novembre, G., Pawar, V.M., Kilintari, M., Bufacchi, R.J., Guo, Y., Rothwell, J.C., et al., 2019. The effect of salient stimuli on neural oscillations, isometric force, and their coupling. Neuroimage 198, 221–230. doi:10.1016/j.neuroimage.2019.05.032.
Oostenveld, R., Fries, P., Maris, E., Schoffelen, J.M., 2011. FieldTrip: open source software for advanced analysis of MEG, EEG, and invasive electrophysiological data. Comput. Intell. Neurosci. 2011, 156869. doi:10.1155/2011/156869.
Opitz, A., Legon, W., Mueller, J., Barbour, A., Paulus, W., Tyler, W.J., 2014. Is sham cTBS real cTBS? The effect on EEG dynamics. Front. Hum. Neurosci. 8, 1043. doi:10.3389/fnhum.2014.01043.
Paus, T., Sipila, P.K., Strafella, A.P., 2001. Synchronization of neuronal activity in the human primary motor cortex by transcranial magnetic stimulation: an EEG study. J. Neurophysiol. 86 (4), 1983–1990. doi:10.1152/jn.2001.86.4.1983.
Premoli, I., Bergmann, T.O., Fecchio, M., Rosanova, M., Biondi, A., Belardinelli, P., et al., 2017. The impact of GABAergic drugs on TMS-induced brain oscillations in human motor cortex. Neuroimage 163, 1–12. doi:10.1016/j.neuroimage.2017.09.023.
Premoli, I., Castellanos, N., Rivolta, D., Belardinelli, P., Bajo, R., Zipser, C., et al., 2014. TMS-EEG signatures of GABAergic neurotransmission in the human cortex. J. Neurosci. 34 (16), 5603–5612. doi:10.1523/JNEUROSCI.5089-13.2014.
Raffin, E., Harquel, S., Passera, B., Chauvin, A., Bougerol, T., David, O, 2020. Probing regional cortical excitability via input-output properties using transcranial magnetic stimulation and electroencephalography coupling. Hum. Brain Mapp. 41 (10), 2741–2761. doi:10.1002/hbm.24975.
Razza, L.B., Moffa, A.H., Moreno, M.L., Carvalho, A.F., Padberg, F., Fregni, F., et al., 2018. A systematic review and meta-analysis on placebo response to repetitive transcranial magnetic stimulation for depression trials. Prog. Neuropsychopharmacol. Biol. Psychiatry 81, 105–113. doi:10.1016/j.pnpbp.2017.10.016.
Rocchi, L., Di Santo, A., Brown, K., Ibanez, J., Casula, E., Rawji, V., et al., 2021. Disentangling EEG responses to TMS due to cortical and peripheral activations. Brain Stimul. 14 (1), 4–18. doi:10.1016/j.brs.2020.10.011.
Rogasch, N.C., Fitzgerald, P.B., 2013. Assessing cortical network properties using TMS-EEG. Hum. Brain Mapp. 34 (7), 1652–1669. doi:10.1002/hbm.22016.
Rogasch, N.C., Thomson, R.H., Farzan, F., Fitzgibbon, B.M., Bailey, N.W., Hernandez-Pavon, J.C., et al., 2014. Removing artefacts from TMS-EEG recordings using independent component analysis: importance for assessing prefrontal and motor cortex network properties. Neuroimage 101, 425–439. doi:10.1016/j.neuroimage.2014.07.037.
Rosanova, M., Casali, A., Bellina, V., Resta, F., Mariotti, M., Massimini, M., 2009. Natural frequencies of human corticothalamic circuits. J. Neurosci. 29 (24), 7679–7685. doi:10.1523/JNEUROSCI.0445-09.2009.
Rossi, S., Ferro, M., Cincotta, M., Ulivelli, M., Bartalini, S., Miniussi, C., et al., 2007. A real electro-magnetic placebo (REMP) device for sham transcranial magnetic stimulation (TMS). Clin. Neurophysiol. 118 (3), 709–716. doi:10.1016/j.clinph.2006.11.005.
Ruddy, K.L., Woolley, D.G., Mantini, D., Balsters, J.H., Enz, N., Wenderoth, N., 2018. Improving the quality of combined EEG-TMS neural recordings: introducing the coil spacer. J. Neurosci. Methods 294, 34–39. doi:10.1016/j.jneumeth.2017.11.001.
Seeck, M., Koessler, L., Bast, T., Leijten, F., Michel, C., Baumgartner, C., et al., 2017. The standardized EEG electrode array of the IFCN. Clin. Neurophysiol. 128 (10), 2070–2077. doi:10.1016/j.clinph.2017.06.254.
Siebner, H.R., Conde, V., Tomasevic, L., Thielscher, A., Bergmann, T.O., 2019. Distilling the essence of TMS-evoked EEG potentials (TEPs): a call for securing mechanistic specificity and experimental rigor. Brain Stimul. 12 (4), 1051–1054. doi:10.1016/j.brs.2019.03.076.
Stenroos, M., Nummenmaa, A., 2016. Incorporating and compensating cerebrospinal fluid in surface-based forward models of magneto- and electroencephalography. PLoS One 11 (7), e0159595. doi:10.1371/journal.pone.0159595.
Stenroos, M., Sarvas, J., 2012. Bioelectromagnetic forward problem: isolated source approach revis(it)ed. Phys. Med. Biol. 57 (11), 3517–3535. doi:10.1088/0031-9155/57/11/3517.
ter Braack, E.M., de Vos, C.C., van Putten, M.J., 2015. Masking the auditory evoked potential in TMS-EEG: a comparison of various methods. Brain Topogr. 28 (3), 520–528. doi:10.1007/s10548-013-0312-z.
Torquati, K., Pizzella, V., Della Penna, S., Franciotti, R., Babiloni, C., Rossini, P.M., et al., 2002. Comparison between SI and SII responses as a function of stimulus intensity. Neuroreport 13 (6), 813–819. doi:10.1097/00001756-200205070-00016.
Tremblay, S., Rogasch, N.C., Premoli, I., Blumberger, D.M., Casarotto, S., Chen, R., et al., 2019. Clinical utility and prospective of TMS-EEG. Clin. Neurophysiol. 130 (5), 802–844. doi:10.1016/j.clinph.2019.01.001.
Wessel, J.R., Aron, A.R, 2017. On the Globality of motor suppression: unexpected events and their influence on behavior and cognition. Neuron 93 (2), 259–280. doi:10.1016/j.neuron.2016.12.013.

2.2 ***Untangling TMS-EEG responses caused by TMS versus sensory input using optimized sham control and GABAergic challenge*** (by Pedro C. Gordon, Yu Fei Song, D. Blair Jovellar, Maryam Rostami, Paolo Belardinelli and Ulf Ziemann; published in J Physiol. 2023 May;601(10):1981-1998. doi: 10.1113/JP283986.)

The Journal of Physiology

J Physiol 601.10 (2023) pp 1981–1998

Untangling TMS-EEG responses caused by TMS *versus* sensory input using optimized sham control and GABAergic challenge

Pedro C. Gordon[1,2], Yu Fei Song[1,2], D. Blair Jovellar[1,2], Maryam Rostami[3], Paolo Belardinelli[1,2,4] and Ulf Ziemann[1,2]

[1] *Department of Neurology & Stroke, University of Tübingen, Tübingen, Germany*
[2] *Hertie Institute for Clinical Brain Research, University of Tübingen, Tübingen, Germany*
[3] *Faculty of Electrical and Computer Engineering, University of Tehran, Tehran, Iran*
[4] *CIMeC, Center for Mind/Brain Sciences, University of Trento, Trento, Italy*

Handling Editors: Richard Carson & Charlotte Stagg

The peer review history is available in the Supporting information section of this article (https://doi.org/10.1113/JP283986#support-information-section).

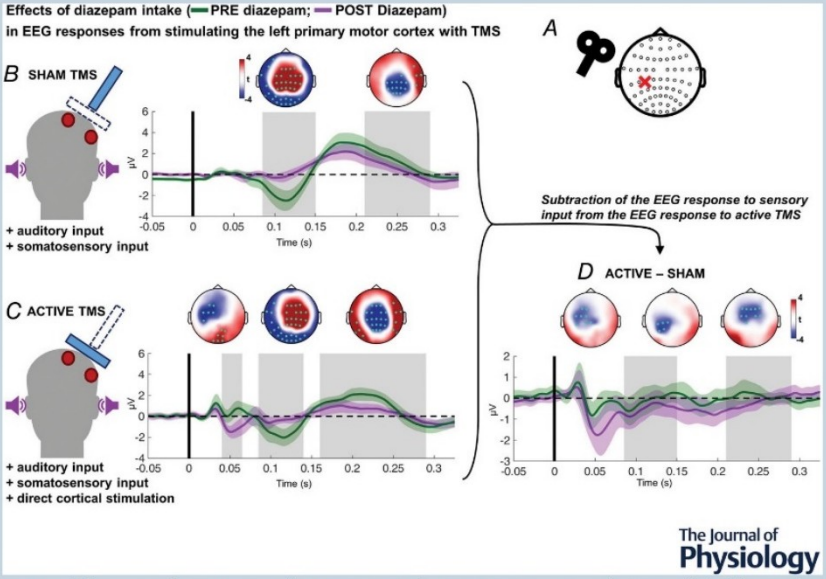

Abstract The combination of transcranial magnetic stimulation (TMS) and electroencephalography (EEG) elegantly probes the excitability and connectivity of the human brain. However, TMS-EEG signals inevitably also contain sensory-evoked responses caused by

Pedro C. Gordon Medical degree at the University of Sao Paulo, Brazil, 2009. Psychiatry specialty at the faculty of medicine of the University of Sao Paulo, Brazil, 2012. Master of science degree at the faculty of medicine of the University of Sao Paulo, Brazil, 2014. Doctor of science degree at the faculty of medicine of the University of Sao Paulo, Brazil, 2018. Postdoctoral researcher at the department of neurology of the University of Tübingen, Germany, since 2018.

DOI: 10.1113/JP283986

TMS-associated auditory and somatosensory inputs, constituting a substantial confounding factor. Here we applied our recently established optimized SHAM protocol (Gordon et al., Neuroimage 2021:118708) to disentangle TMS-EEG responses caused by TMS *vs*. sensory input. One unresolved question is whether these responses superimpose without relevant interaction, a requirement for their disaggregation by the optimized SHAM approach. We applied in 20 healthy subjects a pharmacological intervention using a single oral dose of 20 mg of diazepam, a positive modulator of GABAA receptors. Diazepam decreased the amplitudes of the P60 and P150 components specifically in the ACTIVE TMS and/or the ACTIVE TMS minus SHAM conditions but not in the SHAM condition, pointing to a response caused by TMS. In contrast, diazepam suppressed the amplitude of the N100 component indiscriminately in the ACTIVE TMS and SHAM conditions but not in the ACTIVE TMS minus SHAM condition, pointing to a response caused by sensory input. Moreover, diazepam suppressed the beta-band response observed in the motor cortex specifically after ACTIVE TMS and ACTIVE TMS minus SHAM. These findings demonstrate a lack of interaction of TMS-EEG responses caused by TMS *vs*. sensory input and validate optimized SHAM-controlled TMS-EEG as an appropriate approach to untangle these TMS-EEG responses. This knowledge will enable the proficient use of TMS-EEG to probe the physiology of the human cortex.

(Received 15 October 2022; accepted after revision 17 March 2023; first published online 24 March 2023)
Corresponding author Ulf Ziemann: Department of Neurology & Stroke, Hoppe-Seyler-Straße 3, 72076 Tübingen, Germany. Email: ulf.ziemann@uni-tuebingen.de

Abstract figure legend *A*, representation of the transcranial magnetic stimulation (TMS) target on the scalp (marked as red 'x') indicating the left primary motor cortex (around the location of the C3 electrode). *B*, representation of the SHAM TMS condition, which involved the delivery of auditory (masking nose and sham coil) and somatosensory stimuli (scalp electrical stimulation) of equivalent intensity compared with the ACTIVE TMS. To the right, topographical plots display the results from the statistical comparison between responses post- *vs*. pre-diazepam intake, using cluster-based dependent sample *t* tests (electrodes that comprised the significant clusters in cyan). Below, time-course plot of the EEG responses to the stimuli before (green) and after (purple) the intake of diazepam. Plotted signal corresponds to the average across all significant electrodes, displayed in the topographical plots above. Shaded grey areas indicate the time windows of significant difference between the EEG responses. *C*, representation of the ACTIVE TMS condition, which, in addition to auditory (masking noise and real coil) and somatosensory stimuli (scalp electrical stimulation and real coil), involved the direct activation of the underlying cortex. Time-course plot of EEG responses and topographical plots as in *B*. *D*, by subtracting the individual EEG responses to sensory stimuli (SHAM) from the response to TMS (ACTIVE) we obtain the EEG response attributed solely to the direct cortical activation by TMS. Time-course plot of EEG responses and topographical plots as in *B*.

Key points

- Optimized SHAM disentangles TMS-EEG responses caused by TMS *vs*. sensory input.
- Diazepam differentially modulates TMS-EEG responses caused by TMS *vs*. sensory input.
- Diazepam modulation of P60 and P150 indicate TMS-EEG responses caused by TMS.
- Diazepam modulation of N100 indicate a TMS-EEG response caused by sensory input.

Introduction

The combined use of transcranial magnetic stimulation (TMS) and electroencephalography (EEG) has gained significant attraction as a tool for understanding human neurophysiology (Chung et al., 2015; Tremblay et al., 2019). The technique involves non-invasive brain stimulation with TMS and simultaneous recording of cortical responses using scalp EEG, and provides information on neuronal excitability and connectivity of the stimulated region (Ilmoniemi & Kicic, 2010). TMS-EEG can potentially probe any region on the convexity of the cerebral cortex, obtaining EEG response signatures as markers of cortical responsivity (TMS-evoked potentials, TEPs). The TEP components are commonly referred to as typical positive (P) or negative (N) deflections following the TMS pulse in milliseconds (e.g. P30, N45, P60, N100 and P180 when probing the motor cortex) (Komssi et al., 2004; Lioumis et al., 2009).

Experiments combining TMS-EEG and neuropharmacology have helped to understand the neurophysiological mechanisms involved in TEPs (Darmani & Ziemann, 2019; Ziemann et al., 2015). By measuring TEPs prior to and following the intake of a central nervous system-active drug with a known specific mode of action, it is possible to infer that this mode of action contributes to the TEP components if they are significantly modified by the drug. Positive allosteric modulators of the GABAA receptors (GABAARs), i.e. benzodiazepines and zolpidem, increased the amplitude of the N45 and decreased the N100, whereas the GABABR agonist baclofen increased the N100 amplitude (Premoli et al., 2014). These findings imply that GABAAergic mechanisms contribute to the N45, while the N100 represents a more complex interaction of GABAAergic and GABABergic systems (Premoli et al., 2014). Similar to the positive allosteric modulators of the GABAAR, the antiglutamatergic *N*-methyl-D-aspartate receptor antagonist dextromethorphan increased the N45 amplitude, reinforcing the notion that TMS-EEG responses reflect the state of an excitation/inhibition balance under the control of glutamatergic/GABAergic dynamics (Belardinelli et al., 2021). These and similar other pharmaco-TMS-EEG studies have been important in establishing a neurophysiological basis for further TMS-EEG findings, including its use in the search for potential biomarkers for neuropsychiatric disorders. For instance, TMS-EEG revealed an abnormally low N100 amplitude in patients with attention deficit hyperactivity disorder (ADHD) and schizophrenia, which is in line with models of impaired cortical inhibition secondary to GABAergic dysregulation in these disorders (Bruckmann et al., 2012; Noda et al., 2018).

However, it is known that TMS inevitably generates considerable multisensory input leading to evoked EEG responses (peripherally evoked potentials – PEPs), which overlap with the EEG response from direct cortical activation by TMS, a caveat that has already been identified in early TMS-EEG studies (Nikouline et al., 1999; Paus et al., 2001). This multisensory input includes a high-pitched 'click' sound generated during coil discharge, and somatosensory stimulation of the scalp near the targeted area (Ilmoniemi & Kicic, 2010). This raises the question as to what extent TMS-EEG reflects responses to direct cortical activation by TMS or to the TMS-associated multisensory inputs. If the latter were true, then changes in TMS-EEG responses caused by a neuromodulatory intervention, as well as TMS-EEG response abnormalities in neuropsychiatric disorders, may reflect changes in PEPs rather than TEPs. This would significantly undermine the potential of TMS-EEG to investigate focal brain responsivity.

Here we aimed to test to what extent changes in TMS-EEG responses caused by a single oral dose of a positive allosteric modulator of the GABAAR (diazepam) can be attributed to the modulation of TEPs or PEPs. This investigation is enabled by a newly developed optimized SHAM protocol in TMS-EEG measures, which allows the extraction of TMS-EEG responses that are cleaned from PEPs (Gordon et al., 2021). The rationale of the optimized SHAM was to apply auditory masking, identical auditory input as in ACTIVE TMS, and high-intensity electrical stimulation (ES) of the scalp to saturate somatosensory-evoked potentials. Auditory masking and ES were also applied in ACTIVE TMS. We proposed that ACTIVE TMS minus SHAM responses would reflect true TEPs, under the assumption that TEPs and PEPs are largely independent, i.e. do not non-linearly interact with each other (Gordon et al., 2021). This assumption has been made stronger by the observation that TEPs are not modulated by changing levels of sensory input (Gordon et al., 2023). Therefore, it is possible to identify the modulatory effect of a given intervention over TEPs from the effects over PEPs by isolating these components before and after the intervention. We then tested the existence of modulatory effects of diazepam specifically on components of the ACTIVE TMS minus SHAM response and, at the same time, modulatory effects indiscriminately on other components of ACTIVE TMS and SHAM responses. If true, this would provide evidence of the different effects of neuromodulatory interventions (here a positive allosteric modulator at GABAARs) on EEG responses to sensory inputs and TMS cortical activation, as well as the possibility of disaggregating these responses by the optimized SHAM approach.

Methods

Subjects and design

The study included right-handed healthy volunteers (confirmed by the Edinburgh Handedness Inventory (Oldfield, 1971)) aged between 18 and 50 years for a two-session experiment. Exclusion criteria were: a history or presence of psychiatric or neurological diseases, intake of medication acting on the central nervous system, a history or presence of alcohol or illicit drug abuse, current pregnancy or breastfeeding, and resting motor threshold (RMT) >60% of the maximum stimulator output. This RMT limit was set because higher intensities would involve higher sensory input and potentially compromise the optimized sham procedure (Gordon et al., 2021). Ultimately, no subject was excluded due to this criterion.

A total of 23 subjects were initially included in the study. However, two subjects did not attend the second session and one subject presented a low-quality EEG signal due to excessive movement, preventing further analysis. Therefore, the final analysis included 20 subjects (14 female), with a mean age of 25.5 years (SD ± 4.7). The

study was approved by the ethics committee of the medical faculty of the University of Tübingen (456/2019BO2), conformed to the *Declaration of Helsinki*, and all subjects provided written informed consent prior to enrolment.

The study involved two experimental sessions separated by at least 1 week. Each experimental session involved a pre-intervention measurement with resting-state EEG and single-pulse TMS-EEG, followed by the pharmacological intervention, and then a post-intervention TMS-EEG measurement, identical to the pre-intervention measurement.

Intervention

The pharmacological intervention consisted of the intake of the positive allosteric modulator of the GABAAR diazepam (20 mg diazepam-ratiopharm). We included a control intervention with placebo (P-Tabletten Lichtenstein) in order to clarify that results are specifically due to pharmacological effects, although several studies have consistently confirmed that placebo intake does not result in any significant change in TMS-EEG responses (Belardinelli et al., 2021; Darmani et al., 2019; Premoli et al., 2014; Premoli, Biondi et al., 2017). All subjects received both diazepam and placebo interventions, each assigned to one of the two separate experimental sessions. The order in which the interventions were applied was pseudo-randomized and balanced across subjects. Both experimenters and subjects were blinded to the intervention, as diazepam and placebo tablets were highly similar in appearance and their package labels were covered and replaced by a code that mapped each session to an allocation table, which remained concealed until the end of the study. Drug intake occurred immediately after the pre-intervention measurements. A 60 min waiting time was then inserted prior to the post-intervention measurements in order to allow the plasma peak of diazepam to be reached (Shader et al., 1984).

Experimental set-up

Prior to the TMS-EEG sessions, subjects underwent magnetic resonance imaging (MRI) using a 3T Siemens PRISMA scanner to obtain T1-weighted anatomical images. MRI was used for proper positioning of the TMS coil with respect to the individual's brain anatomy, using a neuronavigation system (Localite GmbH, Sankt Augustin, Germany), and also for the EEG forward model and source reconstruction, explained below.

The experiment was conducted in a quiet room with subjects sitting comfortably on a reclined chair and instructed to keep their eyes open during the measurements. Scalp EEG was recorded from a TMS-compatible 64-channel Ag/AgCl sintered ring electrode cap (EasyCap GmbH, Germany) using a TMS-compatible EEG system and amplifiers (Bittium NeurOne, Finland). Electrode FCz was used as reference. Additionally, surface EMG was recorded through bipolar EMG adhesive hydrogel electrodes (Kendall, Covidien) from the abductor pollicis brevis (APB) and first dorsal interosseus (FDI) muscles of the right hand in a bipolar belly-tendon montage. EEG and EMG data were sampled at 5 kHz, and a 0.16–1.25 kHz bandpass filter was applied. EMG was used to determine RMT with standard methods (Groppa et al., 2012), using neuronavigation to guide the coil's position. The cortical target over the hand area of the left primary motor cortex (M1) that consistently elicited the largest motor-evoked potentials (MEPs) was defined as the hot spot. TMS was delivered using a figure-of-eight coil (external diameter of each wing, 90 mm) connected to a Magstim 200^2 magnetic stimulator (Magstim Company Ltd., UK) with a monophasic current waveform. The induced electrical field in the cortex was directed from lateral-posterior to medial-anterior. Two identical stimulators and coils were used in this experiment, one for the ACTIVE TMS condition and the other for the SHAM TMS condition (Fig. 1*A*). ES of the scalp, as part of the optimized SHAM procedure, was delivered by a Digitimer DS7A electric stimulator (Digitimer Ltd. UK) (Fig. 1*B*) (Gordon et al., 2021).

Resting-state EEG and TMS-EEG

Each pre- and post-intervention measurement included an eyes-open resting-state EEG and a single-pulse TMS-EEG. Resting-state EEG was recorded for 5 min. Subjects were comfortably seated, and instructed to fixate on a black cross 1 m in front of them.

The single-pulse TMS-EEG measurements consisted of 320 TMS pulses, 160 ACTIVE TMS and 160 SHAM TMS, randomly intermixed and applied with an intertrial interval of 3 s (±1 s jitter). Throughout the TMS-EEG measurements, masking noise was delivered through earbuds, set to an intensity high enough to conceal the TMS click noise, or to reach the subject's discomfort threshold. The masking noise was designed to have the same spectral distribution as the coil click sound (Massimini et al., 2005).

The ACTIVE TMS coil was placed tangentially to the scalp and targeted the motor hot spot (Fig. 1*A*). The intensity used for ACTIVE TMS was 90% of RMT. This subthreshold intensity was chosen to avoid somatosensory input via re-afferent feedback from MEP-related muscle twitches (Fecchio et al., 2017; Petrichella et al., 2017), while being sufficient to elicit TEPs (Fecchio et al., 2017; Komssi & Kahkonen, 2006). EMG was recorded during the TMS-EEG measurements to ensure that no MEPs occurred. SHAM TMS involved the application of a click

sound jointly with scalp ES (Fig. 1*A*). This click sound was delivered by the SHAM coil placed atop the ACTIVE TMS coil but angled perpendicular to the scalp, in order to keep the induced electrical field away from the cortex, while still generating the characteristic click sound (Fig. 1*A*). The intensity of SHAM TMS was set to match the auditory sound pressure level of ACTIVE TMS at the ear canals (Gordon et al., 2021).

The optimized SHAM procedure involved ES of the scalp delivered by two pairs of 1 cm diameter electrodes placed between the EEG electrodes: two electrodes of the same polarity at the positions corresponding to FFT9h and AFF5h, according to the International 10−20 system for EEG, and two electrodes of opposite polarity at CPP3h and TPP7h (Fig. 1*B*). Electrode polarity was switched after each pulse to avoid charge accumulation. This array of stimulation electrodes was designed to match the perception of somatosensory input of the TMS pulses, which involves a rather wide area of sensation over the scalp (Conde et al., 2019) and cranial muscle twitches around the target. Importantly, ES was applied in both the ACTIVE TMS and SHAM TMS conditions, using an intensity three times (in four subjects four times) the individual's sensory perception threshold (on average, 25.6 ± 7.5 mA), with a pulse width of 50 μs. ES was delivered exactly concurrently with the TMS trigger. This procedure was employed in order to saturate the PEPs in both the ACTIVE and SHAM TMS conditions and, therefore, equalize them in both conditions (Gordon et al., 2021). This should hold true even when considering that the ACTIVE TMS condition also involves somatosensory input from the TMS pulse, which will become negligible in the presence of the high-intensity saturating somatosensory input provided by ES. Therefore, we argued that it is then possible to subtract the resulting SHAM TMS-EEG response (only PEPs) from the ACTIVE TMS-EEG response (containing both PEPs and TEPs), thus obtaining the brain responses specifically caused by direct cortical activation (TEPs). The sensory perception reported by the subjects was highly comparable between the ACTIVE and SHAM TMS conditions (Fig. 2).

EEG data processing

Offline data analysis was performed using the FieldTrip open-source toolbox (Oostenveld et al., 2011). The resting-state EEG signal was first segmented in 3 s epochs. Spectral power was estimated using the Irregular Resampling Auto-Spectral Analysis (IRASA) method as implemented by the FieldTrip toolbox, and the signal-to-noise ratio was then computed by subtracting the fractal (aperiodic) component from the full spectrum (Donoghue et al., 2020).

To analyse time-domain EEG responses to TMS (TEPs), the signal from each measurement was segmented into epochs aligned to the TMS pulse (−1000 to 1500 ms) in both the ACTIVE and SHAM conditions, and then baseline corrected (−1000 to −50 ms). Both TMS and direct scalp ES are prone to produce a marked decay artefact that can affect the EEG signal from the first few milliseconds up to hundreds of milliseconds. To remove this artefact, we subtracted the best fit of an exponential function from each trial and channel (Conde et al., 2019; Rogasch et al., 2017). For this purpose, we used the 'fit' function from MATLAB to fit the one-term exponential model ($a \times \exp(b \times x)$) over every epoch during the time window 15–500 ms after the TMS pulse. With the prior knowledge that the decay artefact mostly affects early time points, a weighting factor for the exponential model was used, which incorporated a linearly spaced array of 100 to 1 over the course of the fitting time. To prevent the slow

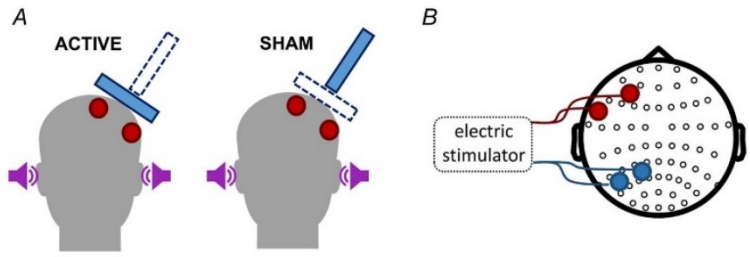

Figure 1. Stimulation set-up
A, representation of the ACTIVE and SHAM TMS set-up, showing delivery of masking noise (purple sound icons) and electrical stimulation of the scalp (red circles) in both stimulation conditions. The difference is with respect to the TMS coil, as ACTIVE TMS involved discharging the coil tangential to the scalp, whereas SHAM TMS involved discharging the coil tilted 90° with respect to the scalp (blue rectangles). *B*, topographical plot illustrating the EEG electrodes over the scalp and the relative position of electrodes for electrical stimulation: two electrodes of the same polarity at FFT9h and AFF5h (red circles), and two electrodes of the opposite polarity at CPP3h and TPP7h (blue circles), connected to the electrical stimulator device. Polarity switched after each pulse. [Colour figure can be viewed at wileyonlinelibrary.com]

waves of artefacts from contaminating the decay model, the exponential fit was obtained from detrended data, in which a fifth degree polynomial was subtracted from every epoch. Following the exponential decay subtraction, the time window between −5 and 15 ms around the TMS pulse, still containing the high-amplitude TMS artefact, was removed and cubic interpolated. EEG data were then downsampled to 1 kHz. Trials were inspected visually, and epochs and channels with excessive noise were excluded, as were trials containing MEPs in the EMG of the right FDI or APB. The average percentage of trials excluded per subject was 19.6% (SD ± 11.2%), with 4.6% due to the presence of MEP (SD ± 5.1%), while the number of channels excluded was on average 5.5 (SD ± 2.1). Further artefacts were removed with independent component analysis (ICA), including artefacts related to muscle activity, eye movement and blinks (Rogasch et al., 2014), using the FastICA algorithm implemented in FieldTrip (Oostenveld et al., 2011). Excluded channels were spline-interpolated. Channels exclusion and interpolation, as well as ICA, were performed separately for each intervention (diazepam, placebo) of a given individual, but combining the data of the measurements before and after drug intake. The TEP signal was finally filtered with a 45 Hz low-pass filter. These procedures yielded the EEG response from the ACTIVE and SHAM conditions. To obtain the ACTIVE minus SHAM condition (i.e. the TMS-EEG response without the PEP) we subtracted the SHAM from the ACTIVE EEG responses. This was done at the individual level, separately for the measurements of each drug intervention (i.e. diazepam *vs.* placebo) and time (i.e. pre- *vs.* post-drug intake).

For the processing of TMS-induced oscillations, time–frequency representations (TFRs) of TMS-related changes in oscillatory power were calculated both trial-by-trial and for the average of all trials. The TFR of the average of all trials was then subtracted from the TFR of each trial, thus removing the evoked oscillatory response and obtaining only the induced oscillatory response (Pellicciari et al., 2017). TFR was calculated using a Morlet wavelet decomposition on single trials, with frequency-dependent width (wavelet width of 2.6 cycles at 4 Hz, adding 0.2 cycles for each 1 Hz). This was followed by standardizing the TFR, by calculating the *z*-value in each frequency band using the pre- and post-stimulus epoch (Grandchamp & Delorme, 2011), and baseline correction (−500 to −50 ms). The procedure was performed trial-by-trial, which entailed separation of the pre- and post-drug conditions. This was relevant in order to standardize the baseline of all measurements in case of a change in the overall oscillatory activity after an intervention.

EEG activity from statistically significant results was localized into the source space. Individual cortical surfaces and dipole arrays were obtained from the individual's MRI, segmented and meshed using the FieldTrip toolbox (Oostenveld et al., 2011), with a forward model for EEG using a customized pipeline, taking into account the positions of the EEG electrodes relative to individual head anatomy (Stenroos & Nummenmaa, 2016; Stenroos & Sarvas, 2012). Source reconstruction was then obtained on the whole cortical surface using the L2-minimum-norm estimate (Hamalainen & Ilmoniemi, 1994). For the TEPs, the final result was obtained by

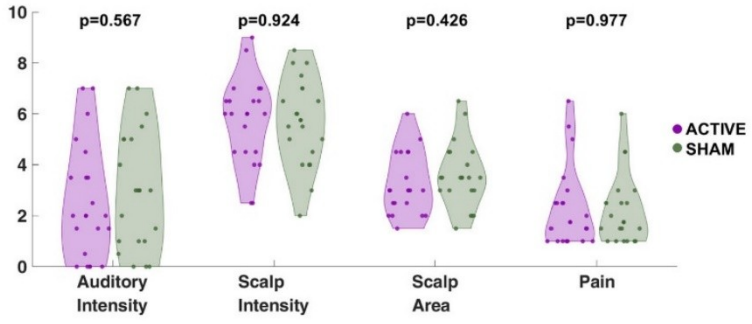

Figure 2. Sensorial perception of the ACTIVE *versus* SHAM TMS conditions
Results from visual analogue scale testing for subjective perception of sensory intensity. Four sensory modalities caused by the ACTIVE *vs.* SHAM TMS conditions were tested: intensity of auditory input, intensity of somatosensory (scalp) input, size of the scalp area where the somatosensory input was perceived, and pain/discomfort caused by the somatosensory input. Reported responses could range from 0 (no perceived sensory modality) to 10 (highest intensity possible). Each point corresponds to the response from one individual subject. Comparisons between the ACTIVE *vs.* SHAM TMS results were performed with Wilcoxon's signed-rank test for non-normal distributions, and resulting *P*-values are displayed above each sensory modality. The tests were performed in the experiment described in Gordon et al. (2021). In the current analysis, only the 20 subjects were included that proceeded to the pharmacological interventions experiment, described in the present report. [Colour figure can be viewed at wileyonlinelibrary.com]

z-transforming the signal of each trial with respect to the mean and standard deviation of the baseline (−500 to −50 ms). For induced oscillations, the EEG signal was first projected to the source space, followed by the TFR calculation, as described above. For the purpose of plotting the final results, data attributed to each individual dipole was pooled and warped into a common MNI space for creating a group average across all subjects.

Statistical analysis

All statistical analyses were performed on the MATLAB platform (R2018b, The Mathworks, USA). Cluster-based permutation t tests were implemented using the FieldTrip toolbox, using 1000 permutations per test (Oostenveld et al., 2011). We compared all EEG-related measures, described above, post-intervention *vs.* pre-intervention, separately for the diazepam and placebo conditions.

The resting-state EEG data were *a priori* divided into frequency bands of interest (FOI): theta (4–7 Hz), alpha (8–12 Hz), low beta (13–20 Hz), high beta (21–29 Hz) and gamma (30–45 Hz). The signal-to-noise ratio from each FOI was then averaged in each channel and submitted to cluster-based t tests for the post- *vs.* pre-intervention comparisons, yielding the significant channel clusters. Because of the multiple testing imposed by the five FOIs, the threshold of statistical significance was Bonferroni-adjusted to $P < 0.01$.

Regarding the TEP analysis, instead of predetermining a set of time windows of interest after the TMS pulse where differences are expected to occur, we relied on the cluster-based t-statistics to determine any time window (between 20 and 500 ms after the TMS) that contained significantly different EEG responses. We first set the cluster-based t tests to include all the channels and time samples, in order to estimate the time windows where the EEG responses were significantly different post- *vs.* pre-intervention. The EEG responses were then averaged within these significant time windows and compared by only including the channels in the cluster calculation, yielding the significant channel clusters. The significance threshold was set to $P < 0.05$. Analyses were performed by comparing the post- *vs.* pre-intervention data separately in the ACTIVE and SHAM TMS conditions. Finally, the post- *vs.* pre-intervention measurements were compared after subtracting the SHAM TMS response from the ACTIVE TMS response.

Statistical analysis of the TMS-induced oscillations followed the same procedure as for the TEPs, but first the data were divided into the same five FOIs as the resting-state EEG data. Therefore, the threshold for statistical significance was adjusted to $P < 0.01$.

Results

Drug effects on resting-state EEG

Diazepam led to significant changes of the resting-state EEG power spectrum (Fig. 3*A*). The cluster-based t-statistics revealed a decrease in alpha power following diazepam intake, observed in a cluster that comprised most of the electrodes. Diazepam also led to an increase in beta power, with low-beta increase detected over the entire scalp, whereas the high-beta increase was limited to the midline regions (Fig. 3 *C*–*D*). Cluster-based t-statistics did not yield any significant cluster when comparing the power spectra post- *vs.* pre-placebo intervention in any frequency band of interest (Fig. 3*B*).

Drug effects on TEPs

Figure 4 shows the butterfly time-course plots of TMS-EEG responses to both drug interventions over all electrodes. As expected, placebo intake did not result in any observable change in either ACTIVE or SHAM TMS (Fig. 4*A*). In contrast, diazepam led to evident changes of the TMS-EEG response, either largely indiscriminately in the ACTIVE and SHAM responses in the period 100−150 ms, or largely selectively in the ACTIVE TMS minus SHAM response in the period around 60 ms (Fig. 4*B*).

The cluster-based t-statistics on the post- *vs.* pre-diazepam SHAM responses revealed a highly significant decrease of the fronto-central negative potential peaking at around 120 ms, and a decrease in the posterior positive potential at around 250 ms (Fig. 5). Given that the SHAM condition involved only multisensory input but not TMS of the brain, these results indicate a specific effect of diazepam on PEPs, consisting of an amplitude reduction of late (>85 ms) TMS-EEG potentials, including an almost complete suppression of the N100 (Figs 5 and 6*A*).

The cluster-based t-statistics on the post- *vs.* pre-diazepam ACTIVE TMS late responses (>80 ms) are similar to those in the SHAM condition (Figs 5 and 6*B*). This is expected, since both conditions involve saturated multisensory input. One difference is a cluster specific to the ACTIVE TMS condition (i.e. not observed in the SHAM condition) comprising left frontal electrodes with increased negativity of the potential around 40–65 ms (P60) (Fig. 5). Source space projection of the signal indicated that this response was located in the stimulated region, around the left M1, extending to frontal regions of the ipsilateral cortex (Fig. 6*B*).

Finally, the post- *vs.* pre-diazepam comparison of the ACTIVE TMS minus SHAM response revealed three significant clusters. The first cluster showed increased negativity of the P60 over left frontal electrodes. Just as for

the ACTIVE TMS condition, the source space projection indicated that this response is located in the area of the stimulated left M1 and respective frontal region (Fig. 6*C*), further suggesting that this modulation is specific to a response caused by TMS rather than by sensory input. The second cluster revealed increased negativity around 140–155 ms (P150) over the left sensorimotor cortex, and the third cluster demonstrated increased negativity at 210−250 ms over bilateral prefrontal cortices (Fig. 6*C*).

Cluster-based *t*-statistics did not yield any significant cluster in the placebo intervention in either SHAM, ACTIVE TMS or ACTIVE TMS minus SHAM conditions.

These results suggest that diazepam has significant effects both on TEPs (represented by the subtraction ACTIVE TMS – SHAM) and on PEPs (represented by indiscriminate effects in the ACTIVE TMS and SHAM conditions). The effects of diazepam on TEPs were also partially represented, as expected, in the ACTIVE TMS signals, but to a lesser or even lacking extent (P150), probably due to the superimposition of diazepam effects on the PEPs at latencies >85 ms.

Finally, although the ACTIVE TMS – SHAM signal showed a clear positive deflection over the stimulated sensorimotor cortex at around 30 ms (P30), this TEP was not significantly modulated by diazepam (Fig. 6 *B* and *C*).

Drug effects on TMS-induced oscillations

The post- *vs.* pre-diazepam comparison revealed no significant difference in the induced oscillations in the SHAM condition (Fig. 7). In the ACTIVE TMS condition, diazepam led to a significant decrease in TMS-induced oscillations in the low- and high-beta frequency bands in the first 200 ms (Fig. 7 *A*–*B*). In the ACTIVE TMS minus SHAM response, a significant cluster was found only in

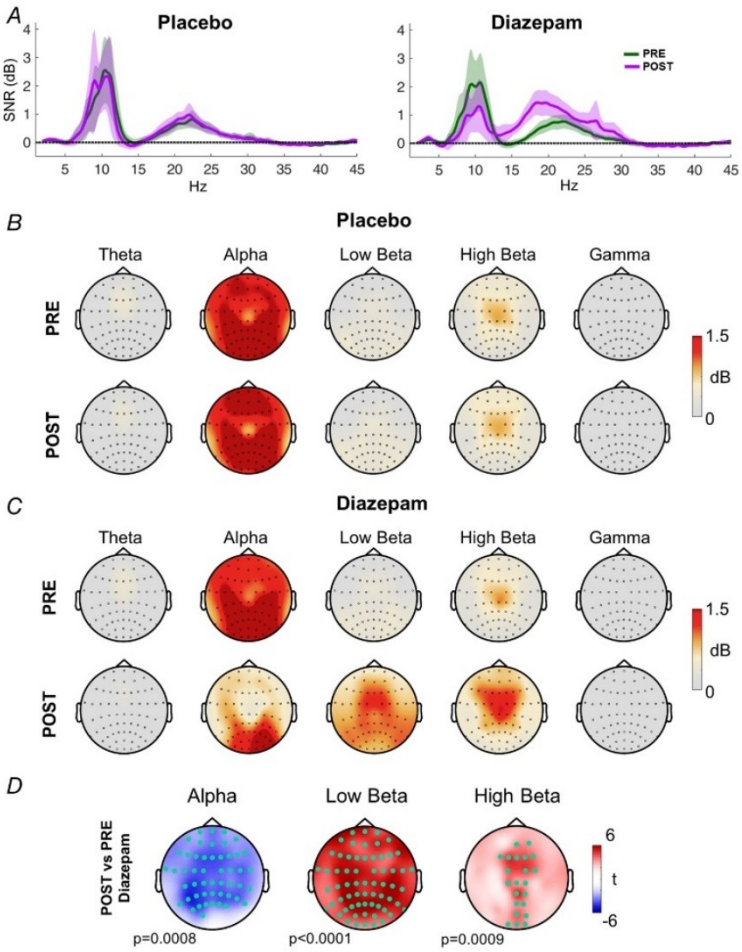

Figure 3. Resting-state EEG analyses post vs. pre drug
A, power spectra of resting-state EEG signal (shades correspond to 1 SD), obtained before (PRE, green line) and after (POST, purple line) intake of placebo (left) or diazepam (right). *B*, scalp distribution of the signal-to-noise ratio (SNR) of each frequency band of interest: theta (4–7 Hz), alpha (8–12 Hz), low beta (13–20 Hz), high beta (21–29 Hz) and gamma (30–45 Hz). Data shown correspond to the PRE (top row) and POST measurements (bottom row) of the placebo intervention. Cluster-based *t*-statistics did not yield any significant cluster when comparing the power spectra post- *vs.* pre-placebo intervention in any frequency band of interest. *C*, scalp distribution of the signal-to-noise ratio of each frequency band of interest, as in *B*, of the PRE and POST measurements of the diazepam intervention. *D*, topographical plots of the cluster-based *t*-statistics comparing the power spectra of resting-state EEG post- *vs.* pre-diazepam, highlighting the electrodes (cyan dots) that comprised the statistically significant clusters. Red and blue colours indicate increase and decrease in power, respectively. [Colour figure can be viewed at wileyonlinelibrary.com]

the low-beta frequency band in left post-central electrodes (Fig. 7 *A–B*). The analysis in source space demonstrated that TMS leads to an increased beta response in the first 200 ms after the stimulus in the stimulated sensorimotor cortical region (Fig. 7*C*), which was absent in the SHAM condition and, therefore, cannot be explained by a modulatory effect of diazepam on the responses to multisensory input.

Discussion

The present observations significantly extend the results from previous studies. In agreement with previous data, diazepam led to modulation of TMS-EEG responses at both early (<80 ms) and later latencies (Premoli et al., 2014). This was observed in the responses to ACTIVE TMS, and persisted after subtraction of the SHAM

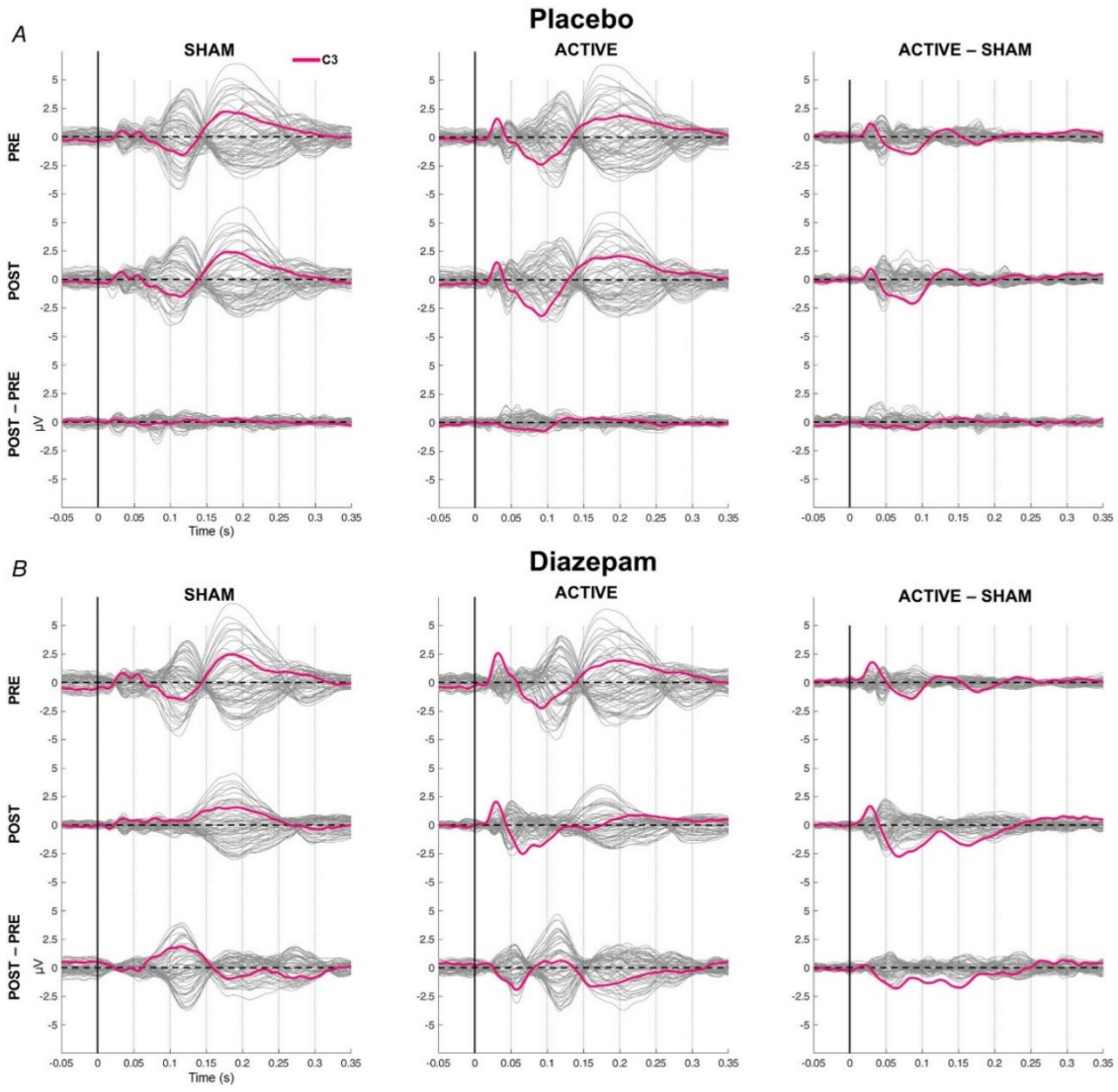

Figure 4. ACTIVE vs. SHAM TMS-EEG responses post vs. pre drug
Time course of the TMS-EEG responses to each intervention (*A*, placebo; *B*, diazepam), time (pre- and post-intervention) and stimulation condition (SHAM, ACTIVE TMS, ACTIVE TMS minus SHAM), with stimulation time marked with a black horizontal line at time = 0. Plots display averages across all subjects (n = 20), each grey line represents the signal from one EEG electrode. Red lines indicate the signals from the C3 electrode. [Colour figure can be viewed at wileyonlinelibrary.com]

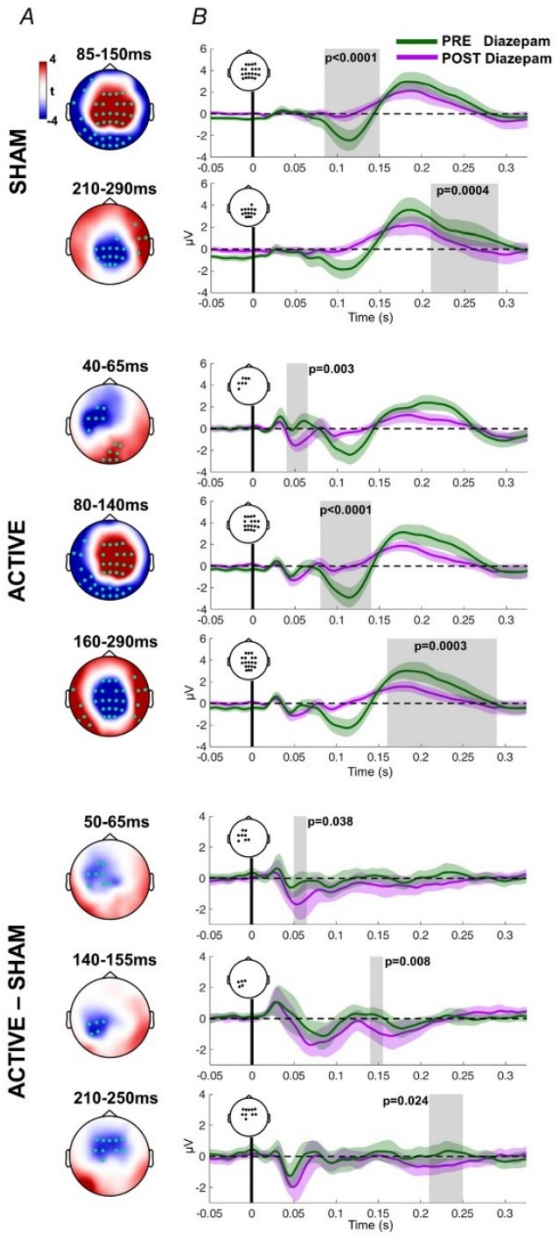

Figure 5. ACTIVE vs. SHAM TMS-EEG responses post vs. pre diazepam
A, topographical plots of the cluster-based *t*-statistics comparing TMS-EEG responses POST- and PRE-diazepam highlighting electrodes that comprised the significant clusters (cyan dots). Results are divided in responses elicited by SHAM TMS (top), ACTIVE TMS (middle) and ACTIVE TMS minus SHAM (bottom). *B*, time course of the EEG response following stimulation (indicated by black bars at time 0 s), averaged across all subjects (n = 20) and the electrodes that composed the significant clusters displayed in the respective top-left inset (black dots in the topographical model). Statistical significance of respective clusters is displayed as *P*-value. Results refer to the POST- *vs.* PRE-diazepam measurements (purple and green, respectively). Shades correspond to 1 SD. Grey areas indicate the time windows of the significant clusters. [Colour figure can be viewed at wileyonlinelibrary.com]

response from the ACTIVE TMS response, strongly suggesting a modulatory effect of diazepam on EEG responses to direct cortical activation by TMS. Another result matching previous findings was the substantial amplitude reduction of the negative TMS-EEG deflection around 100 ms (N100). However, this diazepam effect was observed in the EEG responses elicited by both ACTIVE TMS and SHAM but vanished after subtracting the SHAM from the ACTIVE TMS response. This provides evidence that the diazepam effect on the N100 amplitude was caused by PEP rather than TEP modulation. These findings have critical consequences for the implementation and interpretation of TMS-EEG experiments.

The role of PEPs in TMS-EEG

EEG responses to sensory input have long been observed in TMS-EEG experiments (Ilmoniemi & Kicic, 2010; Nikouline et al., 1999), characterized as a negative cortical deflection peaking at around 100−120 ms, predominantly expressed in the fronto-central midline scalp regions, followed by a positive deflection at around 180−200 ms in posterior regions (Ahn & Frohlich, 2021; Biabani et al., 2019; Ilmoniemi & Kicic, 2010). This pattern fits the profile of EEG responses to perceptual inputs, which are classified as event-related potentials (ERPs) (Boutros et al., 2011; Courchesne et al., 1975; Friedman et al., 2001; Lijffijt et al., 2009; Singhal et al., 2002). These ERPs, often referred to as the N100–P200 complex, can be elicited by a variety of stimuli, suggesting that the response is largely independent of the sensory modality and represents supramodal processing of perceptual inputs (Downar et al., 2002; Kenemans, 2015; Mouraux & Iannetti, 2009; Singhal et al., 2002). Multiple cortical areas contribute to this response, including superior temporal cortex, anterior and posterior cingulum, inferior parietal cortex, and broad regions of the frontal cortex, as determined by both intracranial recordings (Boutros et al., 2011) and functional MRI (Kiehl et al., 2005; Strobel et al., 2008). These ERPs have been interpreted as responses generated by cortical and subcortical networks involved in the modulation of attention and responses to unexpected or salient perceptual events (for review, Wessel & Aron, 2017).

Since TMS-EEG aims at probing focal cortical responses to direct activation by TMS, the overlapping of

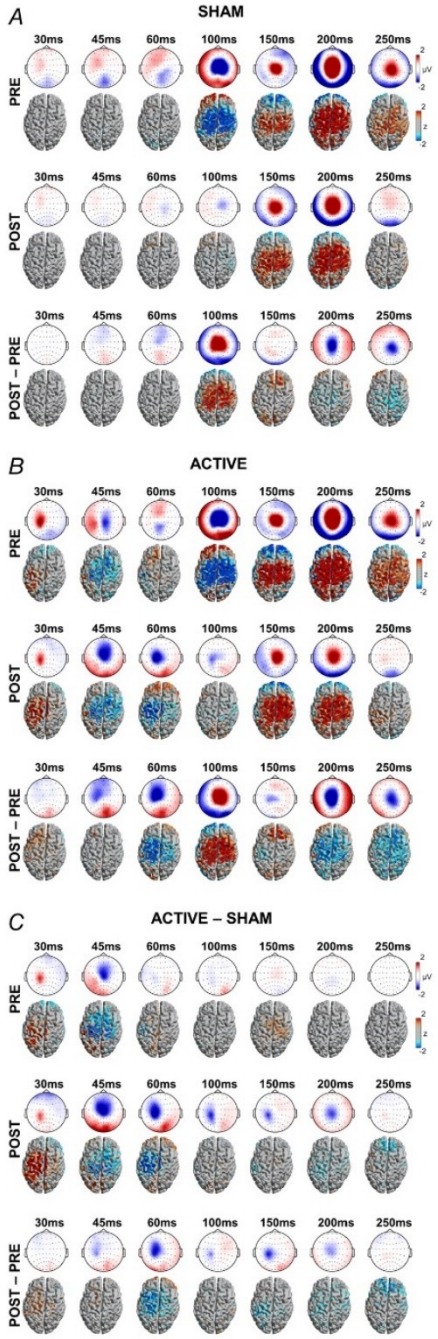

Figure 6. Topographical plots of ACTIVE vs. SHAM TMS-EEG responses post vs. pre diazepam
Topographical plots of the scalp distribution of the TMS-EEG response amplitudes following SHAM TMS (*A*), ACTIVE TMS (*B*) and ACTIVE TMS minus SHAM (*C*), at different time points, averaged across all subjects (n = 20). Data correspond to pre-diazepam (top row), post-diazepam (middle row) and post-diazepam minus pre-diazepam (bottom row). Cortical model plots below the topographical plots show source projections of the corresponding signals, displayed as z-scores. [Colour figure can be viewed at wileyonlinelibrary.com]

PEPs in the response signal represents a relevant limitation of the method. This led to attempts to control for the presence of PEPs, often by employing a control condition that recreates the same sensory inputs as the ACTIVE TMS, in the form of a SHAM TMS condition. The response signal from this sham condition can then be subtracted from the ACTIVE TMS-EEG signal, as we are proposing here. Alternative methods for removing PEP components from the TMS-EEG response include independent components analysis (Ross, Ozdemir et al., 2022) and signal-space projection (Biabani et al., 2019). Other approaches involve analysing signal similarities between TMS-EEG responses elicited by ACTIVE TMS *versus* SHAM TMS using correlation analysis (Conde et al., 2019) and cosine similarity-based analysis (Freedberg et al., 2020). These latter approaches confirmed the notion that TMS-EEG responses <80 ms after the TMS pulse are mostly free from overlapping PEPs, although they were not designed to remove PEPs from the TMS-EEG signal. Moreover, it is important to note that all methods that have attempted to remove PEPs assumed independence between PEPs and TEPs (Biabani et al., 2019). Also, they require information on the signal components that need to be removed from the data of interest, typically obtained with a SHAM TMS condition. Ideally, SHAM TMS should deliver the same multisensory inputs as ACTIVE TMS, thereby allowing the thorough removal of the PEP components from the EEG response elicited by ACTIVE TMS (Biabani et al., 2019; Casali et al., 2010; Du et al., 2017; Gordon et al., 2018; Gordon et al., 2021; Herring et al., 2015).

The role of GABAAR-mediated neurotransmission in PEPs

Several reports have consistently described ERP amplitude reductions by benzodiazepines (Lindhardt et al., 2001; Rockstroh et al., 1991; van Leeuwen et al., 1995), as well as modulation of cortical oscillatory activity (Hall et al., 2010; Saletu et al., 1994). Both ERPs and EEG oscillations are understood to result from complex cortical and sub-cortical mechanisms, including cortico-thalamic circuits involved in the generation of low-frequency oscillations, in which populations of GABAergic neurons have an integral role (Huguenard & McCormick, 2007; Ketz et al., 2015).

Increased GABAAergic tone directly affects neurotransmission in cortico-thalamic circuits, resulting in oscillatory power shifts that can be detected as increased power in the beta band in the resting-state EEG (Fig. 3*A*) and magnetoencephalography recordings (Hall et al., 2010). Several complementary functions have been attributed to cortical beta oscillations. Increased beta power has been associated with an enhanced cortical inhibitory state, which prevents the arrival of incoming information, a necessary mechanism for the maintenance of items in working memory, or the continuous execution of motor planning (Engel & Fries, 2010; Miller et al., 2018). Modulation of beta oscillations and the occurrence of bursts in the beta frequency have also been observed as a response to and processing of sensory cues and motor signals (Schmidt et al., 2019; Zavala et al., 2018). By promoting a state of increased GABAAergic tone and beta activity, diazepam leads to a deficient perception of and response to salient stimuli. This is reflected in the suppression of ERP (N100) and oscillatory responses, which have also been correlated with the behavioural and cognitive deficits caused by positive allosteric modulators of GABAARs (Lozano-Soldevilla et al., 2014).

Therefore, the observed effect of diazepam on the N100 may simply correspond to modulation of the N100–P200 complex, which we had mistakenly interpreted as GABAAergic modulation of the TMS-EEG response to direct cortical activation in previous studies (Premoli et al., 2014). Further, this novel insight may question to what extent interpretation of results from other TMS-EEG studies remain valid. For instance, TMS-EEG studies have shown an abnormally low N100 amplitude in neuropsychiatric disorders such as ADHD, schizophrenia and substance abuse (Bruckmann et al., 2012; Loheswaran et al., 2018; Noda et al., 2018). All these conditions have also been associated with

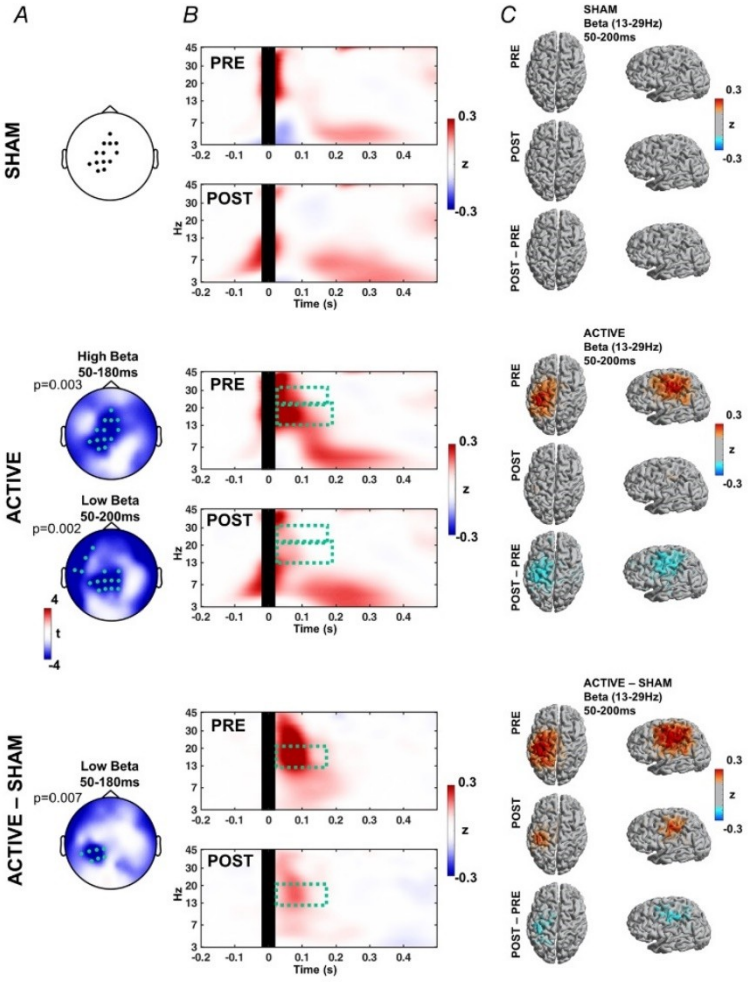

Figure 7. ACTIVE vs. SHAM TMS-induced oscillations post vs. pre diazepam
A, topographical plots of cluster-based *t*-statistics of induced oscillations post- *vs.* pre-diazepam intake, highlighting electrodes (cyan dots) that comprised the statistically significant clusters (note that no significant cluster was found in the SHAM condition). *P*-values of the respective clusters are indicated. Results are divided in induced oscillations elicited by SHAM (top), ACTIVE TMS (middle) and ACTIVE TMS minus SHAM (bottom). *B*, time–frequency plots displaying the subtraction post- minus pre-diazepam intake. Data averaged across all subjects (n = 20) and channels comprising the respective significant clusters in (*A*). For the SHAM condition, the same electrodes were used that comprised the significant cluster in the high-beta band in the ACTIVE TMS condition. Time–frequency regions of the significant clusters are outlined with cyan dotted boxes. *C*, cortical model plots show source projections of the induced oscillations post- minus pre-diazepam intake within the specified frequency and time windows. [Colour figure can be viewed at wileyonlinelibrary.com]

pathologically low sensory ERP amplitudes (Cheng et al., 2016; Rangaswamy & Porjesz, 2014; Rosburg, 2018). Likewise, consistent modulation of the N100 potential has been described following theta-burst stimulation to the prefrontal cortex (Che et al., 2019; Chung et al., 2017; Chung et al., 2019), which, given the role of prefrontal regions in the generation of ERPs, might simply indicate modulation of PEP rather than TEP amplitudes.

However, our results do not automatically imply that other previous TMS-EEG studies are to be considered invalid. In particular, TMS-EEG responses at latencies <80 ms after the TMS pulse are at low risk for being contaminated with PEPs (Ahn & Frohlich, 2021; Conde et al., 2019) and, therefore, likely represent genuine focal cortical responses to direct activation by TMS. Nevertheless, the present findings reinforce the argument that the use of proper control for PEPs is crucial in TMS-EEG experiments, to allow removal of PEPs from the TMS-EEG signal and reveal responses specifically attributed to direct cortical activation by TMS, including responses that might otherwise have been concealed by PEPs. This is the case for the positive deflection observed in the stimulated sensorimotor cortex around 150 ms after the stimulus. In a recent report (Gordon et al., 2021), we demonstrated the existence of this response to TMS of M1. However, the P150 became visible only in the ACTIVE TMS minus SHAM response. Here we show, in addition, that the P150 is suppressed by diazepam, and again, this effect could be demonstrated only in the ACTIVE TMS minus SHAM response (Figs 5 and 6*C*).

Revisiting the role of GABAAR-mediated neurotransmission in TMS-EEG

The earliest TMS-EEG response was a clearly identifiable positive deflection around 30 ms after the TMS pulse, at the stimulation site, which has been described by several previous reports (Bonato et al., 2006; Komssi et al., 2004; Lioumis et al., 2009; Paus et al., 2001). However, this deflection remained unaffected by the intake of diazepam (Fig. 6*B*). This reproduces the observations from our previous study, suggesting that this component is insensitive to GABAAR modulation (Premoli et al., 2014), while it may be suppressed by blockers of voltage-gated sodium channels, such as carbamazepine (Darmani et al., 2019). Although the origin of this component is not well understood, its amplitude is affected by the direction of the induced electrical field in the sensorimotor cortex, and some studies demonstrated a correlation with MEP amplitude, although other reports could not replicate this finding (Ahn & Frohlich, 2021; Bonato et al., 2006; Maki & Ilmoniemi, 2010).

We showed previously that the anti-glutamatergic drug perampanel (antagonist at the α-amino-3-hydroxy-5-methyl-4-isoxazole propionic acid receptor) also caused suppression of the P60 (Belardinelli et al., 2021). In combination with the diazepam effect of the present study, these results suggest that the P60 amplitude reflects an excitation/inhibition balance. Shifts towards less excitation/more inhibition result in P60 amplitude depression.

Finally, the time window and location of the P150 are similar to those of the low beta-band oscillatory response, which is also a specific response to TMS of M1 independent of sensory inputs (Gordon et al., 2021; Hannah et al., 2022). Moreover, both of these responses are suppressed by diazepam (Fig. 7) (Premoli, Bergmann et al., 2017).

Comparison with the previous pharmaco-TMS-EEG study by Premoli et al. (2014)

There are relevant methodological differences between the present and the previous pharmaco-TMS-EEG study (Premoli et al., 2014), which are most likely responsible for differences in the findings between the two studies. Firstly, we applied here subthreshold TMS intensity, whereas the previous study (Premoli et al., 2014) used TMS pulses at threshold intensity. TMS of motor cortex at suprathreshold intensities results in different TMS-EEG responses compared with subthreshold TMS (Gordon et al., 2018; Romero et al., 2019). In particular, suprathreshold stimulation elicits a prominent negative deflection in bilateral frontal and contralateral sensorimotor cortex (N45) (Biabani et al., 2019; Bonato et al., 2006; Gordon et al., 2018), compared with a more localized and lower amplitude potential elicited by subthreshold TMS (Fig. 6*B*) (Biabani et al., 2019; Bonato et al., 2006; Gordon et al., 2018). Given the capacity of suprathreshold TMS to effectively depolarize pyramidal neurons in deeper cortical layers (Romero et al., 2019), TMS pulses are likely to result in the propagation of action potentials from the target region, causing the activation of connected distant cortical areas, such as the contralateral sensorimotor cortex. Premoli et al. (2014) concluded that diazepam acted in modulating this propagation, resulting in the observed change in the N45 contralateral to the stimulation site (Premoli et al., 2014). This effect, however, was not observed in the present study, most likely because of the use of subthreshold stimulation intensity.

Moreover, suprathreshold TMS of M1 elicits negative deflections between 100 and 200 ms centred at the site of stimulation (Biabani et al., 2019; Gordon et al., 2018). Conversely, subthreshold TMS of M1 elicits a positive deflection in the stimulated sensorimotor region around 150 ms after the stimulus, which is independent of sensory input, as demonstrated here (Fig. 5) and in previous reports (Gordon et al., 2021; Hannah et al., 2022). In addition, suprathreshold TMS pulses are accompanied by another peripherally evoked response, the re-afferent

feedback resulting from the MEP-related muscle twitch (Fecchio et al., 2017; Petrichella et al., 2017). This would constitute an additional confounding factor to the TMS-EEG analysis, which explains our present choice of using a subthreshold stimulation intensity. Another crucial difference is that the previous study lacked a SHAM condition (Premoli et al., 2014). This incapacitated the previous study from disentangling TEPs from PEPs, a major limitation for interpretation of TMS-EEG responses at latencies >80 ms.

Limitations

As evident from the reported sensory input (Fig. 2), a considerable proportion of subjects could identify the TMS 'click' sound despite the masking noise. This failure to completely suppress the TMS sensory input occurs as some subjects and stimulation conditions require high TMS intensities, which produce auditory inputs that surpass the masking noise (Conde et al., 2019; Gassmann et al., 2022). TMS-related auditory inputs, however, have been successfully controlled with the introduction of a sham coil that produced the same 'click' sound as the active coil. Nevertheless, the design of effective masking noise for specific TMS setups has been facilitated with the recent development of open-source toolboxes for this purpose (Russo et al., 2022), which can create a device-specific masking noise capable of suppressing the TMS 'click' even at lower sound intensities, thus dispensing with the need for a sham control for auditory inputs.

Proper control for somatosensory inputs, however, are still necessary, especially when applying TMS to sensitive regions of the scalp or using high TMS intensities. This is evident by the detection of PEPs in TMS-EEG signal even after thorough control for auditory sources (Ross, Sarkar et al., 2022). In the present experiment, we controlled for somatosensory inputs by means of an optimized sham procedure, which is based on the assumption that the TEPs and PEPs are linearly superimposed. However, this would not be true in the case of an interaction effect between TEPs and PEPs, which would invalidate the procedure. This motivated us to design a further experiment to test this hypothesis, recently published (Gordon et al., 2023). In that experiment, we observed no evidence of TEP modulation by sensory inputs, which remained stable regardless of the concomitant PEPs. Therefore, there is currently no evidence that sensory responses interact with the cortical responses from TMS measured by EEG, further supporting the validity of the PEP subtraction from TEPs in TMS-EEG studies.

The use of high-intensity ES may still have other limitations, such as subject discomfort and increased risk of electrical artefacts in the EEG. Therefore, despite the efficacy of the present optimized SHAM procedure in removing the PEPs from the TMS-EEG signal, there is room for improvement. A possible solution could be to determine the amplitude of the PEPs elicited by TMS, and titrate ES intensity to elicit the same response, thus eliminating the need to apply ES in the ACTIVE TMS condition (Gordon et al., 2023). Moreover, other procedures to remove PEPs from the TMS-EEG response might be more reliable than the plain signal subtraction, such as the use of ICA and signal-space projection (Biabani et al., 2019; Ross, Ozdemir et al., 2022), although this will have to be further tested in future experiments.

A final issue concerns the concept of 'true' TEPs. In the present study we successfully extracted the EEG response from TMS by removing the spurious responses to sensory input. Nevertheless, the characteristics of these responses, both in time and cortical distribution, are considerably variable and dependent on several factors, including TMS intensity, exact cortical target, brain state during the stimulation and inter-individual variability. Despite standardization procedures to account for most of these factors, the inter-individual variability is still an issue that has not been systematically tackled, and which we could not address in the present study due to its limited sample size. In addition to properly controlling for PEPs, future TMS-EEG studies would benefit from accessing the role of inter-individual variability in the EEG responses to cortical TMS.

Conclusions

We demonstrated that diazepam, a positive allosteric modulator of GABAARs, specifically suppressed certain components (P60, P150, induced oscillations in the low-beta frequency band) of the ACTIVE TMS minus SHAM response, and indiscriminately suppressed the N100 component of the ACTIVE TMS and SHAM responses. These findings provide compelling evidence that the optimized SHAM condition can be used to clean PEPs from TEPs by subtraction of the SHAM from the ACTIVE TMS response. This advancement of knowledge of the physiology of TMS-EEG responses will facilitate their utilization in further physiological and clinical investigations.

References

Ahn, S., & Frohlich, F. (2021). Pinging the brain with transcranial magnetic stimulation reveals cortical reactivity in time and space. *Brain Stimulation*, **14**(2), 304–315.

Belardinelli, P., Konig, F., Liang, C., Premoli, I., Desideri, D., Muller-Dahlhaus, F., Gordon, P. C., Zipser, C., Zrenner, C., & Ziemann, U. (2021). TMS-EEG signatures of glutamatergic neurotransmission in human cortex. *Scientific Reports*, **11**(1), 8159.

Biabani, M., Fornito, A., Mutanen, T. P., Morrow, J., & Rogasch, N. C. (2019). Characterizing and minimizing the contribution of sensory inputs to TMS-evoked potentials. *Brain Stimulation*, **12**(6), 1537–1552.

Bonato, C., Miniussi, C., & Rossini, P. M. (2006). Transcranial magnetic stimulation and cortical evoked potentials: A TMS/EEG co-registration study. *Clinical Neurophysiology*, **117**(8), 1699–1707.

Boutros, N. N., Gjini, K., Urbach, H., & Pflieger, M. E. (2011). Mapping repetition suppression of the N100 evoked response to the human cerebral cortex. *Biological Psychiatry*, **69**(9), 883–889.

Bruckmann, S., Hauk, D., Roessner, V., Resch, F., Freitag, C. M., Kammer, T., Ziemann, U., Rothenberger, A., Weisbrod, M., & Bender, S. (2012). Cortical inhibition in attention deficit hyperactivity disorder: New insights from the electroencephalographic response to transcranial magnetic stimulation. *Brain*, **135**(7), 2215–2230.

Casali, A. G., Casarotto, S., Rosanova, M., Mariotti, M., & Massimini, M. (2010). General indices to characterize the electrical response of the cerebral cortex to TMS. *Neuroimage*, **49**(2), 1459–1468.

Che, X., Cash, R., Chung, S. W., Bailey, N., Fitzgerald, P. B., & Fitzgibbon, B. M. (2019). The dorsomedial prefrontal cortex as a flexible hub mediating behavioral as well as local and distributed neural effects of social support context on pain: A Theta Burst Stimulation and TMS-EEG study. *Neuroimage*, **201**, 116053.

Cheng, C. H., Chan, P. S., Hsieh, Y. W., & Chen, K. F. (2016). A meta-analysis of mismatch negativity in children with attention deficit-hyperactivity disorders. *Neuroscience Letters*, **612**, 132–137.

Chung, S. W., Lewis, B. P., Rogasch, N. C., Saeki, T., Thomson, R. H., Hoy, K. E., Bailey, N. W., & Fitzgerald, P. B. (2017). Demonstration of short-term plasticity in the dorsolateral prefrontal cortex with theta burst stimulation: A TMS-EEG study. *Clinical Neurophysiology*, **128**(7), 1117–1126.

Chung, S. W., Rogasch, N. C., Hoy, K. E., & Fitzgerald, P. B. (2015). Measuring brain stimulation induced changes in cortical properties using TMS-EEG. *Brain Stimulation*, **8**(6), 1010–1020.

Chung, S. W., Sullivan, C. M., Rogasch, N. C., Hoy, K. E., Bailey, N. W., Cash, R. F. H., & Fitzgerald, P. B. (2019). The effects of individualised intermittent theta burst stimulation in the prefrontal cortex: A TMS-EEG study. *Human Brain Mapping*, **40**(2), 608–627.

Conde, V., Tomasevic, L., Akopian, I., Stanek, K., Saturnino, G. B., Thielscher, A., Bergmann, T. O., & Siebner, H. R. (2019). The non-transcranial TMS-evoked potential is an inherent source of ambiguity in TMS-EEG studies. *Neuroimage*, **185**, 300–312.

Courchesne, E., Hillyard, S. A., & Galambos, R. (1975). Stimulus novelty, task relevance and the visual evoked potential in man. *Electroencephalography and Clinical Neurophysiology*, **39**(2), 131–143.

Darmani, G., Bergmann, T. O., Zipser, C., Baur, D., Muller-Dahlhaus, F., & Ziemann, U. (2019). Effects of antiepileptic drugs on cortical excitability in humans: A TMS-EMG and TMS-EEG study. *Human Brain Mapping*, **40**(4), 1276–1289.

Darmani, G., & Ziemann, U. (2019). Pharmacophysiology of TMS-evoked EEG potentials: A mini-review. *Brain Stimulation*, **12**(3), 829–831.

Donoghue, T., Haller, M., Peterson, E. J., Varma, P., Sebastian, P., Gao, R., Noto, T., Lara, A. H., Wallis, J. D., Knight, R. T., Shestyuk, A., & Voytek, B. (2020). Parameterizing neural power spectra into periodic and aperiodic components. *Nature Neuroscience*, **23**(12), 1655–1665.

Downar, J., Crawley, A. P., Mikulis, D. J., & Davis, K. D. (2002). A cortical network sensitive to stimulus salience in a neutral behavioral context across multiple sensory modalities. *Journal of Neurophysiology*, **87**(1), 615–620.

Du, X., Choa, F. S., Summerfelt, A., Rowland, L. M., Chiappelli, J., Kochunov, P., & Hong, L. E. (2017). N100 as a generic cortical electrophysiological marker based on decomposition of TMS-evoked potentials across five anatomic locations. *Experimental Brain Research*, **235**(1), 69–81.

Engel, A. K., & Fries, P. (2010). Beta-band oscillations–signalling the status quo? *Current Opinion in Neurobiology*, **20**(2), 156–165.

Fecchio, M., Pigorini, A., Comanducci, A., Sarasso, S., Casarotto, S., Premoli, I., Derchi, C. C., Mazza, A., Russo, S., Resta, F., Ferrarelli, F., Mariotti, M., Ziemann, U., Massimini, M., & Rosanova, M. (2017). The spectral features of EEG responses to transcranial magnetic stimulation of the primary motor cortex depend on the amplitude of the motor evoked potentials. *PLoS ONE*, **12**(9), e0184910.

Freedberg, M., Reeves, J. A., Hussain, S. J., Zaghloul, K. A., & Wassermann, E. M. (2020). Identifying site- and stimulation-specific TMS-evoked EEG potentials using a quantitative cosine similarity metric. *PLoS ONE*, **15**(1), e0216185.

Friedman, D., Cycowicz, Y. M., & Gaeta, H. (2001). The novelty P3: An event-related brain potential (ERP) sign of the brain's evaluation of novelty. *Neuroscience and Biobehavioral Reviews*, **25**(4), 355–373.

Gassmann, L., Gordon, P. C., & Ziemann, U. (2022). Assessing effective connectivity of the cerebellum with cerebral cortex using TMS-EEG. *Brain Stimulation*, **15**(6), 1354–1369.

Gordon, P. C., Desideri, D., Belardinelli, P., Zrenner, C., & Ziemann, U. (2018). Comparison of cortical EEG responses to realistic sham versus real TMS of human motor cortex. *Brain Stimulation*, **11**(6), 1322–1330.

Gordon, P. C., Jovellar, D. B., Song, Y., Zrenner, C., Belardinelli, P., Siebner, H. R., & Ziemann, U. (2021). Recording brain responses to TMS of primary motor cortex by EEG - utility of an optimized sham procedure. *Neuroimage*, **245**, 118708.

Gordon, P. C., Song, Y., Jovellar, B., Belardinelli, P., & Ziemann, U. (2023). No evidence for interaction between TMS-EEG responses and sensory inputs. *Brain Stimulation*, **16**(1), 25–27.

Grandchamp, R., & Delorme, A. (2011). Single-trial normalization for event-related spectral decomposition reduces sensitivity to noisy trials. *Frontiers in Psychology*, **2**, 236.

Groppa, S., Oliviero, A., Eisen, A., Quartarone, A., Cohen, L. G., Mall, V., Kaelin-Lang, A., Mima, T., Rossi, S., Thickbroom, G. W., Rossini, P. M., Ziemann, U., Valls-Sole, J., & Siebner, H. R. (2012). A practical guide to diagnostic transcranial magnetic stimulation: Report of an IFCN committee. *Clinical Neurophysiology*, **123**(5), 858–882.

Hall, S. D., Barnes, G. R., Furlong, P. L., Seri, S., & Hillebrand, A. (2010). Neuronal network pharmacodynamics of GABAergic modulation in the human cortex determined using pharmaco-magnetoencephalography. *Human Brain Mapping*, **31**(4), 581–594.

Hamalainen, M. S., & Ilmoniemi, R. J. (1994). Interpreting magnetic fields of the brain: Minimum norm estimates. *Medical & Biological Engineering & Computing*, **32**(1), 35–42.

Hannah, R., Muralidharan, V., & Aron, A. R. (2022). Motor cortex oscillates at its intrinsic post-movement beta rhythm following real (but not sham) single pulse, rhythmic and arrhythmic transcranial magnetic stimulation. *Neuroimage*, **251**, 118975.

Herring, J. D., Thut, G., Jensen, O., & Bergmann, T. O. (2015). Attention modulates TMS-locked alpha oscillations in the visual cortex. *Journal of Neuroscience*, **35**(43), 14435–14447.

Huguenard, J. R., & McCormick, D. A. (2007). Thalamic synchrony and dynamic regulation of global forebrain oscillations. *Trends in Neuroscience (Tins)*, **30**(7), 350–356.

Ilmoniemi, R. J., & Kicic, D. (2010). Methodology for combined TMS and EEG. *Brain Topography*, **22**(4), 233–248.

Kenemans, J. L. (2015). Specific proactive and generic reactive inhibition. *Neuroscience and Biobehavioral Reviews*, **56**, 115–126.

Ketz, N. A., Jensen, O., & O'Reilly, R. C. (2015). Thalamic pathways underlying prefrontal cortex-medial temporal lobe oscillatory interactions. *Trends in Neuroscience (Tins)*, **38**(1), 3–12.

Kiehl, K. A., Stevens, M. C., Laurens, K. R., Pearlson, G., Calhoun, V. D., & Liddle, P. F. (2005). An adaptive reflexive processing model of neurocognitive function: Supporting evidence from a large scale (n = 100) fMRI study of an auditory oddball task. *Neuroimage*, **25**(3), 899–915.

Komssi, S., & Kahkonen, S. (2006). The novelty value of the combined use of electroencephalography and transcranial magnetic stimulation for neuroscience research. *Brain Research Reviews*, **52**(1), 183–192.

Komssi, S., Kahkonen, S., & Ilmoniemi, R. J. (2004). The effect of stimulus intensity on brain responses evoked by transcranial magnetic stimulation. *Human Brain Mapping*, **21**(3), 154–164.

Lijffijt, M., Lane, S. D., Meier, S. L., Boutros, N. N., Burroughs, S., Steinberg, J. L., Moeller, F. G., & Swann, A. C. (2009). P50, N100, and P200 sensory gating: Relationships with behavioral inhibition, attention, and working memory. *Psychophysiology*, **46**(5), 1059–1068.

Lindhardt, K., Gizurarson, S., Stefansson, S. B., Olafsson, D. R., & Bechgaard, E. (2001). Electroencephalographic effects and serum concentrations after intranasal and intravenous administration of diazepam to healthy volunteers. *British Journal of Clinical Pharmacology*, **52**(5), 521–527.

Lioumis, P., Kicic, D., Savolainen, P., Makela, J. P., & Kahkonen, S. (2009). Reproducibility of TMS-Evoked EEG responses. *Human Brain Mapping*, **30**(4), 1387–1396.

Loheswaran, G., Barr, M. S., Zomorrodi, R., Rajji, T. K., Blumberger, D. M., Le Foll, B., & Daskalakis, Z. J. (2018). Alcohol impairs N100 response to dorsolateral prefrontal cortex stimulation. *Scientific Reports*, **8**(1), 3428.

Lozano-Soldevilla, D., ter Huurne, N., Cools, R., & Jensen, O. (2014). GABAergic modulation of visual gamma and alpha oscillations and its consequences for working memory performance. *Current Biology*, **24**(24), 2878–2887.

Maki, H., & Ilmoniemi, R. J. (2010). The relationship between peripheral and early cortical activation induced by transcranial magnetic stimulation. *Neuroscience Letters*, **478**(1), 24–28.

Massimini, M., Ferrarelli, F., Huber, R., Esser, S. K., Singh, H., & Tononi, G. (2005). Breakdown of cortical effective connectivity during sleep. *Science*, **309**(5744), 2228–2232.

Miller, E. K., Lundqvist, M., & Bastos, A. M. (2018). Working memory 2.0. *Neuron*, **100**(2), 463–475.

Mouraux, A., & Iannetti, G. D. (2009). Nociceptive laser-evoked brain potentials do not reflect nociceptive-specific neural activity. *Journal of Neurophysiology*, **101**(6), 3258–3269.

Nikouline, V., Ruohonen, J., & Ilmoniemi, R. J. (1999). The role of the coil click in TMS assessed with simultaneous EEG. *Clinical Neurophysiology*, **110**(8), 1325–1328.

Noda, Y., Barr, M. S., Zomorrodi, R., Cash, R. F. H., Rajji, T. K., Farzan, F., Chen, R., George, T. P., Daskalakis, Z. J., & Blumberger, D. M. (2018). Reduced short-latency afferent inhibition in prefrontal but not motor cortex and its association With executive function in Schizophrenia: A combined TMS-EEG study. *Schizophrenia Bulletin*, **44**(1), 193–202.

Oldfield, R. C. (1971). The assessment and analysis of handedness: the Edinburgh inventory. *Neuropsychologia*, **9**(1), 97–113.

Oostenveld, R., Fries, P., Maris, E., & Schoffelen, J. M. (2011). FieldTrip: Open source software for advanced analysis of MEG, EEG, and invasive electrophysiological data. *Computational Intelligence and Neuroscience*, **2011**, 156869.

Paus, T., Sipila, P. K., & Strafella, A. P. (2001). Synchronization of neuronal activity in the human primary motor cortex by transcranial magnetic stimulation: An EEG study. *Journal of Neurophysiology*, **86**(4), 1983–1990.

Pellicciari, M. C., Veniero, D., & Miniussi, C. (2017). Characterizing the cortical oscillatory response to TMS pulse. *Frontiers in Cellular Neuroscience*, **11**, 38.

Petrichella, S., Johnson, N., & He, B. (2017). The influence of corticospinal activity on TMS-evoked activity and connectivity in healthy subjects: A TMS-EEG study. *PLoS ONE*, **12**(4), e0174879.

Premoli, I., Bergmann, T. O., Fecchio, M., Rosanova, M., Biondi, A., Belardinelli, P., & Ziemann, U. (2017). The impact of GABAergic drugs on TMS-induced brain oscillations in human motor cortex. *Neuroimage*, **163**, 1–12.

Premoli, I., Biondi, A., Carlesso, S., Rivolta, D., & Richardson, M. P. (2017). Lamotrigine and levetiracetam exert a similar modulation of TMS-evoked EEG potentials. *Epilepsia*, **58**(1), 42–50.

Premoli, I., Castellanos, N., Rivolta, D., Belardinelli, P., Bajo, R., Zipser, C., Espenhahn, S., Heidegger, T., Muller-Dahlhaus, F., & Ziemann, U. (2014). TMS-EEG signatures of GABAergic neurotransmission in the human cortex. *Journal of Neuroscience*, **34**(16), 5603–5612.

Rangaswamy, M., & Porjesz, B. (2014). Understanding alcohol use disorders with neuroelectrophysiology. *Handbook of Clinical Neurology*, **125**, 383–414.

Rockstroh, B., Elbert, T., Lutzenberger, W., & Altenmuller, E. (1991). Effects of the anticonvulsant benzodiazepine clonazepam on event-related brain potentials in humans. *Electroencephalography and Clinical Neurophysiology*, **78**(2), 142–149.

Rogasch, N. C., Sullivan, C., Thomson, R. H., Rose, N. S., Bailey, N. W., Fitzgerald, P. B., Farzan, F., & Hernandez-Pavon, J. C. (2017). Analysing concurrent transcranial magnetic stimulation and electroencephalographic data: A review and introduction to the open-source TESA software. *Neuroimage*, **147**, 934–951.

Rogasch, N. C., Thomson, R. H., Farzan, F., Fitzgibbon, B. M., Bailey, N. W., Hernandez-Pavon, J. C., Daskalakis, Z. J., & Fitzgerald, P. B. (2014). Removing artefacts from TMS-EEG recordings using independent component analysis: Importance for assessing prefrontal and motor cortex network properties. *Neuroimage*, **101**, 425–439.

Romero, M. C., Davare, M., Armendariz, M., & Janssen, P. (2019). Neural effects of transcranial magnetic stimulation at the single-cell level. *Nature Communications*, **10**(1), 2642.

Rosburg, T. (2018). Auditory N100 gating in patients with schizophrenia: A systematic meta-analysis. *Clinical Neurophysiology*, **129**(10), 2099–2111.

Ross, J. M., Ozdemir, R. A., Lian, S. J., Fried, P. J., Schmitt, E. M., Inouye, S. K., Pascual-Leone, A., & Shafi, M. M. (2022). A structured ICA-based process for removing auditory evoked potentials. *Scientific Reports*, **12**(1), 1391.

Ross, J. M., Sarkar, M., & Keller, C. J. (2022). Experimental suppression of transcranial magnetic stimulation-electroencephalography sensory potentials. *Human Brain Mapping*.**43**(17), 5141–5153.

Russo, S., Sarasso, S., Puglisi, G. E., Dal Palu, D., Pigorini, A., Casarotto, S., D'Ambrosio, S., Astolfi, A., Massimini, M., Rosanova, M., & Fecchio, M. (2022). TAAC - TMS adaptable auditory control: A universal tool to mask TMS clicks. *Journal of Neuroscience Methods*, **370**, 109491.

Saletu, B., Grunberger, J., Linzmayer, L., Semlitsch, H. V., Anderer, P., & Chwatal, K. (1994). Pharmacokinetic and -dynamic studies with a new anxiolytic, suriclone, utilizing EEG mapping and psychometry. *British Journal of Clinical Pharmacology*, **37**(2), 145–156.

Schmidt, R., Herrojo Ruiz, M., Kilavik, B. E., Lundqvist, M., Starr, P. A., & Aron, A. R. (2019). Beta oscillations in working memory, executive control of movement and thought, and sensorimotor function. *Journal of Neuroscience*, **39**(42), 8231–8238.

Shader, R. I., Pary, R. J., Harmatz, J. S., Allison, S., Locniskar, A., & Greenblatt, D. J. (1984). Plasma concentrations and clinical effects after single oral doses of prazepam, clorazepate, and diazepam. *Journal of Clinical Psychiatry*, **45**(10), 411–413.

Singhal, A., Doerfling, P., & Fowler, B. (2002). Effects of a dual task on the N100-P200 complex and the early and late Nd attention waveforms. *Psychophysiology*, **39**(2), 236–245.

Stenroos, M., & Nummenmaa, A. (2016). Incorporating and compensating cerebrospinal fluid in surface-based forward models of magneto- and electroencephalography. *PLoS ONE*, **11**(7), e0159595.

Stenroos, M., & Sarvas, J. (2012). Bioelectromagnetic forward problem: Isolated source approach revis(it)ed. *Physics in Medicine and Biology*, **57**(11), 3517–3535.

Strobel, A., Debener, S., Sorger, B., Peters, J. C., Kranczioch, C., Hoechstetter, K., Engel, A. K., Brocke, B., & Goebel, R. (2008). Novelty and target processing during an auditory novelty oddball: A simultaneous event-related potential and functional magnetic resonance imaging study. *Neuroimage*, **40**(2), 869–883.

Tremblay, S., Rogasch, N. C., Premoli, I., Blumberger, D. M., Casarotto, S., Chen, R., Di Lazzaro, V., Farzan, F., Ferrarelli, F., Fitzgerald, P. B., Hui, J., Ilmoniemi, R. J., Kimiskidis, V. K., Kugiumtzis, D., Lioumis, P., Pascual-Leone, A., Pellicciari, M. C., Rajji, T., Thut, G., … Daskalakis, Z. J. (2019). Clinical utility and prospective of TMS-EEG. *Clinical Neurophysiology*, **130**(5), 802–844.

van Leeuwen, T. H., Verbaten, M. N., Koelega, H. S., Slangen, J. L., van der Gugten, J., & Camfferman, G. (1995). Effects of oxazepam on event-related brain potentials, EEG frequency bands, and vigilance performance. *Psychopharmacology*, **122**(3), 244–262.

Wessel, J. R., & Aron, A. R. (2017). On the globality of motor suppression: Unexpected events and their influence on behavior and cognition. *Neuron*, **93**(2), 259–280.

Zavala, B., Jang, A., Trotta, M., Lungu, C. I., Brown, P., & Zaghloul, K. A. (2018). Cognitive control involves theta power within trials and beta power across trials in the prefrontal-subthalamic network. *Brain*, **141**(12), 3361–3376.

Ziemann, U., Reis, J., Schwenkreis, P., Rosanova, M., Strafella, A., Badawy, R., & Muller-Dahlhaus, F. (2015). TMS and drugs revisited 2014. *Clinical Neurophysiology*, **126**(10), 1847–1868.

Additional information

Data availability statement

Data can be made available upon request.

MATLAB scripts, including the EEG pre-processing pipeline and statistics, are available at https://github.com/pcgordon/optimized_supraliminal_sham. These codes were designed for using the open-source toolbox Fieldtrip, version 20 210 212 (https://www.fieldtriptoolbox.org/).

Competing interests

U.Z. reports a grant from TAKEDA Millennium Pharmaceuticals, Inc., and personal consulting fees from CorTec GmbH, all outside the submitted work. All other authors declare no further competing financial interests.

Author contributions

The experiments described in this study were performed in the Brain Networks and Plasticity Laboratory, University of Tübingen. P.C.G. and U.Z. designed the study protocol. P.C.G. set up the experiment and obtained ethics committee approval; P.B. and P.C.G. designed the algorithms for experiments and analyses. M.R. contributed with the exponential decay artefact removal algorithm. P.B. created the head models. B.J., P.C.G, and Y.F.S. conducted the experiments. P.C.G. analysed the experimental data. U.Z. critically reviewed the final manuscript. All authors contributed to the writing of the manuscript and approved its final version.

Funding

P.C.G. reports funding from the German Research Foundation (Deutsche Forschungsgemeinschaft – DFG – project number 466 458 984). Furthermore, this project has received funding to U.Z. from the European Research Council (ERC) under the European Union's Horizon 2020 research and innovation programme (ConnectToBrain, ERC synergy grant agreement No 810 377).

Acknowledgements

Open access funding enabled and organized by Projekt DEAL.

Keywords

electroencephalography, GABA, inhibition, peripherally evoked potentials, pharmaco-TMS-EEG, sham stimulation, TMS-EEG, transcranial magnetic stimulation

Supporting information

Additional supporting information can be found online in the Supporting Information section at the end of the HTML view of the article. Supporting information files available:

Statistical Summary Document
Peer Review History

2.3 *No evidence for interaction between TMS-EEG responses and sensory inputs*

(by Pedro C. Gordon, Yu Fei Song, D. Blair Jovellar, Paolo Belardinelli and Ulf Ziemann; published in Brain Stimul. 2023 Jan-Feb;16(1):25-27. doi: 10.1016/j.brs.2022.12.010.)

Brain Stimulation 16 (2023) 25–27

Contents lists available at ScienceDirect

Brain Stimulation

journal homepage: http://www.journals.elsevier.com/brain-stimulation

No evidence for interaction between TMS-EEG responses and sensory inputs

There is considerable ongoing discussion on the relevance of peripherally evoked potentials (PEPs) in TMS-EEG measurements. These PEPs are elicited by the auditory and somatosensory inputs caused by TMS, potentially becoming overlapped with TMS evoked potentials (TEPs). There is consensus that this overlapping presents an inherent challenge for TMS-EEG investigations [1–3]. Nevertheless, there is to this date no agreement on how to best address this issue [4,5]. Proposed solutions commonly involve the use of a control condition in the form of sham TMS that aims at eliciting sensory input akin to real TMS. In principle, once one has identified the EEG responses to such sensory input, these can be removed from the real TMS response signal [6,7]. However, previous attempts suffered from methodological flaws [2,5], as the proposed sham conditions have failed to fully mimic the sensory inputs from real TMS, leaving the issue unresolved.

To overcome these challenges, we have designed a method which aimed at equivalence of EEG responses to sensory inputs from the real and the sham TMS [1]. In brief, our method consisted of causing somatosensory input in both the sham and real TMS conditions by means of high-intensity electrical stimulation (ES) of the scalp, to the extent to saturate the PEP amplitude. Therefore, additional somatosensory input from the real TMS condition becomes negligible in this saturated somatosensory evoked potential. Subtracting the EEG response to sham TMS from the EEG response to real TMS should then remove the somatosensory evoked potentials. The resulting EEG deflections <80 ms after the TMS pulse are minimally affected by PEPs. Later responses were predominantly localized at the site of the stimulated motor cortex, but obscured by PEPs without the subtraction [1].

Our proposed method, however, was criticized for its use of high-intensity somatosensory inputs. It was suggested that high-intensity peripheral stimulation might interact with the brain response to TMS. This has been, for example, inferred from recent work that showed modulation of corticospinal excitability by auditory and somatosensory stimuli [8]. Although modulation of TEPs by sensory inputs has not been directly demonstrated to this date, it would imply that EEG responses observed by our method would not correspond to “true” TEPs, but instead to TEPs that are modulated by concomitant sensory input. Moreover, this possible interaction between PEPs and TEPs would also imply that these responses are non-linearly intertwined, which would challenge attempts by us and others to remove PEPs from TMS-EEG responses by simple subtraction.

Given the importance of this unresolved issue for the TMS-EEG field, we sought to experimentally test TEP modulation by somatosensory input. We compared EEG responses from three different single-pulse TMS conditions in 12 healthy right-handed volunteers: 6 female (50%), mean age 25 years, age range 20–32 years. All 3 conditions consisted of REAL TMS targeting the left primary motor cortex at an intensity 90% of the resting motor threshold, and 140 pulses per condition were applied. Moreover, in all conditions 140 trials of SHAM TMS were randomly interleaved with the REAL TMS trials, using a sham coil to produce click sound and ES of the scalp. ES was delivered by 2 pairs of 1 cm diameter electrodes placed between the EEG electrodes, one pair of opposite polarity placed at the FCC4h and CCP4h EEG electrode positions, and the other at TPP7h and TPP9h. These positions were chosen to generate somatosensory input from a broad scalp region around the TMS target. Masking noise was used throughout all measurements (Fig. 1A).

The 3 TMS conditions differed as follows: In Condition 1, ES (pulse width, 200 μs) was applied to the scalp with an intensity of 400% sensory perception threshold, both during the REAL TMS and SHAM trials (as described in our previous report [1]). In Condition 2, ES was also applied in both REAL TMS and SHAM trials, but the intensity was 800% of sensory perception threshold. Condition 3 consisted simply of REAL TMS without concomitant ES. However, somatosensory inputs from the TMS pulse *per se* also cause PEPs in TMS-EEG experiments [2,9], suggesting that the SHAM condition should contain an equivalent somatosensory input. For this reason, SHAM in Condition 3 consisted of individually titrated ES intensity, so that the PEP amplitude in this SHAM condition matched the PEP amplitude in the REAL TMS condition (Fig. 1A). In summary, REAL TMS is the same in all conditions, while the intensity of concomitant somatosensory input is considerably different. Crucially, for interpretation of our experimental data, the existence of any significant modulatory effect of somatosensory input on the EEG response evoked by TMS should then translate into differences between conditions, detectable in the EEG responses to REAL TMS after subtraction of the EEG responses to SHAM TMS. In contrast, absence of a significant modulatory effect should result in identical EEG responses after subtraction.

https://doi.org/10.1016/j.brs.2022.12.010

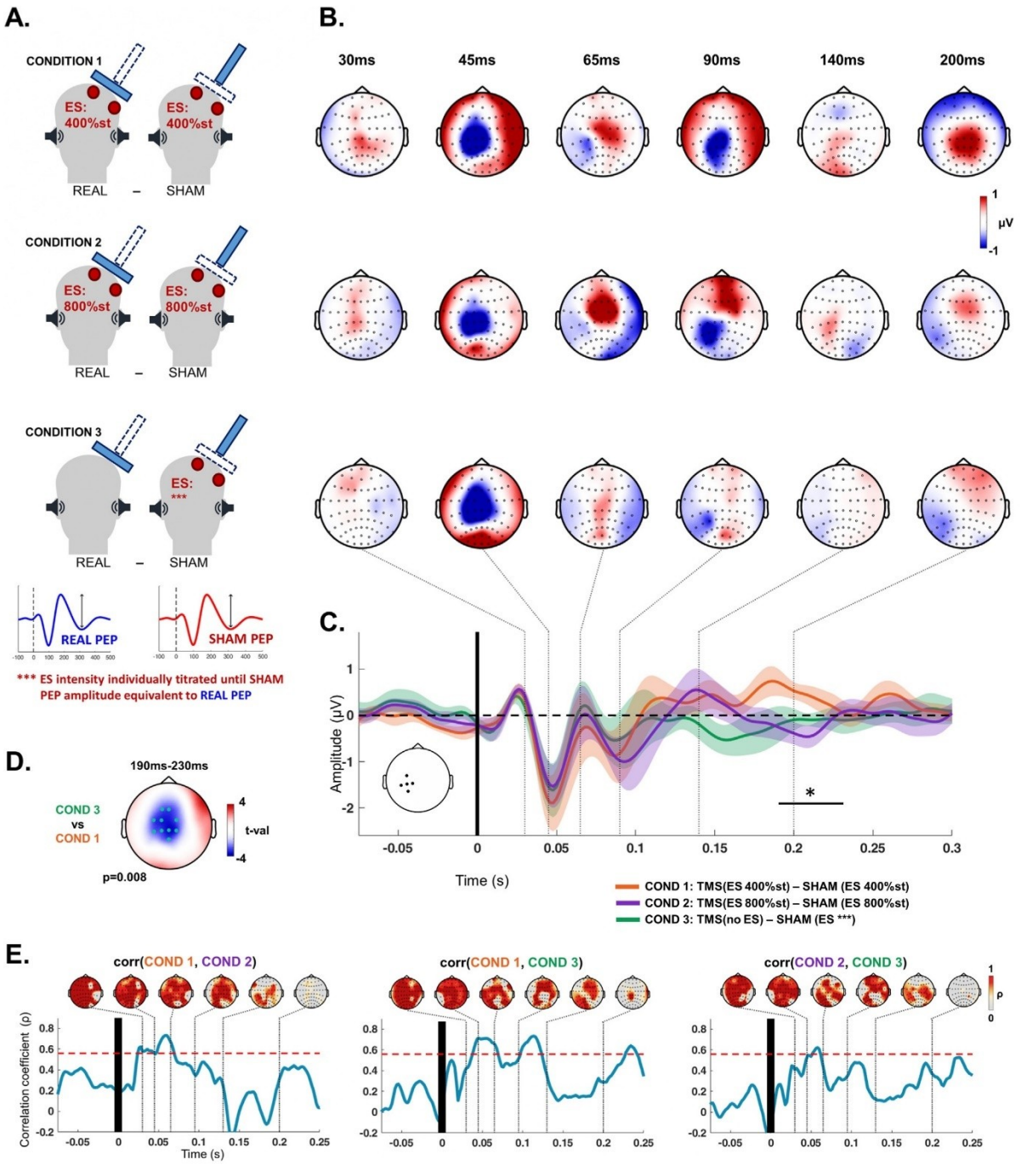
A.
CONDITION 1
ES: 400%st
ES: 400%st
REAL – SHAM
CONDITION 2
ES: 800%st
ES: 800%st
REAL – SHAM
CONDITION 3
ES: ***
REAL – SHAM
REAL PEP
SHAM PEP
*** ES intensity individually titrated until SHAM PEP amplitude equivalent to REAL PEP
B.
30ms
45ms
65ms
90ms
140ms
200ms
1
μV
-1
C.
Amplitude (μV)
Time (s)
COND 1: TMS(ES 400%st) – SHAM (ES 400%st)
COND 2: TMS(ES 800%st) – SHAM (ES 800%st)
COND 3: TMS(no ES) – SHAM (ES ***)
D.
190ms-230ms
COND 3
vs
COND 1
t-val
p=0.008
E.
corr(COND 1, COND 2)
corr(COND 1, COND 3)
corr(COND 2, COND 3)
Correlation coefficient (ρ)
Time (s)
ρ

Fig. 1. A. Representation of the 3 stimulation conditions. The blue rectangle represents the TMS coil (real coil parallel to the scalp, sham coil perpendicular to the scalp). Black sound icons represent the masking noise. Red dots represent the electrodes for the electric stimulation (ES), with the intensity of the ES specified in the figure. Note that the ES for Condition 3 was individually titrated. This was done by delivering 40 pulses using REAL TMS to left primary motor cortex at 90% of resting motor threshold, and calculating the amplitude of the response signal from electrode FCz (against an average reference) by taking the difference between the positive peak at around 200 ms and the negative peak at around 300 ms. The procedure was then repeated, but using scalp ES instead of the REAL TMS, until the amplitude of the evoked response matched that from the REAL TMS (average of 30 trials per intensity step).
B. Topographical plots representing the scalp distribution of the EEG response amplitudes (REAL TMS minus SHAM TMS) divided by the 3 stimulation conditions, as indicated to the left (A.).
C. Time course of the EEG response from the 3 conditions, averaged across all subjects (n = 12) and electrodes around the stimulated region (depicted in the scalp electrodes model). The shaded areas represent ±1 S E M. Horizontal black bar (*) indicate the time window where the cluster-based ANOVA identified significant differences between conditions.
D. Topographical plot of the *post-hoc* cluster-based *t*-statistics showing the single statistically significant cluster (between Conditions 1 and 3). Cyan dots represent the electrodes that compose the significant cluster. The p-value is indicated.
E. Spearman correlation statistics of the signals (REAL TMS minus SHAM TMS) between the 3 stimulation conditions, averaged across all subjects (coefficients are z-transformed). Topographical plots display the spatial distribution of the correlation coefficients (ρ) in selected time windows after the stimulus (as in B.). Time course plots display the temporal progression of the correlation coefficients (ρ) averaged across all channels. Red dotted lines represent the significance threshold (p = 0.05) for 10° of freedom (df = n−2; n = sample size). (For interpretation of the references to colour in this figure legend, the reader is referred to the Web version of this article.)

The TMS-EEG signals were processed using established methods, which included visual inspection and exclusion of individual trials containing excessive artifacts, followed by the clipping and interpolation of the signal within the time window around the TMS artifact (−2 ms–14 ms), and lastly independent component analysis aimed at removing further artifacts, namely eye blinks, eye movement and cranial muscle activity [10]. The resulting TMS-EEG responses from the 3 conditions were statistically compared using a cluster-based ANOVA aimed at identifying time-windows of significantly difference, followed by post hoc cluster-based dependent samples t-tests. The TMS-EEG responses were also compared with respect to their spatial similarity by means of pairwise correlation analysis [2].

Fig. 1B–C shows that the EEG responses to REAL TMS after subtraction of SHAM TMS were similar across the 3 conditions. Moreover, Fig. 1E demonstrates that these responses are significantly correlated in their time course and spatial distribution, especially within the first 100 ms after stimulation. Together, this is compelling evidence in favor of the notion that somatosensory input does not significantly interact with the EEG response caused by TMS. Therefore, the EEG response to REAL TMS after subtraction of the response to SHAM TMS can be considered a "true" TEP.

Only one significant difference was detected in the amplitude of late potentials from Condition 3 compared to Condition 1 (Fig. 1C–D). However, these late potentials are not typical of TEPs, and given their latency and midline distribution, most likely represent PEPs. It is possible that the individually titrated SHAM in Condition 3 did not appropriately match the PEPs from the REAL TMS condition and/or that the 400% ES was insufficient to saturate the PEPs.

In summary, this implies that the optimized sham method that we have proposed [1], which depends on application of high-intensity somatosensory stimulation to saturate the somatosensory evoked potential, is valid for removing PEPs and obtaining the true EEG responses to direct cortical activation by TMS. On a more general note, it follows that methods of PEP removal from the TEP signals that assume independence of the two signals, such as independent component analysis [7], SSP-SIR [6], or a simple arithmetical subtraction, are valid, provided that the PEPs in the SHAM condition match those caused by REAL TMS.

It is important to note that the present data does not constitute incontrovertible evidence against modifiability of motor cortex excitability by sensory input. It is simply possible that TMS-EEG just is not sensitive to this modulatory effect.

Declaration of competing interest

The authors declare that they have no known competing financial interests or personal relationships that could have appeared to influence the work reported in this paper.

References

[1] Gordon PC, Jovellar DB, Song Y, Zrenner C, Belardinelli P, Siebner HR, et al. Recording brain responses to TMS of primary motor cortex by EEG - utility of an optimized sham procedure. Neuroimage 2021;245:118708.
[2] Conde V, Tomasevic L, Akopian I, Stanek K, Saturnino GB, Thielscher A, et al. The non-transcranial TMS-evoked potential is an inherent source of ambiguity in TMS-EEG studies. Neuroimage 2019;185:300–12.
[3] Rocchi L, Di Santo A, Brown K, Ibanez J, Casula E, Rawji V, et al. Disentangling EEG responses to TMS due to cortical and peripheral activations. Brain Stimul 2021;14(1):4–18.
[4] Belardinelli P, Biabani M, Blumberger DM, Bortoletto M, Casarotto S, David O, et al. Reproducibility in TMS-EEG studies: a call for data sharing, standard procedures and effective experimental control. Brain Stimul 2019;12(3):787–90.
[5] Siebner HR, Conde V, Tomasevic L, Thielscher A, Bergmann TO. Distilling the essence of TMS-evoked EEG potentials (TEPs): a call for securing mechanistic specificity and experimental rigor. Brain Stimul 2019;12(4):1051–4.
[6] Biabani M, Fornito A, Mutanen TP, Morrow J, Rogasch NC. Characterizing and minimizing the contribution of sensory inputs to TMS-evoked potentials. Brain Stimul 2019;12(6):1537–52.
[7] Ross JM, Ozdemir RA, Lian SJ, Fried PJ, Schmitt EM, Inouye SK, et al. A structured ICA-based process for removing auditory evoked potentials. Sci Rep 2022;12(1):1391.
[8] Novembre G, Pawar VM, Kilintari M, Bufacchi RJ, Guo Y, Rothwell JC, et al. The effect of salient stimuli on neural oscillations, isometric force, and their coupling. Neuroimage 2019;198:221–30.
[9] Ross JM, Sarkar M, Keller CJ. Experimental suppression of transcranial magnetic stimulation-electroencephalography sensory potentials. Hum Brain Mapp 2022;43(17):5141–53.
[10] Rogasch NC, Sullivan C, Thomson RH, Rose NS, Bailey NW, Fitzgerald PB, et al. Analysing concurrent transcranial magnetic stimulation and electroencephalographic data: a review and introduction to the open-source TESA software. Neuroimage 2017;147:934–51.

Pedro C. Gordon, Yufei Song, Blair Jovellar
Department of Neurology & Stroke, University of Tübingen, Germany
Hertie Institute for Clinical Brain Research, University of Tübingen, Germany
Paolo Belardinelli
Department of Neurology & Stroke, University of Tübingen, Germany
Hertie Institute for Clinical Brain Research, University of Tübingen, Germany
CIMeC, Center for Mind/Brain Sciences, University of Trento, Italy
Ulf Ziemann*
Department of Neurology & Stroke, University of Tübingen, Germany
Hertie Institute for Clinical Brain Research, University of Tübingen, Germany

* Corresponding author.
E-mail address: ulf.ziemann@uni-tuebingen.de (U. Ziemann).

30 September 2022
Available online 22 December 2022

3. Discussion

3.1 Designing the optimized sham procedure for TMS-EEG

As stated in the Aims/Objectives, the optimized sham procedure for TMS-EEG needed to both reliably recreate the same sensory inputs as the real TMS pulse and evoke the same electrophysiological responses to its sensory inputs. We reasoned that the optimized sham should contain an auditory and a somatosensory component, with the auditory component being generated by a sham coil and the somatosensory component by electric stimulation (ES) to the scalp, as applied in several previous studies (Biabani et al., 2019; Conde et al., 2019; Gordon et al., 2018; Raffin et al., 2020; Rocchi et al., 2021). Differently from these previous attempts, however, we aimed to test several possible configurations of sensory stimuli that would make the sham condition optimal according to our stated criteria and, thus, succeeding where others have failed.

To evaluate whether the sham condition evokes the same sensorial perception as the real TMS we applied two measures: a quantitative assessment of perceived stimuli from the sham and the real TMS, in the form of a visual analogue scale, and the accuracy with which one can distinguish between these two, in the form of a series of two-alternative forced choice trials that blindly presented either the sham or real TMS.

In the pilot phase of the first experiment, we ascertained through sound pressure measurements that the incoming sound from both the real and sham TMS were reaching the subject's ears with the same intensity, then calibrating the sham coil intensity accordingly. To further blur the auditory inputs from these two sources we also added the delivery of masking noise, a standard procedure in TMS-EEG (Russo et al., 2022; ter Braack et al., 2015). The pilot measurements suggested that the conditions for an optimized sham procedure were easily satisfied with regards to the auditory stimulus. However, the same could not be said for the somatosensory input. Regardless of the set-up arrangement tested, be it electrode array disposition on the scalp, pulse width, ES intensity used, or even with precisely calibrated intensity to try to match the real TMS sensation; most subjects could still effortlessly distinguish real and sham TMS. This sobering realization clarifies a possible reason why previous attempts have failed.

Our solution to this problem was to apply high-intensity ES in the sham condition as well as in the real TMS condition, forcing the two conditions to be indistinguishable. This is based on the psychophysical principle that states that the „noticeable difference“ threshold to distinguish between two stimuli of increasing intensity rises in a fractional way, not absolute (Gescheider, 1997). For instance, given a condition in which the first stimulus with a pressure of 100 kPa can be discriminated from a second stimulus when the latter reaches a pressure of 110 kPa (10% higher), then if the first stimulus is increased to 1000 kPa the second stimulus will only be discriminated with intensities around 1100kPa (fractional difference of 10%), and not 1010 kPa (which would be the case for absolute differences). That means that by delivering high-intensity ES in both conditions, any further small somatosensory inputs would not result in a detectable increase in the SEP amplitude, including the somatosensory input from real TMS. Moreover, the same principle applies for electrophysiological responses, so that the constant increasing of a given stimulus intensity pushes the PEP amplitudes closer to a saturation point in which small stimuli differences do not lead to a measurable difference in response (Lin et al., 2003; Torquati et al., 2002). These properties could yield an optimized sham procedure for TMS-EEG that could satisfy our established necessary criteria for optimized sham.

3.2 Testing the optimized sham procedure for TMS-EEG

We first attempted to ascertain whether our optimized sham procedure satisfied the first criterion, namely that it reliably recreates the same sensory inputs as the real TMS. On the quantitative assessment of perceived stimuli, the reported perception showed no statistical difference between the sham and real TMS conditions, regardless of the sensory modality (2.1 Figure 3A), suggesting a satisfactory match. However, when testing the accuracy of distinguishing the 2 conditions, 44% of subjects had an accuracy above the level for random answers, with 3 subjects having an accuracy above 95%, thus clearly being able to distinguish the two conditions (2.1 Figure 3B).

A possible explanation for some subjects being able to distinguish the two conditions might be that, in their cases, there was a trend towards different perceived sensorial stimuli, which might have not been observable in the analysis of the whole population. However, by dividing the quantitative assessment of perceived stimuli between individuals who were able to distinguish the conditions and those who were not, there was no significant difference (2.1 Figure 3E). Interestingly, this is in line with our

observations from the pilot measurements, in which no matter how we designed an ES condition to be similar to the real TMS, subjects were still able to tell them apart, even if they could not clearly formulate what sensorial phenomenon indicated the difference. This should not come as a surprise, given that the resulting electric fields from TMS and electric stimuli to the scalp have very different conformations and most certainly activate peripheral nerves differently, likely resulting in the individual identifying the nature of each condition, even if only at a subliminal level.

In summary, regarding the attempt to fulfill the first criterion, our optimized sham procedure was a partial success. While the perceived sensory input between the two conditions was highly comparable, almost half the sample could, to some extent, detect slight differences between the sham and real TMS, indicating some difference in sensory inputs between the real and sham conditions.

Regarding the second criterion, we reasoned that for our current design of optimized sham procedure to elicit the same PEPs as the real TMS, both containing high intensity ES, any further increase in sensory stimulus above the set ES intensity (3 times higher than the sensory threshold) should not lead to a change in PEP amplitude. We verified that increasing the intensity of the somatosensory input indeed reaches a saturation around the intensities we applied in the experiment (2.1 Figure 2). This suggests that the addition of extra sensory input, as is the case of the real TMS condition, should not result in detectable changes in the PEP. This, however, is an indirect test. To confirm the second criterion, the PEP from the sham condition should match that from the real TMS, so that the true TEP should contain no PEP component that cannot be observed also in the response to the sham condition.

By comparing the sham and the real TMS responses we observed a match in late components, specifically the frontocentral negative potential around 100ms after the pulse, followed by the positive potential around 200ms, strongly suggesting that these are PEPs. Indeed, these EEG responses have been several times described as sensory evoked potentials, often referred to as the N100–P200 complex. This complex can be elicited by a variety of sensory stimuli and is thought to represent supramodal processing of perceptual inputs (Downar et al., 2002; Kenemans, 2015; Mouraux & Iannetti, 2009; Singhal et al., 2002). Although some have argued that the frontocentral N100 in TMS-EEG might represent a generic cortical response to direct stimulation,

given that it is observed in probing different cortical regions (Du et al., 2017), it is far more likely that, no matter the cortical target, TMS application will involve multisensory stimuli that will inevitably elicit PEPs.

When subtracting the sham response from the real TMS response, the N100–P200 is completely removed, in agreement with the notion that it contains only PEP components. The remaining responses are EEG potentials between 30-150ms after the pulse and are mostly limited to the region around the stimulated primary motor cortex (2.1 Figure 4; 2.2 Figure 4). Early components of the TEPs from motor cortex stimulation have been properly described in previous studies, including a positive potential around 30ms after the pulse (P30) followed by a negative potential around 45ms (N45) (Hallett et al., 2017; Hill et al., 2016; Komssi & Kähkönen, 2006). This was likely possible due to the absence of overlap with PEP in this early time window. Conversely, some discrepancies are found with the later P70 potential and the positive potential around 100-150ms on the stimulated cortex, with some uncontrolled or incompletely sham-controlled studies not properly identifying them (Ahn & Fröhlich, 2021; Belardinelli et al., 2021; Bonato et al., 2006; Cash et al., 2017; Darmani et al., 2019; Gordon et al., 2018; Komssi & Kähkönen, 2006; Premoli et al., 2014).

In summary, the confirmation of true TEPs around 30-70ms after the pulse agrees with previous reports, as this time window is mostly free of PEPs (Ahn & Fröhlich, 2021; Conde et al., 2019). However, in later time windows the signal overlapping of the PEPs hinders the analysis of TEPs, and sham control procedures that do not fully reproduce the sensory input from the real TMS may lead to components of PEPs mistakenly interpreted as TEPs.

The analysis of the oscillatory responses induced by TMS also leads to a similar conclusion. TMS to the motor cortex has been described to induce a broadband oscillatory response that lasts for up to 300ms and encompasses several cortical regions (Biabani et al., 2019; Fecchio et al., 2017; Premoli, Bergmann, et al., 2017; Rosanova et al., 2009). However, very similar results are obtained by applying solely sensory stimuli (2.1 Figure 5), indicating that these cortical oscillatory changes occur in response to incoming sensory information, and largely not to direct cortical activation by TMS. The result from subtracting the oscillatory response to sham from the response to real TMS reveals as a genuine response to TMS only a short increase in

the beta band oscillation, that lasts up to 100ms after the stimulus, precisely around the stimulated cortical target (2.1 Figure 5).

3.3 Applying the optimized sham procedure for TMS-EEG in a pharmacological study

It is now evident that a considerable component of the TMS-EEG response is attributed to PEPs. This raises the question to what extent previous studies that revealed modulation of TMS-EEG responses, be it by neuromodulatory interventions, drugs or different brain states, were describing changes of the true TEPs or of PEPs. Also, whether we can apply the optimized sham procedure to reliably separate the effects on these two responses. To address these questions, we designed an experiment to reproduce the findings of previous pharmacological TMS-EEG studies (Premoli, Bergmann, et al., 2017; Premoli et al., 2014) while using the optimized sham procedure.

The initial results from our experiment were similar to the findings by Premoli et al, with Diazepam modulating the EEG evoked responses to TMS. However, Diazepam intake also modulated EEG evoked responses to the sham condition. Specifically, it decreased the N100 amplitude, a result also observed by Premoli et al (2.2 Figure 5 and 6), demonstrating that an intervention (here Diazepam intake) can indeed modulate PEPs in TMS-EEG experiments. Not surprisingly, the same modulatory effect of benzodiazepines on EEG evoked responses to sensory stimuli had been observed in previous studies (Lindhardt et al., 2001; van Leeuwen et al., 1995). Accordingly, after subtracting the EEG response to sham from that of the real TMS the N100-P200 complex is thoroughly removed before and after Diazepam intake. What is left is the modulation of potentials mostly contained in the stimulated cortical area, which included an increase in negativity of the potential around 50ms after the pulse (2.2 Figure 5 and 6), which was also described in the previous studies (Premoli, Bergmann, et al., 2017; Premoli et al., 2014).

An analogous issue affects TMS-EEG studies that claimed to have identified signatures of focal disturbance to direct cortical activation by TMS in neuropsychiatric disorders. This is the case of TMS-EEG studies that have shown an abnormally low N100 amplitude in neuropsychiatric disorders such as ADHD, schizophrenia and substance abuse (Bruckmann et al., 2012; Loheswaran et al., 2018; Noda et al., 2018).

However, these neuropsychiatric conditions have also been associated with pathologically low sensory evoked responses' amplitudes (Cheng et al., 2016; Rangaswamy & Porjesz, 2014; Rosburg, 2018).

In summary, there is a real risk that studies applying TMS-EEG are simply observing the effects on PEP. Since TMS-EEG aims at probing the responses of specific cortical regions to direct activation by TMS, this exposes a severe limitation of the method. Nevertheless, in this process we demonstrated that it is possible to use an optimized sham procedure to reliably remove the PEPs from the EEG response signal and reveal the true TEPs, and consequently disentangle the modulatory effect of an intervention (in this case Diazepam intake) on the true TEPs.

3.4 Do high intensity somatosensory inputs modulate TEPs?

In the development of the optimized sham procedure for TMS-EEG we were faced with a potential limitation of the method, namely the possibility that the high intensity somatosensory stimulus could have a modulatory effect over the motor cortex response evoked by TMS. If this were the case, then the delivery of high-intensity multisensory inputs in the real TMS sham conditions might warp the true TEP, thus further obscuring the real EEG response signature to direct cortical activation by TMS. This possibility has gained support by evidence that sensory inputs modulate motor cortex excitability measured by MEP amplitudes (Novembre et al., 2019).

To test this hypothesis, we conducted a third experiment, in which we obtained TEPs (EEG response to TMS after subtraction of the EEG response to sham) using the optimized sham procedure of high-intensity ES in both sham and real TMS conditions (as in 2.1 and 2.2), and compared with the TEP from the same conditions but with ES of double the intensity. If the TEPs are modulated by somatosensory input intensity, the results from these two measurements should differ. However, we observed that the resulting TEPs from these conditions were not significantly different (2.3 Figure 1).

A limitation of this approach is that in both conditions a higher than usual ES intensity was used. It might be that the modulatory effects of somatosensory inputs over motor cortex excitability are also subject to a saturating effect. In other words, there might be an observable modulatory effect when using high-intensity ES as compared to "standard" TMS (without concomitant ES), however, using a "double" high-intensity ES

would not recruit further observable modulation. We addressed this issue by creating another sham design, in which the ES intensity is carefully calibrated so that the elicited PEP has the same amplitudes as the PEP elicited by the real TMS. This guarantees that the PEPs from both sham and real TMS are matched, making it possible to obtain the true TEPs by subtracting the sham response from the real TMS response, without the need of high-intensity ES. As before, we observed that the resulting TEPs from all these conditions were not significantly different (2.3 Figure 1), indicating that the optimized sham with high-intensity ES does not significantly modulate the true TEPs, and is thus valid.

It should be noted that this approach of PEP-calibrated sham procedure does not satisfy the first criterion for an optimized sham, as subjects are clearly able to distinguish between the real and the sham conditions. In fact, the lengthy calibration procedure offers enough opportunity for the subjects to learn the differences between the conditions. However, this introduces the question of whether being able to identify the two conditions is relevant in the present setting. It is evident that being able to distinguish between two stimuli involves different neurophysiological processes, yet these might be too subtle to be identified by TMS-EEG. Ultimately our goal was to apply a control condition that elicits PEPs in the EEG that are equal to those elicited by the real TMS, so that these could be subtracted and reveal the true TEP. In this regard, both optimized sham and PEP-calibrated sham were successful.

3.5 Conclusion

Our project describes two methods of controlling TMS-EEG responses for PEPs using a sham procedure: an optimized sham and PEP-calibrated sham. The PEP-calibrated sham offers a more elegant solution and might be preferred for targets that require TMS pulses of high intensity, and thus harder to find a corresponding saturating somatosensory stimulus. The drawback, however, is the lengthy and careful calibration procedure, which involves repeated measures of stimulus response needed to attain an ES intensity that elicits a matching PEP amplitude with respect to the real TMS. Still, both procedures were shown to reliably remove the PEPs from the TMS-EEG signal and reveal the genuine TEP response to direct cortical activation by TMS.

The application of these sham procedures conclusively confirmed the superposition of PEPs on the TMS-EEG response, which to a concerning degree had been

misinterpreted as true TEP components in several previous publications. The use of a proper sham is also imperative for TMS-EEG experiments aimed at testing the effects of interventions, as these can also modulate PEPs. Therefore, the use of an optimized sham control is indispensable for obtaining reliable responses from direct cortical activation by TMS, and assuring appropriate interpretation of TMS-EEG results.

4. Summary

The combination of transcranial magnetic stimulation (TMS) and electroencephalography (EEG) is increasingly used to investigate changes in cortical excitability and responsivity caused by neuropsychiatric disorders, drug intake and neuromodulatory interventions. However, TMS-EEG suffers from a considerable methodological challenge posed by peripherally evoked potentials (PEPs) in the response signal, which are elicited by auditory and somatosensory stimuli from the TMS device activation. This represents a considerable limitation, as it is unclear to what extent the results observed in TMS-EEG measurements refer to specific responses to TMS indicating direct cortical activation or simply unspecific cortical responses to sensory input. Attempts to tackle this issue have not been able to reliably remove the PEP components from the TMS-EEG response signal, leaving the issue unresolved.

The objective of the present project was to design an optimized sham procedure that reliably recreates all sensory inputs generated by the TMS application. Being able to elicit matching PEPs will allow the subtraction of the sham condition response from the real TMS response, thus revealing the true TMS-evoked potentials (TEPs). A further objective was the application of the optimized sham to a pharmacological TMS-EEG experiment using Diazepam, which in previous studies has been shown to modulate TMS-EEG responses. The aim was to test whether it is possible to use the optimized sham procedure to disentangle the modulatory effects on PEPs from the effects on TEPs.

The experiments described in the published articles reveal the successful design of a sham procedure for TMS-EEG, which recreates matching electrophysiological responses elicited by TMS-related sensory inputs. This was possible with the delivery of a high-intensity somatosensory stimulus to both the sham and the real TMS conditions. The procedure allowed the subtraction of the PEP components in the sham condition from the EEG signal to TMS, thus revealing the specific electrophysiological signatures of direct cortical activation by TMS, the true TEPs.

By applying this sham procedure to a pharmacological TMS-EEG experiment it became evident that both TEPs and PEPs are modulated by Diazepam intake. In

addition to demonstrating the feasibility and utility of the method, it also constitutes a warning that studies that do not apply proper sham procedures to TMS-EEG experiments might be simply observing modulation of PEPs. Finally, a possible shortcoming of the method was addressed, namely the possibility that the sham procedure might alter the true TEP conformation. An additional experiment to test this hypothesis could dismiss this possibility, indicating the validity of the optimized sham procedure.

In summary, the present project emphasizes the limitations of TMS-EEG measurements when not properly accounting for the non-specific EEG responses to sensory inputs, while also presenting reliable solutions by applying proper sham control conditions. These findings are relevant for future TMS-EEG experiments that aim at measuring regional brain target engagement.

5. German summary

Die Kombination von transkranieller Magnetstimulation (TMS) und Elektroenzephalographie (EEG) wird zunehmend eingesetzt, um Veränderungen der kortikalen Erregbarkeit und Reaktivität zu untersuchen, die durch neuropsychiatrische Erkrankungen, Medikamenteneinnahme und neuromodulatorische Interventionen hervorgerufen werden. TMS-EEG hat jedoch eine wichtige methodologische Einschränkung, nämlich die Entstehung von peripher evozierten Potentialen (PEPs) im Antwortsignal, die durch auditive und somatosensorische Stimuli von der Aktivierung des TMS-Gerätes hervorgerufen werden. Dies ist eine erhebliche Herausforderung, da es unklar ist, ob die Ergebnisse einer TMS-EEG-Messung eine direkte kortikale TMS-Aktivierung oder eine unspezifische kortikale Reaktion auf sensorische Inputs darstellt. Bis dato konnten Studien PEP-Komponenten nicht zuverlässig aus dem TMS-EEG-Antwortsignal bereinigen, so dass dieses Problem ungelöst blieb.

Das Ziel dieses Projektes war die Entwicklung eines optimierten Sham-Verfahrens, das alle sensorischen Inputs, die durch die TMS-Anwendung erzeugt werden, zuverlässig reproduziert. Die Möglichkeit, gleichartige PEPs auszulösen, erlaubt es, die EEG-Antwort des Sham-Verfahrens von der EEG-Antwort des TMS zu subtrahieren und so die echten TMS-evozierten Potentialen (TEPs) aufzudecken. Ein weiteres Ziel dieser Studie ist die Anwendung dieses entwickelten Sham-Verfahrens auf ein pharmakologisches TMS-EEG-Experiment mit Diazepam, von dem in früheren Studien eine Modulation der TMS-EEG-Antwort gezeigt werden konnte. Hiermit untersuchten wir, ob es möglich ist, mit Hilfe des optimierten Sham-Verfahrens die modulierenden Effekte von Diazepam auf PEPs von den Effekten auf TEPs zu trennen.

Die publizierten Artikel beschreiben die erfolgreiche Entwicklung eines TMS-EEG Sham-Verfahrens, welches die elektrophysiologischen EEG-Antworten auf TMS-bezogene sensorische Inputs präzise reproduziert. Dies wurde erreicht, indem hochintensive somatosensorische Stimuli sowohl in der Sham-Bedingung als auch in der realen TMS-Bedingung appliziert wurden. Das Verfahren erlaubte die Subtraktion der PEP-Komponenten in der Sham-Bedingung vom EEG-Signal in der realen TMS-Bedingung und zeigte die spezifischen elektrophysiologischen Signaturen der direkten kortikalen Aktivierung durch TMS (TEPs).

Die Anwendung dieser Sham-Verfahren auf ein pharmakologisches TMS-EEG-Experiment zeigte, dass sowohl TEPs als auch PEPs durch die Einnahme von Diazepam moduliert werden können. Dies demonstriert die Anwendbarkeit und den Nutzen der Methode. Gleichzeitig sind die Ergebnisse eine Warnung für andere Studien, die keine geeigneten Sham-Verfahren bei TMS-EEG-Experimenten einsetzen und daher möglicherweise lediglich eine Modulation durch PEPs beobachten. Schließlich wurde in der letzten Studie eine mögliche Einschränkung der Methode untersucht, nämlich die Möglichkeit, dass die Sham-Verfahren selbst die TEPs modulieren könnten. Das Experiment zur Überprüfung dieser Hypothese konnte dies nicht bestätigen, was die Validität der optimierten Sham-Verfahren unterstreicht.

Zusammenfassend unterstreichen die vorliegenden Experimente die Einschränkung von TMS-EEG-Messungen, wenn für kortikale EEG-Antworten auf sensorische Inputs nicht geeignet kontrolliert wird. Die Experimente zeigen auch eine zuverlässige Lösung durch die Anwendung eines optimierten Sham-Verfahrens. Diese Ergebnisse sind hoch-relevant für zukünftige TMS-EEG-Experimente, die darauf abzielen, die regionale neuronale Erregbarkeit des Gehirns zu untersuchen.

6. List of References

Ahn, S., & Fröhlich, F. (2021). Pinging the brain with transcranial magnetic stimulation reveals cortical reactivity in time and space. *Brain Stimul*, *14*(2), 304-315. https://doi.org/10.1016/j.brs.2021.01.018

Barker, A. T., Jalinous, R., & Freeston, I. L. (1985). Non-invasive magnetic stimulation of human motor cortex. *Lancet*, *1*(8437), 1106-1107. https://doi.org/10.1016/s0140-6736(85)92413-4

Belardinelli, P., König, F., Liang, C., Premoli, I., Desideri, D., Müller-Dahlhaus, F., Gordon, P. C., Zipser, C., Zrenner, C., & Ziemann, U. (2021). TMS-EEG signatures of glutamatergic neurotransmission in human cortex. *Sci Rep*, *11*(1), 8159. https://doi.org/10.1038/s41598-021-87533-z

Benussi, A., Di Lorenzo, F., Dell'Era, V., Cosseddu, M., Alberici, A., Caratozzolo, S., Cotelli, M. S., Micheli, A., Rozzini, L., Depari, A., Flammini, A., Ponzo, V., Martorana, A., Caltagirone, C., Padovani, A., Koch, G., & Borroni, B. (2017). Transcranial magnetic stimulation distinguishes Alzheimer disease from frontotemporal dementia. *Neurology*, *89*(7), 665-672. https://doi.org/10.1212/wnl.0000000000004232

Benussi, A., Grassi, M., Palluzzi, F., Koch, G., Di Lazzaro, V., Nardone, R., Cantoni, V., Dell'Era, V., Premi, E., Martorana, A., di Lorenzo, F., Bonni, S., Ranieri, F., Capone, F., Musumeci, G., Cotelli, M. S., Padovani, A., & Borroni, B. (2020). Classification Accuracy of Transcranial Magnetic Stimulation for the Diagnosis of Neurodegenerative Dementias. *Ann Neurol*, *87*(3), 394-404. https://doi.org/10.1002/ana.25677

Biabani, M., Fornito, A., Mutanen, T. P., Morrow, J., & Rogasch, N. C. (2019). Characterizing and minimizing the contribution of sensory inputs to TMS-evoked potentials. *Brain Stimul*, *12*(6), 1537-1552. https://doi.org/10.1016/j.brs.2019.07.009

Bonato, C., Miniussi, C., & Rossini, P. M. (2006). Transcranial magnetic stimulation and cortical evoked potentials: a TMS/EEG co-registration study. *Clin Neurophysiol*, *117*(8), 1699-1707. https://doi.org/10.1016/j.clinph.2006.05.006

Bruckmann, S., Hauk, D., Roessner, V., Resch, F., Freitag, C. M., Kammer, T., Ziemann, U., Rothenberger, A., Weisbrod, M., & Bender, S. (2012). Cortical inhibition in attention deficit hyperactivity disorder: new insights from the electroencephalographic response to transcranial magnetic stimulation. *Brain*, *135*(Pt 7), 2215-2230. https://doi.org/10.1093/brain/aws071

Burke, D., Hicks, R., Stephen, J., Woodforth, I., & Crawford, M. (1995). Trial-to-trial variability of corticospinal volleys in human subjects. *Electroencephalogr Clin Neurophysiol*, *97*(5), 231-237. https://doi.org/10.1016/0013-4694(95)00005-j

Casarotto, S., Comanducci, A., Rosanova, M., Sarasso, S., Fecchio, M., Napolitani, M., Pigorini, A., A, G. C., Trimarchi, P. D., Boly, M., Gosseries, O., Bodart, O., Curto, F., Landi, C., Mariotti, M., Devalle, G., Laureys, S., Tononi, G., & Massimini, M. (2016). Stratification of unresponsive patients by an independently validated index of brain complexity. *Ann Neurol*, *80*(5), 718-729. https://doi.org/10.1002/ana.24779

Cash, R. F., Noda, Y., Zomorrodi, R., Radhu, N., Farzan, F., Rajji, T. K., Fitzgerald, P. B., Chen, R., Daskalakis, Z. J., & Blumberger, D. M. (2017). Characterization of Glutamatergic and GABAA-Mediated Neurotransmission in Motor and Dorsolateral Prefrontal Cortex Using Paired-Pulse TMS-EEG. *Neuropsychopharmacology*, *42*(2), 502-511. https://doi.org/10.1038/npp.2016.133

Cheng, C. H., Chan, P. S., Hsieh, Y. W., & Chen, K. F. (2016). A meta-analysis of mismatch negativity in children with attention deficit-hyperactivity disorders. *Neurosci Lett*, *612*, 132-137. https://doi.org/10.1016/j.neulet.2015.11.033

Conde, V., Tomasevic, L., Akopian, I., Stanek, K., Saturnino, G. B., Thielscher, A., Bergmann, T. O., & Siebner, H. R. (2019). The non-transcranial TMS-evoked potential is an inherent source of ambiguity in TMS-EEG studies. *Neuroimage*, *185*, 300-312. https://doi.org/10.1016/j.neuroimage.2018.10.052

Darmani, G., Bergmann, T. O., Zipser, C., Baur, D., Müller-Dahlhaus, F., & Ziemann, U. (2019). Effects of antiepileptic drugs on cortical excitability in humans: A TMS-EMG and TMS-EEG study. *Hum Brain Mapp*, *40*(4), 1276-1289. https://doi.org/10.1002/hbm.24448

Davey, K., & Epstein, C. M. (2000). Magnetic stimulation coil and circuit design. *IEEE Trans Biomed Eng*, *47*(11), 1493-1499. https://doi.org/10.1109/10.880101

Dayan, E., Censor, N., Buch, E. R., Sandrini, M., & Cohen, L. G. (2013). Noninvasive brain stimulation: from physiology to network dynamics and back. *Nat Neurosci*, *16*(7), 838-844. https://doi.org/10.1038/nn.3422

Di Lazzaro, V., Oliviero, A., Profice, P., Pennisi, M. A., Di Giovanni, S., Zito, G., Tonali, P., & Rothwell, J. C. (2000). Muscarinic receptor blockade has differential effects on the excitability of intracortical circuits in the human motor cortex. *Exp Brain Res*, *135*(4), 455-461. https://doi.org/10.1007/s002210000543

Di Lazzaro, V., Oliviero, A., Saturno, E., Dileone, M., Pilato, F., Nardone, R., Ranieri, F., Musumeci, G., Fiorilla, T., & Tonali, P. (2005). Effects of lorazepam on short latency afferent inhibition and short latency intracortical inhibition in humans. *J Physiol*, *564*(Pt 2), 661-668. https://doi.org/10.1113/jphysiol.2004.061747

Di Lazzaro, V., Pilato, F., Dileone, M., Tonali, P. A., & Ziemann, U. (2005). Dissociated effects of diazepam and lorazepam on short-latency afferent inhibition. *J Physiol*, *569*(Pt 1), 315-323. https://doi.org/10.1113/jphysiol.2005.092155

Downar, J., Crawley, A. P., Mikulis, D. J., & Davis, K. D. (2002). A cortical network sensitive to stimulus salience in a neutral behavioral context across multiple sensory modalities. *J Neurophysiol*, *87*(1), 615-620. https://doi.org/10.1152/jn.00636.2001

Du, X., Choa, F. S., Summerfelt, A., Rowland, L. M., Chiappelli, J., Kochunov, P., & Hong, L. E. (2017). N100 as a generic cortical electrophysiological marker based on decomposition of TMS-evoked potentials across five anatomic locations. *Exp Brain Res*, *235*(1), 69-81. https://doi.org/10.1007/s00221-016-4773-7

Fecchio, M., Pigorini, A., Comanducci, A., Sarasso, S., Casarotto, S., Premoli, I., Derchi, C. C., Mazza, A., Russo, S., Resta, F., Ferrarelli, F., Mariotti, M., Ziemann, U., Massimini, M., & Rosanova, M. (2017). The spectral features of EEG responses to transcranial magnetic stimulation of the primary motor cortex

depend on the amplitude of the motor evoked potentials. *PLoS One*, *12*(9), e0184910. https://doi.org/10.1371/journal.pone.0184910

Gescheider, G. A. (1997). *Psychophysics: The Fundamentals* (3rd Edition ed.). Psychology Press. https://doi.org/https://doi.org/10.4324/9780203774458

Gordon, P. C., Desideri, D., Belardinelli, P., Zrenner, C., & Ziemann, U. (2018). Comparison of cortical EEG responses to realistic sham versus real TMS of human motor cortex. *Brain Stimul*, *11*(6), 1322-1330. https://doi.org/10.1016/j.brs.2018.08.003

Gosseries, O., Sarasso, S., Casarotto, S., Boly, M., Schnakers, C., Napolitani, M., Bruno, M. A., Ledoux, D., Tshibanda, J. F., Massimini, M., Laureys, S., & Rosanova, M. (2015). On the cerebral origin of EEG responses to TMS: insights from severe cortical lesions. *Brain Stimul*, *8*(1), 142-149. https://doi.org/10.1016/j.brs.2014.10.008

Groppa, S., Oliviero, A., Eisen, A., Quartarone, A., Cohen, L. G., Mall, V., Kaelin-Lang, A., Mima, T., Rossi, S., Thickbroom, G. W., Rossini, P. M., Ziemann, U., Valls-Sole, J., & Siebner, H. R. (2012). A practical guide to diagnostic transcranial magnetic stimulation: Report of an IFCN committee. *Clin Neurophysiol*, *123*(5), 858-882. https://doi.org/10.1016/j.clinph.2012.01.010

Hallett, M., Di Iorio, R., Rossini, P. M., Park, J. E., Chen, R., Celnik, P., Strafella, A. P., Matsumoto, H., & Ugawa, Y. (2017). Contribution of transcranial magnetic stimulation to assessment of brain connectivity and networks. *Clin Neurophysiol*, *128*(11), 2125-2139. https://doi.org/10.1016/j.clinph.2017.08.007

Harquel, S., Bacle, T., Beynel, L., Marendaz, C., Chauvin, A., & David, O. (2016). Mapping dynamical properties of cortical microcircuits using robotized TMS and EEG: Towards functional cytoarchitectonics. *Neuroimage*, *135*, 115-124. https://doi.org/10.1016/j.neuroimage.2016.05.009

Herring, J. D., Thut, G., Jensen, O., & Bergmann, T. O. (2015). Attention Modulates TMS-Locked Alpha Oscillations in the Visual Cortex. *J Neurosci*, *35*(43), 14435-14447. https://doi.org/10.1523/JNEUROSCI.1833-15.2015

Hill, A. T., Rogasch, N. C., Fitzgerald, P. B., & Hoy, K. E. (2016). TMS-EEG: A window into the neurophysiological effects of transcranial electrical stimulation in non-motor brain regions. *Neurosci Biobehav Rev*, *64*, 175-184. https://doi.org/10.1016/j.neubiorev.2016.03.006

Ilmoniemi, R. J., & Kicic, D. (2010). Methodology for combined TMS and EEG. *Brain Topogr*, *22*(4), 233-248. https://doi.org/10.1007/s10548-009-0123-4

Ilmoniemi, R. J., Virtanen, J., Ruohonen, J., Karhu, J., Aronen, H. J., Naatanen, R., & Katila, T. (1997). Neuronal responses to magnetic stimulation reveal cortical reactivity and connectivity. *Neuroreport*, *8*(16), 3537-3540. https://doi.org/10.1097/00001756-199711100-00024

Kenemans, J. L. (2015). Specific proactive and generic reactive inhibition. *Neurosci Biobehav Rev*, *56*, 115-126. https://doi.org/10.1016/j.neubiorev.2015.06.011

Komssi, S., & Kähkönen, S. (2006). The novelty value of the combined use of electroencephalography and transcranial magnetic stimulation for neuroscience research. *Brain Res Rev*, *52*(1), 183-192. https://doi.org/10.1016/j.brainresrev.2006.01.008

Kujirai, T., Caramia, M. D., Rothwell, J. C., Day, B. L., Thompson, P. D., Ferbert, A., Wroe, S., Asselman, P., & Marsden, C. D. (1993). Corticocortical inhibition in human motor cortex. *J Physiol*, *471*, 501-519. https://doi.org/10.1113/jphysiol.1993.sp019912

Lefaucheur, J. P., & Picht, T. (2016). The value of preoperative functional cortical mapping using navigated TMS. *Neurophysiol Clin*, *46*(2), 125-133. https://doi.org/10.1016/j.neucli.2016.05.001

Liepert, J., Schwenkreis, P., Tegenthoff, M., & Malin, J. P. (1997). The glutamate antagonist riluzole suppresses intracortical facilitation. *J Neural Transm (Vienna)*, *104*(11-12), 1207-1214. https://doi.org/10.1007/bf01294721

Lin, Y. Y., Shih, Y. H., Chen, J. T., Hsieh, J. C., Yeh, T. C., Liao, K. K., Kao, C. D., Lin, K. P., Wu, Z. A., & Ho, L. T. (2003). Differential effects of stimulus intensity on peripheral and neuromagnetic cortical responses to median nerve stimulation. *Neuroimage*, *20*(2), 909-917. https://doi.org/10.1016/s1053-8119(03)00387-2

Lindhardt, K., Gizurarson, S., Stefansson, S. B., Olafsson, D. R., & Bechgaard, E. (2001). Electroencephalographic effects and serum concentrations after intranasal and intravenous administration of diazepam to healthy volunteers. *Br J Clin Pharmacol*, *52*(5), 521-527. https://doi.org/10.1046/j.0306-5251.2001.01486.x

Loheswaran, G., Barr, M. S., Zomorrodi, R., Rajji, T. K., Blumberger, D. M., Le Foll, B., & Daskalakis, Z. J. (2018). Alcohol Impairs N100 Response to Dorsolateral Prefrontal Cortex Stimulation. *Sci Rep*, *8*(1), 3428. https://doi.org/10.1038/s41598-018-21457-z

Massimini, M., Ferrarelli, F., Huber, R., Esser, S. K., Singh, H., & Tononi, G. (2005). Breakdown of cortical effective connectivity during sleep. *Science*, *309*(5744), 2228-2232. https://doi.org/10.1126/science.1117256

McDonnell, M. N., Orekhov, Y., & Ziemann, U. (2006). The role of GABA(B) receptors in intracortical inhibition in the human motor cortex. *Exp Brain Res*, *173*(1), 86-93. https://doi.org/10.1007/s00221-006-0365-2

Mohammadi, B., Krampfl, K., Petri, S., Bogdanova, D., Kossev, A., Bufler, J., & Dengler, R. (2006). Selective and nonselective benzodiazepine agonists have different effects on motor cortex excitability. *Muscle Nerve*, *33*(6), 778-784. https://doi.org/10.1002/mus.20531

Mouraux, A., & Iannetti, G. D. (2009). Nociceptive laser-evoked brain potentials do not reflect nociceptive-specific neural activity. *J Neurophysiol*, *101*(6), 3258-3269. https://doi.org/10.1152/jn.91181.2008

Nikouline, V., Ruohonen, J., & Ilmoniemi, R. J. (1999). The role of the coil click in TMS assessed with simultaneous EEG. *Clin Neurophysiol*, *110*(8), 1325-1328. https://doi.org/10.1016/s1388-2457(99)00070-x

Noda, Y., Barr, M. S., Zomorrodi, R., Cash, R. F. H., Rajji, T. K., Farzan, F., Chen, R., George, T. P., Daskalakis, Z. J., & Blumberger, D. M. (2018). Reduced Short-Latency Afferent Inhibition in Prefrontal but not Motor Cortex and Its Association With Executive Function in Schizophrenia: A Combined TMS-EEG Study. *Schizophr Bull*, *44*(1), 193-202. https://doi.org/10.1093/schbul/sbx041

Novembre, G., Pawar, V. M., Kilintari, M., Bufacchi, R. J., Guo, Y., Rothwell, J. C., & Iannetti, G. D. (2019). The effect of salient stimuli on neural oscillations,

isometric force, and their coupling. *Neuroimage*, *198*, 221-230. https://doi.org/10.1016/j.neuroimage.2019.05.032

Paus, T., Sipila, P. K., & Strafella, A. P. (2001). Synchronization of neuronal activity in the human primary motor cortex by transcranial magnetic stimulation: an EEG study. *J Neurophysiol*, *86*(4), 1983-1990. https://doi.org/10.1152/jn.2001.86.4.1983

Peterchev, A. V., Wagner, T. A., Miranda, P. C., Nitsche, M. A., Paulus, W., Lisanby, S. H., Pascual-Leone, A., & Bikson, M. (2012). Fundamentals of transcranial electric and magnetic stimulation dose: definition, selection, and reporting practices. *Brain Stimul*, *5*(4), 435-453. https://doi.org/10.1016/j.brs.2011.10.001

Picht, T., Krieg, S. M., Sollmann, N., Rosler, J., Niraula, B., Neuvonen, T., Savolainen, P., Lioumis, P., Makela, J. P., Deletis, V., Meyer, B., Vajkoczy, P., & Ringel, F. (2013). A comparison of language mapping by preoperative navigated transcranial magnetic stimulation and direct cortical stimulation during awake surgery. *Neurosurgery*, *72*(5), 808-819. https://doi.org/10.1227/NEU.0b013e3182889e01

Pitkanen, M., Kallioniemi, E., Jarnefelt, G., Karhu, J., & Julkunen, P. (2018). Efficient Mapping of the Motor Cortex with Navigated Biphasic Paired-Pulse Transcranial Magnetic Stimulation. *Brain Topogr*, *31*(6), 963-971. https://doi.org/10.1007/s10548-018-0660-9

Premoli, I., Bergmann, T. O., Fecchio, M., Rosanova, M., Biondi, A., Belardinelli, P., & Ziemann, U. (2017). The impact of GABAergic drugs on TMS-induced brain oscillations in human motor cortex. *Neuroimage*, *163*, 1-12. https://doi.org/10.1016/j.neuroimage.2017.09.023

Premoli, I., Biondi, A., Carlesso, S., Rivolta, D., & Richardson, M. P. (2017). Lamotrigine and levetiracetam exert a similar modulation of TMS-evoked EEG potentials. *Epilepsia*, *58*(1), 42-50. https://doi.org/10.1111/epi.13599

Premoli, I., Castellanos, N., Rivolta, D., Belardinelli, P., Bajo, R., Zipser, C., Espenhahn, S., Heidegger, T., Muller-Dahlhaus, F., & Ziemann, U. (2014). TMS-EEG signatures of GABAergic neurotransmission in the human cortex. *J Neurosci*, *34*(16), 5603-5612. https://doi.org/10.1523/jneurosci.5089-13.2014

Radhu, N., de Jesus, D. R., Ravindran, L. N., Zanjani, A., Fitzgerald, P. B., & Daskalakis, Z. J. (2013). A meta-analysis of cortical inhibition and excitability using transcranial magnetic stimulation in psychiatric disorders. *Clin Neurophysiol*, *124*(7), 1309-1320. https://doi.org/10.1016/j.clinph.2013.01.014

Raffin, E., Harquel, S., Passera, B., Chauvin, A., Bougerol, T., & David, O. (2020). Probing regional cortical excitability via input-output properties using transcranial magnetic stimulation and electroencephalography coupling. *Hum Brain Mapp*, *41*(10), 2741-2761. https://doi.org/10.1002/hbm.24975

Rangaswamy, M., & Porjesz, B. (2014). Understanding alcohol use disorders with neuroelectrophysiology. *Handb Clin Neurol*, *125*, 383-414. https://doi.org/10.1016/b978-0-444-62619-6.00023-9

Rocchi, L., Di Santo, A., Brown, K., Ibáñez, J., Casula, E., Rawji, V., Di Lazzaro, V., Koch, G., & Rothwell, J. (2021). Disentangling EEG responses to TMS due to cortical and peripheral activations. *Brain Stimul*, *14*(1), 4-18. https://doi.org/10.1016/j.brs.2020.10.011

Rosanova, M., Casali, A., Bellina, V., Resta, F., Mariotti, M., & Massimini, M. (2009). Natural frequencies of human corticothalamic circuits. *J Neurosci*, *29*(24), 7679-7685. https://doi.org/10.1523/jneurosci.0445-09.2009

Rosburg, T. (2018). Auditory N100 gating in patients with schizophrenia: A systematic meta-analysis. *Clin Neurophysiol*, *129*(10), 2099-2111. https://doi.org/10.1016/j.clinph.2018.07.012

Rosler, K. M., Petrow, E., Mathis, J., Aranyi, Z., Hess, C. W., & Magistris, M. R. (2002). Effect of discharge desynchronization on the size of motor evoked potentials: an analysis. *Clin Neurophysiol*, *113*(11), 1680-1687. https://doi.org/10.1016/s1388-2457(02)00263-8

Ruohonen, J., Virtanen, J., & Ilmoniemi, R. J. (1997). Coil optimization for magnetic brain stimulation. *Ann Biomed Eng*, *25*(5), 840-849. https://doi.org/10.1007/bf02684168

Russo, S., Sarasso, S., Puglisi, G. E., Dal Palu, D., Pigorini, A., Casarotto, S., D'Ambrosio, S., Astolfi, A., Massimini, M., Rosanova, M., & Fecchio, M. (2022). TAAC - TMS Adaptable Auditory Control: A universal tool to mask TMS clicks. *J Neurosci Methods*, *370*, 109491. https://doi.org/10.1016/j.jneumeth.2022.109491

Schramm, S., Mehta, A., Auguste, K. I., & Tarapore, P. E. (2021). Navigated transcranial magnetic stimulation mapping of the motor cortex for preoperative diagnostics in pediatric epilepsy. *J Neurosurg Pediatr*, 1-8. https://doi.org/10.3171/2021.2.Peds20901

Siebner, H. R., Conde, V., Tomasevic, L., Thielscher, A., & Bergmann, T. O. (2019). Distilling the essence of TMS-evoked EEG potentials (TEPs): A call for securing mechanistic specificity and experimental rigor. *Brain Stimul*, *12*(4), 1051-1054. https://doi.org/10.1016/j.brs.2019.03.076

Singhal, A., Doerfling, P., & Fowler, B. (2002). Effects of a dual task on the N100-P200 complex and the early and late Nd attention waveforms. *Psychophysiology*, *39*(2), 236-245. https://doi.org/10.1017/s0048577202011009

ter Braack, E. M., de Vos, C. C., & van Putten, M. J. (2015). Masking the Auditory Evoked Potential in TMS-EEG: A Comparison of Various Methods. *Brain Topogr*, *28*(3), 520-528. https://doi.org/10.1007/s10548-013-0312-z

Tokimura, H., Di Lazzaro, V., Tokimura, Y., Oliviero, A., Profice, P., Insola, A., Mazzone, P., Tonali, P., & Rothwell, J. C. (2000). Short latency inhibition of human hand motor cortex by somatosensory input from the hand. *J Physiol*, *523 Pt 2*, 503-513. https://doi.org/10.1111/j.1469-7793.2000.t01-1-00503.x

Torquati, K., Pizzella, V., Della Penna, S., Franciotti, R., Babiloni, C., Rossini, P. M., & Romani, G. L. (2002). Comparison between SI and SII responses as a function of stimulus intensity. *Neuroreport*, *13*(6), 813-819. https://doi.org/10.1097/00001756-200205070-00016

Tremblay, S., Rogasch, N. C., Premoli, I., Blumberger, D. M., Casarotto, S., Chen, R., Di Lazzaro, V., Farzan, F., Ferrarelli, F., Fitzgerald, P. B., Hui, J., Ilmoniemi, R. J., Kimiskidis, V. K., Kugiumtzis, D., Lioumis, P., Pascual-Leone, A., Pellicciari, M. C., Rajji, T., Thut, G., . . . Daskalakis, Z. J. (2019). Clinical utility and prospective of TMS-EEG. *Clin Neurophysiol*, *130*(5), 802-844. https://doi.org/10.1016/j.clinph.2019.01.001

Valls-Sole, J., Pascual-Leone, A., Wassermann, E. M., & Hallett, M. (1992). Human motor evoked responses to paired transcranial magnetic stimuli. *Electroencephalogr Clin Neurophysiol*, *85*(6), 355-364. https://doi.org/10.1016/0168-5597(92)90048-g

van der Kamp, W., Zwinderman, A. H., Ferrari, M. D., & van Dijk, J. G. (1996). Cortical excitability and response variability of transcranial magnetic stimulation. *J Clin Neurophysiol*, *13*(2), 164-171. https://doi.org/10.1097/00004691-199603000-00007

van Leeuwen, T. H., Verbaten, M. N., Koelega, H. S., Slangen, J. L., van der Gugten, J., & Camfferman, G. (1995). Effects of oxazepam on event-related brain potentials, EEG frequency bands, and vigilance performance. *Psychopharmacology (Berl)*, *122*(3), 244-262. https://doi.org/10.1007/bf02246546

Ziemann, U., Reis, J., Schwenkreis, P., Rosanova, M., Strafella, A., Badawy, R., & Muller-Dahlhaus, F. (2015). TMS and drugs revisited 2014. *Clin Neurophysiol*, *126*(10), 1847-1868. https://doi.org/10.1016/j.clinph.2014.08.028

Ziemann, U., Rothwell, J. C., & Ridding, M. C. (1996). Interaction between intracortical inhibition and facilitation in human motor cortex. *J Physiol*, *496 (Pt 3)*, 873-881. https://doi.org/10.1113/jphysiol.1996.sp021734